Membranes for Hydrogen Separation

Nathan W. Ockwig† and Tina M. Nenoff*,‡

Geochemistry, and Surface and Interface Sciences, Sandia National Laboratories, P.O. Box 5800, M.S. 1415, Albuquerque, New Mexico 87185

Received November 27, 2006

Contents

* To whom correspondence should be addressed. Telephone: 505-844-0340. Fax: 505-844-5470. E-mail: tmnenof@sandia.gov; Internet: www.sandia.gov/nenoff.
† Geochemistry.
‡ Surface and Interface Sciences.

1. Introduction

The increasing demand for "clean" and efficient energy has resulted in an increased global willingness to embrace the proposed "hydrogen economy" as a potential long term solution to the growing energy crisis. With global energy consumption predicted to nearly double by 2050 and our present fossil fuel reserves under increasingly urgent environmental, political, and economic pressures, we must unambiguously overcome the many scientific and technological hurdles that exist between the present state of hydrogen production, utilization, and storage capabilities and those required for a competitive sustainable hydrogen economy.[1] Although many multifaceted technological barriers exist, before we can completely realize the full potential of a hydrogen economy two economic barriers, namely the cost of fuel cells and the cost of hydrogen production, must be reduced by factors of 10 and 4, respectively.[2] In an extensive effort to address these goals, the $1.2B Hydrogen Fuel Initiative was announced in January of 2003 as a presidential directive. Since then tremendous cooperative efforts have been brought to bear on the safe economic production and storage H_2.

Nearly 2% or ~6 Exajoules (1 EJ = 10^{18} joules) of the world's primary energy is stored in the 41 MM tons of H_2 which is produced industrially on a yearly basis. Over 90% of this 0.85 trillion m^3/year is generated from fossil fuel sources (mainly steam reforming of natural gas) while the remaining fraction (~8%) is produced through electrolysis of water. Much of this H_2 is used for large-scale processes in the metallurgical, chemical, petrochemical, pharmaceutical, and textile industries to manufacture a diverse range of products from semiconductors and steel alloys to vitamins and raw chemical materials such as ammonia, methanol, and hydrogen peroxide.[3] However, large-scale production of H_2 for these industries often requires an almost prohibitively large capital investment for the separation and purification processes which significantly drives up the cost of H_2. Regardless of which method is used to produce H_2, the need will always exist for a cost effective and efficient means to separate it from other less desirable species. Currently, H_2 can be purified through one (or a combination) of three major processes: (1) pressure swing adsorption (PSA),[4,5] (2)

10.1021/cr0501792 CCC: $65.00
Published on Web 10/10/2007

Tina M. Nenoff obtained her B.A. degree in Chemistry in 1987 from the University of Pennsylvania. She obtained her Ph.D. in 1993 at the University of California, Santa Barbara, in the Chemistry Department under the guidance of Dr. Galen D. Stucky. She then joined the staff at Sandia National Laboratories. Her research has been directed toward the synthesis and application of novel condensed and microporous oxide phases for catalysis and separations. She is focused on defect-free inorganic thin-film membranes for H_2 purification and on hydrocarbon feedstock separations. Another area of focus is on the synthesis and characterization of oxide ion exchangers for the removal and fixation of radioisotopes from caustic solutions containing many competing ions. Dr. Nenoff has published over 100 papers in various material science and chemistry journals and has presented at over 50 national and international conferences. She is a member of both the MRS and ACS societies.

Nathan W. Ockwig was born in Granite Falls, Minnesota, and obtained his B.S. in Chemistry (1996) from St. Cloud State University in St. Cloud, Minnesota. He earned both an M.S. (2002) and Ph.D. (2005) in the Department of Chemistry at the University of Michigan while working on the synthesis, classification, and characterization of new Metal-Organic Framework (MOF) materials under the guidance of Professor Omar M. Yaghi. Currently, Dr. Ockwig is a postdoctoral appointee in the Geochemistry Department of Sandia National Laboratories under the technical guidance of Randall T. Cygan and Tina M. Nenoff. His research at Sandia is focused on the dynamic behavior of small molecules and solvated ions in microporous zeolite and MOF materials using a variety of molecular modeling, structural, and spectroscopic characterization techniques.

fractional/cryogenic distillation, or (3) membrane separation.[6,7] While PSA and fractional/cryogenic distillation systems are in commercial operation, they are generally not cost effective and are quite energetically demanding for the separation and purification of H_2. In addition, neither of these methods provides sufficient purity for the targeted applications in the hydrogen economy. The third method, membrane separation, is currently considered to be the most promising because of low energy consumption, possibility for continuous operation, dramatically lower investment cost, its ease of operation, and ultimately cost effectiveness.[8]

Many H_2 membrane separation technologies are based on the most widely used method of hydrogen production, that is, the steam reforming of light hydrocarbons, mainly methane.[9] This process, called steam-methane reforming (SMR), consists of two basic steps. In the initial reforming step, methane (CH_4) and excess steam (H_2O) react to form carbon monoxide (CO) and hydrogen (H_2) at ~820 °C (reaction 1). Additional H_2 is obtained by the subsequent

Initial reforming reaction:

$$CH_4 + H_2O \rightarrow CO + 3H_2 \qquad \text{(reaction 1)}$$

Water-gas shift (WGS) reaction:

$$CO + H_2O \rightarrow CO_2 + H_2 \qquad \text{(reaction 2)}$$

Steam-methane reforming (SMR) reaction:

$$CH_4 + 2H_2O \rightarrow CO_2 + 4H_2 \qquad \text{(reaction 3)}$$

reaction of CO with H_2O in the water-gas shift (WGS) reaction (reaction 2). For each mole of CH_4 consumed, the overall SMR process (reaction 3) theoretically yields 4 mol of H_2 and 1 mol of CO_2, although in practice this is seldom achieved. The H_2 product composition prior to purification depends on the exact nature of the shift process used. Typically, in a high-temperature shift reactor operating at 350 °C, a product stream composition is 73.9% H_2, 17.7% CO_2, 6.9% CH_4, and 1.0% CO.[10] However, a second shift process involving a lower temperature (190−210 °C) shift reaction is often used with a resulting product composition of 74.1% H_2, 18.5% CO_2, 6.9% CH_4, and 0.1% CO.[10] Regardless of the method, H_2 purification ultimately equates to a CO_2 removal process.

Within the arena of gaseous H_2 separations, membrane compositions span the entire periodic table and range from metallic alloys and organic polymers to inorganic oxides and composites (i.e., cermets, metal−organic frameworks, and composites).[11] The diversity of structures synthesized for gas separation applications cannot possibly be encompassed in a single review. However, some generalized principles can be extracted if we categorize them in a deliberate way to highlight their compositions and distinct performance characteristics. This article is intended to provide a critical and comprehensive review of the diverse membrane materials which are under investigation for H_2 separation and purification technologies. We have chosen to put limits on the scope of materials presented herein. In particular, we have chosen to report on recent research into membrane categories that encompass broad and thematic trends of structure/property relationships between membrane class and H_2 separation ability. Older technology, individual phases, and less developed categories of membranes, such as mixed ionic−electronic proton conductors for H_2 separation, remain vital to the research field and are covered in detail elsewhere.[12,13]

Classification by composition is perhaps the simplest way of categorizing membrane materials, and they are delineated as follows: metallic (pure metals or alloys), inorganics (including oxides, zeolites, glasses, and ceramics), porous carbons, purely organic polymers, and hybrids or composites. Beyond composition, the properties (mechanical, thermal, and chemical stabilities) and performance characteristics (processability, maximum H_2 flux, permeability, selectivity, transport mechanism, lifetime) of a given membrane material are the most critical issues for any given application. The

Table 1. Current Status and Future H_2 Membrane Property Targets[1,2,14]

property	2003	2007	2010	2015
cost (USD/ft^2)	178	150	100	<100
operating T (°C)	300−600	400−700	300−600	250−500
operating ΔP (MPa)	0.69	1.38	≤2.75	2.75−6.90
H_2 recovery (% gas processed)	60	70	80	90
H_2 purity (% of dry gas)	>99.9	>99.9	>99.95	99.99
durability (years)	<1	1	3	>5

combined result of these composition and performance issues ultimately determines the cost and viability of a given material for application in commercial H_2 separation technologies. The five performance targets for H_2 separation set forth by the U.S. Department of Energy reflect the present capabilities and highlight the distinct research and development opportunities which are necessary components to fully realize the hydrogen economy.[14] The specific targets are as follows: (1) higher H_2 flux rates; (2) lower material costs; (3) improved durability; (4) lower parasitic power requirements; and (5) lower membrane production/fabrication costs (see Table 1 for target values).[1,2,14]

Although efficient and cost effective fuel cells utilizing H_2 have taken the center stage of global energy interests, research surrounding both the production and storage of H_2 is gaining international attention. This is because the purification and separation stages of nearly all large-scale manufacturing processes are often the most technological challenging and economically limiting factors. Hydrogen has been reported as "A Clean and Secure Energy Future"[15] due to its natural abundance and the nonpolluting nature of its combustion products (H_2O). However, significantly less attention has been drawn to the fact that other forms of energy (nuclear, fossil, solar, etc.)[16] must be consumed to manufacture and purify H_2 for various fuel and energy applications. Virtually all naturally occurring hydrogen is a substituent of a more complex molecule (i.e., H_2O or CH_4), and as such, a specific amount of energy is required to liberate the hydrogen from these compounds, plus the energy necessary for its purification, compression, and/or liquefaction. In addition, many of these processes are known to produce undesirable greenhouse gases as a byproduct and therefore must be combined with (carbon) sequestration technologies to significantly reduce the level of emissions. This complex set of criteria culminates into a very energetically demanding and technically challenging obstacle which must be fully addressed before the hydrogen economy can be embraced at local, national, and global levels. Despite these challenges and regardless of the advances in H_2 production methods, the need will always exist for cheaper and more efficient ways to purify and separate it from other gases.[17] Currently, the most promising of these separation technologies are based on membranes which are capable of operating under a wide variety of conditions while maintaining their efficiency. However, each class of membranes offers its own unique advantages and disadvantages to H_2 separation and purification which are primarily governed by their inherent chemical, thermal, and mechanical stabilities.

In the broadest sense, a membrane is simply a barrier which selectively allows certain molecules to permeate across it. In terms of gaseous H_2 purification and separation, this means that either H_2 molecules or impurities selectively interact with or permeate the membrane. Either of these very simplistic H_2 separation processes can be attributed to one

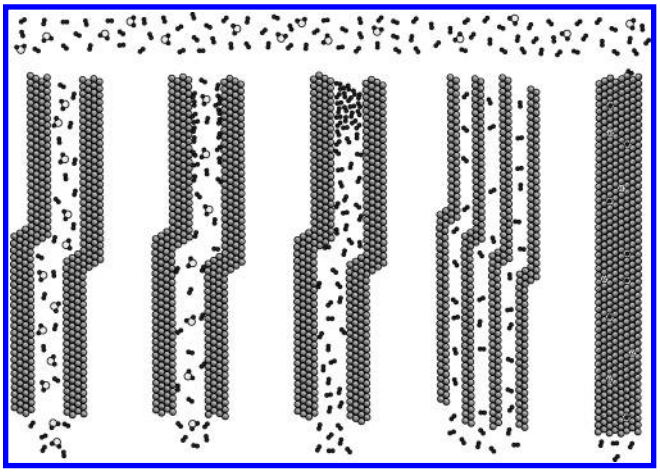

Figure 1. Illustration of five H_2 separation mechanisms: (i) Knudson diffusion; (ii) surface diffusion; (iii) capillary condensation; (iv) molecular sieving; (v) solution diffusion.

(or more) of five separation mechanisms (Figure 1):[18,19] (i) Knudson diffusion,[20] (ii) surface diffusion, (iii) capillary condensation, (iv) molecular sieving, and (v) solution diffusion.[21,22] Ultimately, the contribution of these mechanisms in a specific material culminates in its overall performance and efficiency characteristics.

The most commonly reported and compared performance characteristics of gas separation membranes are permeance (or flux) and selectivity: the flux, J, is the amount (mass or moles) of gas which permeates through the membrane (i.e., flow or flux) per unit time and unit surface area; the permeability coefficient, ρ, is the quantitative expression of a specific measure of gas moving through a membrane; and the selectivity, α, is the separating ability of a given membrane.[23]

Diffusion through dense membranes is driven by an underlying chemical potential or concentration gradient across the membrane and is well described by Ficks' first law (eq 1):[24]

$$J_{H_2} = -D_{H_2}\nabla C_{(x,y,z)} \quad \nabla C_{(x,y,z)} = \hat{\imath}\frac{\partial C}{\partial x} + \hat{\jmath}\frac{\partial C}{\partial y} + \hat{k}\frac{\partial C}{\partial z} \quad (1)$$

where D_{H_2} is the diffusion coefficient and the differential vector operator, $\nabla C_{(x,y,z)}$, is the three-dimensional equilibrium concentration in Cartesian coordinates. However, since we are primarily interested in the steady-state flux across the membrane itself, this equation is simplified to a single dimension. Permeability becomes important when the surface concentrations of the gas are not known. In these cases, Henry's law ($S_H = C_{gas}/P_{gas}$) is used, where S_H is a constant relating the vapor pressure of a nondissociative gas to its dilute concentration in a liquid or solid (i.e., the solution phase). C_{gas} and P_{gas} are the concentration and pressure of the gas, respectively. Since inlet and outlet pressures are easily measured, pressure is substituted into Fick's first law. In the case of diatomic molecules such as H_2, which dissociate prior to dissolution (i.e., in metals), a modification of Henry's law is needed; this is called Sieverts' law ($S_H = C_{gas}/P_{gas}^{1/2}$). This is then used to convert Fick's law into a usable form (eq 2):

$$J_{H_2} = \frac{-D_{H_2}\partial C_{H_2}}{\partial l} = \frac{-D_{H_2}S_{H_2}\partial P_{H_2}^{1/2}}{\partial l} \cong \frac{-D_{H_2}S_{H_2}\Delta P_{H_2}^{1/2}}{\Delta l} = \frac{-\rho_{H_2}(P_{H_2,l}^{1/2} - P_{H_2,0}^{1/2})}{l} \quad (2)$$

where J_{H_2} is the hydrogen flux, D_{H_2} is the concentration independent diffusion coefficient (not universally true), S_{H_2} is the Sieverts' law constant or solubility, l is the membrane thickness, and ρ_{H_2} is $D_{H_2}S_{H_2}$, the hydrogen permeability, while $P_{H_2,0}$ and $P_{H_2,l}$ are the measured pressures of H_2 on the feedstock and product sides of the membrane, respectively. If the individual permeabilities (ρ_i) of a given gas pair are known, the ratio of these values is defined as the *ideal* selectivity of the membrane, symbolized as $\alpha^*_{i,j}$. The separation factor ($\alpha_{i,j}$) is given by the mole fractions of both components on the feed stock (χ_i^f or χ_j^f) and product sides (χ_i^p or χ_j^p) and is related to the *ideal* selectivity through the follow expression (eq 3 and Table 2):

$$\alpha_{i,j} = \alpha^*_{i,j}\left(\frac{\chi_i^f P_i^f - \chi_i^p P_i^p}{\chi_j^f P_j^f - \chi_j^p P_j^p}\right)\left(\frac{\chi_j^f}{\chi_i^f}\right) = \left(\frac{\rho_i}{\rho_j}\right)\frac{\left(\frac{\Delta P_i}{P_i^f}\right)}{\left(\frac{\Delta P_j}{P_j^f}\right)} = \left(\frac{D_i}{D_j}\right)\left(\frac{S_i}{S_j}\right)\frac{\left(\frac{\Delta P_i}{P_i^f}\right)}{\left(\frac{\Delta P_j}{P_j^f}\right)} \quad (3)$$

The permeation and selectivity values associated with any and all membranes can be related to each other for direct comparison on performance. However, much of the similarity ends there. The fundamental science of each membrane type is unique and has its own set of questions to address in order to make membranes specifically selective for H_2 or related gases found in the production processes. Furthermore, the ability to take the laboratory bench-scale research to production scale with defect-free, highly selective membranes for large-scale applications is an involved and detailed endeavor. The ability to take concept to commercialization is the route necessary for success in any new membrane technology.

2. Metallic Membranes

This section of our review focuses specifically on metallic membranes for the separation of H_2. Metallic membranes are typically dense sheets or films which H_2 permeates through as its component protons and electrons. The fundamental mechanism of action in these dense metallic membranes requires the conduction of free electrons and the presence of specific catalytic surfaces to dissociate H_2 on the raw feed stream side and reassociate the protons and electrons on the product side (Figure 2). Hydrogen selectivity is typically very high in these systems, since the dense structure prevents the passage of large atoms and molecules such as CO, CO_2, O_2, N_2, etc.). This high selectivity translates to very high purity H_2 and the increased thermal stabilities allow higher operating temperatures. These are the primary advantages that metallic membranes offer over other materials. The metals which are most suitable for H_2 separation membranes typically have high H_2 permeabilities,[25] high diffusivities or solubilities,[26] and good thermal stability at elevated temperatures.[27] These include but are not limited exclusively to tantalum, niobium, and vanadium, and unlike platinum and palladium, they are abundant and comparatively cheap. Historically, H_2 separations were performed with Pd-based membranes, since they naturally catalyze the surface dissociation/reassociation processes and are highly permeable to H_2. There is extensive information in the literature regarding many years of research into Pd membranes. For a review of recent advances in these membranes, see refs 28−

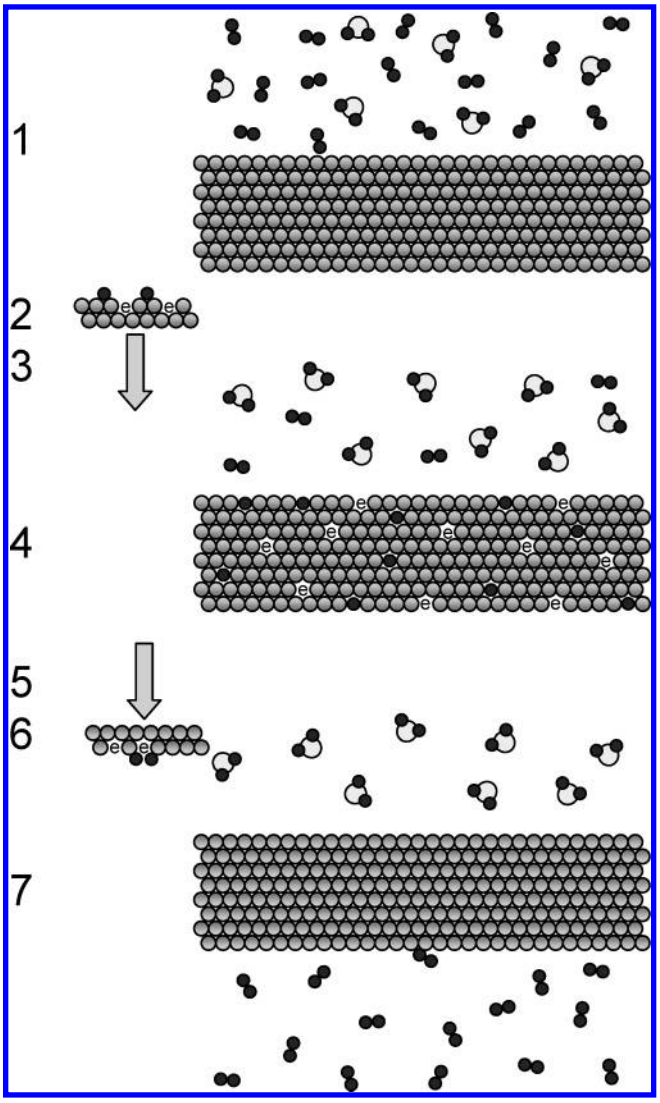

Figure 2. Seven-step diffusion mechanism in dense metal phases: (1) movement of the raw gas (mixture of H_2 and undesired) to the feed stream surface of the membrane; (2) dissociation of chemisorbed H_2 into hydrogen ions (H^+) and electrons (e^{-1}); (3) adsorption of H^+ ions into the membrane bulk; (4) diffusion of the H^+ ions and electrons through the membrane; (5) desorption of H^+ ions from the membrane bulk to the product stream surface of the membrane; (6) reassociation of the H^+ ions and the electrons into discrete molecules of H_2; and, finally, (7) diffusion of the H_2 from the product surface of the membrane.

Table 2. Engineering Strategies for Hydrogen Separation Membranes

selectivity	general	H_2 selective	H_2 rejective
$\frac{D_{H2}}{D_{gas}}$	>>>1	>>>>1	>>1
$\frac{S_{H2}}{S_{gas}}$	<<1	<1	<<<1
$\frac{P_{H2}}{P_{gas}}$	>1	>>>1	<1

30. In particular, Ma's research into Pd-based membranes has been at the forefront for years.[31−34] From an economic perspective, Pd-based membranes are generally considered prohibitively expensive for finding global integration for hydrogen production through large-scale industrial processes,[30,35] though a recent economic study has shown economic competitiveness for steam reforming using Pd-based membranes versus a conventional plant.[36] Pd- and Pt-based membranes are plagued by a very high sensitivity to surface contamination from a wide variety of impurities (H_2S, CO, thiophene, chlorine, and iodine), which severely reduce their performance.[37] This dramatic reduction in performance is primarily due to the more favorable interaction energies between the membrane and the contaminant than H_2 or irreversible chemisorptive reactions. For example, palladium membranes and catalysts have a well documented history of poisoning in the presence of sulfur containing species.[38−40] Additionally, while Pd membranes still out-perform many other prospective materials, the Pd−H phase transition at ~300 °C often leads to membrane degradation in the presence of H_2 due to a significant difference in their lattice constants.[41−43] This problem of hydrogen embrittlement can be minimized in Pd membranes by alloying them with Ag, Cu, or Au or controlling the operating conditions to avoid a two-phase region.[44] A more detailed description of alloys is given below, and recent advances in Pd-based membranes are readily available in a variety of reviews.[28,29,30,45,46] Recently, several efforts have made significant advances in non-Pd metallic membranes, and this review will largely focus on these systems.[47,48] Membranes made from metals with high diffusivity or solubility are more prone to degradation by hydrogen embrittlement[27,49] and are consequently less durable. Of course, each H_2 separation/production process has its own unique performance characteristics and requirements which must be met by the membrane employed. For example, the mildest thermal requirements (300−500 °C) are present in processes based on the water-gas shift (WGS) reaction.[50,51] Significantly higher thermal conditions are required for the reformation of natural gas (800−950 °C),[52] while the gasification of coal often requires temperatures exceeding 1000 °C.[53] However, these operating conditions are continually changing with improvements of these processes. For a detailed example, see the reports by Amadeo[54] and Andreeva[55] of the low-temperature and -pressure (180−230 °C and 101.325 kPa) WGS reactions. One further consideration which should not be overlooked is performance effects and possible interactions between the WGS catalysts and undesired products with the specific metal membrane.

Following the taxonomy used by Wipf et al.,[26] a metallic membrane material can be classified as (1) pure (single element), (2) crystalline, or (3) amorphous. This allows for the direct comparison of H_2 performance characteristics in terms of both underlying chemical structure and basic elemental composition.[26] The characteristic H_2 flux of a metallic membrane is measured directly using a standard gas permeation cell[37,56,57] which places a gas pressure differential (ΔP) on the membrane with a variety of gas mixtures and under various operating conditions (typically temperature, pressure, and cycling to determine lifetime). The analysis is typically coupled to a gas chromatograph (GC), a mass spectrometer (MS), or both (GC-MS) to determine exact gas compositions, to detect membrane leaks, and, most importantly, to quantify the permeability under a given set of conditions.[25,58,59,60]

The fundamental concepts, mechanisms, and equations governing the performance of dense metallic membranes have been the subject of numerous reviews.[25,61−65] In a dense metallic membrane, H_2 permeates through the solid material via the solution diffusion mechanism outlined in the first section (type v).[18] The solution diffusion mechanism involves a total of seven steps, which are illustrated in Figure 2: (1) movement of the raw gas (mixture of H_2 and undesired) to the feed stream surface of the membrane; (2) dissociation of chemisorbed H_2 into hydrogen ions (H^+) and electrons (e^{-1}); (3) adsorption of H^+ ions into the membrane bulk; (4) diffusion of the H^+ ions and electrons through the membrane; (5) desorption of H^+ ions from the membrane bulk to the product stream surface of the membrane; (6) reassociation of the H^+ ions and the electrons into discrete molecules of H_2; and, finally, (7) diffusion of the H_2 from the product surface of the membrane. The most commonly compared performance characteristic of H_2 selective membranes is the steady-state flux (J)[23,66] of hydrogen atoms through a membrane. This steady-state flux is simply the quantity (typically given in moles) of H_2 permeating through a certain area (cm^2) over a given period of time (s) at a specified temperature and applied pressure differential (ΔP), and it is typically expressed in units of mol $H_2/(cm^2\ s)$ for H_2 permeation through metal membranes. Reported J values (H_2 flux) through metallic membranes commonly range from 10^{-4} to 10^{-1} mol $H_2/(cm^2\ s)$ and are closely dependent on the elemental composition, the underlying chemical structure, and the fabrication method(s) used to produce the membrane.[37,54,55,64,67,68]

Ficks' first law (eq 1) describes the atomic permeation flux of hydrogen through a homogeneous metal phase as a function of the concentration gradients and a diffusion coefficient, D_{H_2} (cm^2/s), which is the concentration gradient resulting from ΔP across the membrane. Sieverts' law (eq 2) may be used under certain conditions to describe the relationship between the concentration (C_{H_2}) and the square root of pressure ($P_{H_2}^{1/2}$). This model assumes that the bulk diffusion of H_2 (step 4) occurs very quickly and it does not adversely affect the overall rate of membrane permeation. It should be noted however that Sieverts' law is limited to systems where the H_2 concentrations are low and the M−H interaction is significantly less than 1.[42] Although beyond the scope of this review, there are several modifications to this model which can account for grain boundaries complications,[69] contamination of the feed stream, and various surface phenomena.[25,70−73] Corrections to account for other H_2 diffusion modes can also be implemented.[74,75] In addition, Ward[64] proposed an elaborate model which attempts to account for all individual steps in the "solution diffusion" mechanism.

For the purposes of this review, any crystalline, single-element metal is defined as a "pure" metal. The permeability of H_2 through these types of membranes is a function of the underlying lattice structure and various types of lattice defects (i.e., vacancies, contaminant atoms, or dislocations) and reactivity toward H_2 or other feed stream gases. Body centered cubic (bcc) forms of Fe, V, Nb, and Ta commonly exhibit exceptionally high H_2 permeabilities.[25,26] Face centered cubic (fcc) metals such as Ni and Pd also exhibit favorable H_2 permeabilities, with Pd possessing significantly higher H_2 permeability than Ni.[76] Because Ni is far cheaper, its alloys are being actively investigated in a range of

Table 3. Interaction Properties of H_2 for Pure Metals[46,107,469,470]

packing	metal	hydride composition	H solubility (H/M @ 27 °C)	hydride ΔH formation (kJ/mol)	H_2 permeability @ 500 °C (mol/ms $Pa^{1/2}$)[a]
fcc	Ni	Ni_2H	$\sim 7.6 \times 10^{-5}$	−6	7.8×10^{-11}
	Cu		$\sim 8 \times 10^{-7}$		4.9×10^{-12}
	Pd	PdH	0.03	+20	1.9×10^{-8}
	Pt	PtH	$\sim 1 \times 10^{-5}$	+26	2.0×10^{-12}
bcc	V	VH_2	0.05	−54	1.9×10^{-7}
	Fe	FeH	3×10^{-8}	+14	1.8×10^{-10}
	Nb	NbH_2	0.05	−60	1.6×10^{-6}
	Ta	Ta_2H	0.20	−78	1.3×10^{-7}
hcp	Ti	γ-TiH_2	$\alpha \sim 0.0014$ $\beta \sim 1.0$	−126	
	Zr	ZrH_2	<0.01	−165	
	Hf	HfH_2	$\alpha \sim 0.01$ $\beta \sim 1.0$	−133	

[a] For unit conversions, please see p 19 of ref 46.

compositions for more favorable H_2 separation properties.[30,72,77,78]

2.1. Pure Metals

The fundamental properties of pure metals critical to H_2 separation membranes are summarized in Table 3. Higher permeation rates result from higher H_2 solubilities and lowered activation energies; decreased permeation rates originate with increased hydride formation enthalpies, resulting in the formation of stable hydrides and consequently increasing the risk of hydrogen embrittlement.[79] This embrittlement is primarily a result of changes in chemical structure and unit cell dimensions which introduce stress through abrupt changes in lattice constants. The slow dissociation and reassociation of H_2 for group IV or V metal surfaces such as V, Nb, and Ta precludes reasonably high flux rates.[56] Decreased permeation in metals also results from the formation of very stable passive oxides on the surface which consequently hinder H_2 molecule dissociation, dissolution, and H absorption by the bulk.[56,58] Without substantially removing or modifying these metallic surfaces, H_2 separation membranes based on these particular metals are severely limited.

2.2. Alloys

Group IV (Zr, Ti, Hf) and V (V, Nb, Ta) metallic crystalline alloys are known to exhibit high H_2 permeabilities.[80−82] Alloying is primarily employed to improve a pure metal's physical characteristics (e.g., strength, durability, degradation resistance) while maintaining a single-phase bcc structure that is required for high H_2 permeation. Alloying is a very well established process and commonly includes a vast variety of elements: Fe, Mn, Mo, Cu, Ni, Ga, Ge, Sn, Si, W, La, and Be.[79] However, Co, Cr, and Al are the most commonly used for binary and ternary systems.[78,79] The atomic percentages of second or third elements in binary and ternary systems to form bcc single-phase alloys with V, Nb, Ta, or Zr are easily established from the binary and ternary alloy phase diagrams (Table 4).[79,83,84] Certain alloys of the highly permeable group IV and V metals have been considered, because of their ability to reduce the susceptibility to hydride formation and increase their resistance to H_2 embrittlement caused through hydride formation pathways.[79,85−88] In particular, small percentages of metals such as Zr, Mo, Ru, and Rh have been shown to suppress the embrittlement mechanism caused by increased hydride formation enthalpies.[85,89] Alloying with Cu, Ni, Ag, or Fe is one of the methods employed to reduce surface susceptibility to gaseous impurities (e.g., H_2S, CO, H_2O) and subsequent surface contamination.[28] There are many examples of such alloys in the journal and patent literature.[78,79,90,91]

Table 4. Select Crystalline Single-Phase Body-Centered Cubic Binary and Ternary Alloy Compositions of V, Zr, Nb, and Ta $[M_{1-\alpha-\beta}M'_\alpha M''_\beta]$[81]

M′	α-max	M″	β-max
Al	0.35	Fe	0.40
	0.40	Ge	0.03
	0.40	Cu	0.05
	0.40	Zr	0.05
	0.40	Ni	0.08
	0.40	Ga	0.12
	0.40	Mn	0.53
	0.40	Mo	1
	0.40	Nb	1
	0.40	Ta	1
	0.50	Ti	0.90
Co	0.10	Fe	0.30
	0.12	Si	0.07
	0.12	Ni	0.10
	0.12	Ga	0.12
Cr	1	Hf	0.02
	1	Zr	0.04
	1	Ni	0.09
	1	Ta	0.10
	1	Fe	0.25
	1	Ti	0.80
	1	Mo	1
	1	Nb	1
	1	W	1
Ga	0.10	Ge	0.04
	0.10	Si	0.04
	0.10	Ni	0.08
	0.10	Mn	0.50
	0.10	Nb	1
	0.15	Ln	0.15
Mo	1	Si	0.04
	1	Ni	0.22
	1	Ti	0.25
	1	Nb	1
	1	Ta	1

Another area of intense research is directed toward understanding the effects of microcrystalline or polycrystalline grain size (typically 0.5−20 μm) on the H_2 permeation rates. Since alloy grain size directly correlates to the volume and morphology of its grain boundaries, it is predicted to directly influence the specific H_2 permeation rates and embrittlement resistance. The production and processing methods employed to synthesize a specific metallic alloy directly affect both the nucleation and size of the individual grains. These processes include, but are not limited to, chemical vapor deposition (CVD), plating, sputtering, and melt cooling, all of which typically increase the grain size of an alloy. Cold working methods such as rolling, drawing, pressing, spinning, extruding, and heading can actually reduce an alloy's specific grain size.

Since alloys with very small grains have a higher volume percentage of boundaries and more significant defects, they are expected to exhibit atypical diffusion mechanisms.[92] These alloys have the potential of producing diffusion rates which exceed those of traditional lattice diffusion.[93−95] One such example, nanostructured Pd−Fe supported membranes,[37,96−98] exhibit higher H_2 fluxes (attributed to grain boundary diffusion) than their coarse-grained counterparts.[37] Conversely, the Pd−Ag membranes reported by Ying and co-workers[37,96−98] and Lin et al.[99,100] showed an increase in

the H_2 permeation flux with increasing grain size. However, in this particular case, the elevated H_2 permeation was also accompanied by an increase in He permeation and gaps in the grain boundaries.[97] Unfortunately, direct comparison of these two studies is not meaningful because of the differences in manner of preparation and associated sample thicknesses. However, the difference in diffusion behaviors is tentatively attributed to the differing nanostructures and grain boundary regions. In yet another set of studies of the Pd−Ag alloys, McCool and Lin[99] describe the preparation of dense thin-film Pd−Ag membranes via dc magnetron sputtering. Heinze and co-workers[69] investigated the effect of grain size on H_2 diffusion in commercially available Pd−Ag foils ($Ag_{23}Pd_{77}$, 23% Ag) and found that grain size had no significant effect on the overall H_2 diffusion rates despite observing different operating mechanisms with different sized grains.

There are at least two other factors within crystalline alloys which directly affect the diffusivity and permeation of H_2. These are (1) specific H_2 interactions with chemical or structural defects and (2) quasi-crystallinity. The H_2 interactions ultimately lead to H_2 trapping within or around the specific chemical and/or structural defects in the alloy.[101] This factor becomes increasingly significant when H_2 concentrations decrease due to reduced H_2 fluxes through immobilization of hydrogen or by H_2 degradation of the alloy itself. The effect of quasi-crystallinity[102−104] on the behavior of H_2 in alloys remains completely unaddressed in the open literature. Quasi-crystals possess forbidden symmetry of five-fold or greater than six-fold rotational symmetry in a periodic system.[105] Further work is needed to understand the effects of processing and preparatory methods on the viability of both noble metal- and non-noble metal-based alloys for H_2 separation.

2.3. Amorphous Metals

H_2 separation membranes based on amorphous metals are generally more attractive than their crystalline equivalents because they typically exhibit improved mechanical and structural properties without concern for defect-free film growth. This is primarily a result of the fact that these structured materials are readily stabilized in alloy form. Amorphous metals are commonly reported to exhibit increased strength, ductility, corrosion resistance, and, more importantly, H_2 solubility[106] than their crystalline analogues. Furthermore, they usually contain a more open lattice[66] which decreases the embrittlement dangers associated with H_2 purification.[47] Amorphous metallic H_2 membranes are capable of withstanding repeated cycling, high temperatures, and high pressures, all of which are common operating conditions for industrial scale H_2 separations. This class of membrane material offers the additional advantage of outstanding compositional flexibility and homogeneity and high catalytic surface activities for enhanced H_2−surface interactions.[73] This can be highly composition dependent, as is the case for the amorphous nickel-based alloys: $(Zr_{36}Ni_{64})_{1-a}(Ti_{39}Ni_{61})_a$ and $(Zr_{36}Ni_{64})_{1-a}(Hf_{36}Ni_{64})_a$, where $0 < a < 1$ and which required catalytic surface coatings to lower the surface activation energies. It is important to note that the durability of the surface coating needs further research, as intermetallic diffusion of coating metals into bulk metals is commonly observed at high temperatures. In contrast, $(Zr_{36}Ni_{64})$ did not require surface coatings and $Ti_{39}Ni_{61}$ was far too brittle for use in H_2 separation applications.[45,64,66]

While measured H_2 permeabilities for amorphous alloys have yet to equal or exceed that of Pd, considerable advances have been made and this area is still an entirely open field (Table 5). The variety of amorphous alloys available to explore for H_2 separation membranes is limited only by the imagination, and there remains many unexplored compositions to consider. To date, most alloys examined for H_2 separations have been V, Nb, Ta, or Zr based because of their relatively high pure metal H_2 permeabilities.[107] A range of other Zr−Ni alloys have been investigated and shown to have relatively good mechanical and thermal stability.[108,109] The ternary Ni−Nb−Zr alloys have also been studied, including the effects of additional elements (e.g., quaternary phases including Al, Co, Cu, P, Pd, Si, Sn, Ta, and Ti), and they have been shown to be reasonably successful for H_2 separations.[47,110] Amorphous Fe-based alloys have also been explored, although the surface behaviors of these particular alloys severely inhibited the adsorption/desorption of H_2 and dramatically reduced permeation.[111,112] Another heavily researched group of alloys is based on V because of its high H_2 permeability and solubility. However, the severe H_2 embrittlement characteristics of V require the addition of other elements, which can dramatically change the permeability, mechanical, and thermal properties.[113−117]

To efficiently optimize amorphous alloys for H_2 separation membranes, multiple physical and chemical characteristics must be known and ideally understood. These characteristics

Table 5. Permeability Data for Some Recent Alloys Reported in the Literature[46]

alloy	H_2 permeability (mol/m·s·$Pa^{1/2}$)[a]	temp (°C)
VCr_4Ti_4 [472]	1×10^{-5} to 1.3×10^{-8}	500−650
Ni_3Al−6Fe [473]	4×10^{-12}	375
Ni_3Al−Zr [473]	1×10^{-12}	375
$V_{99.98}Al_{0.02}$ [116]	$0.7-1.8 \times 10^{-9}$	250−400
$V_{99.1}Al_{0.9}$ [116]	$0.7-1.8 \times 10^{-9}$	250−400
$V_{97.1}Al_{2.9}$ [116]	$0.7-1.8 \times 10^{-9}$	250−400
$V_{90.2}Al_{9.8}$ [116]	$2-3 \times 10^{-9}$	250−400
$V_{81.3}Al_{18.7}$ [116]	$3.7-6 \times 10^{-8}$	250−400
$V_{71.8}Al_{28.2}$ [116]	$0.7-1.8 \times 10^{-9}$	250−400
$V_{90}Al_{10}$ [115]	$1.3-2 \times 10^{-7}$	250−400
$V_{70}Al_{30}$ [115]	$0.7-1.8 \times 10^{-9}$	250−400
$V_{85}Ni_{14.91}Al_{0.09}$ [114]	$3-4.5 \times 10^{-7}$	250−400
$V_{85}Ni_{14.1}Al_{0.9}$ [114]	$3-4.5 \times 10^{-7}$	250−400
$V_{85}Ni_{12.4}Al_{2.6}$ [114]	$4-6 \times 10^{-7}$	250−400
$V_{85}Ni_{10.5}Al_{4.5}$ [114]	$5-7 \times 10^{-7}$	250−400
$Nb_{10}Zr_{45}Ni_{45}$ [473]	$\sim 2.5 \times 10^{-8}$	350
$Nb_{95}Zr_5$ [474]	$\sim 1.3 \times 10^{-7}$	300
$Nb_{95}Mo_5$ [475]	$\sim 1.3 \times 10^{-7}$	300
$Nb_{95}Ru_5$ [475]	$\sim 1.3 \times 10^{-7}$	300
$Nb_{95}Pd_5$ [475]	$\sim 1.3 \times 10^{-7}$	300
Fe_3Al [475]	$0.6-1.01 \times 10^{-10}$	25
$Nb_{29}Ti_{31}Ni_{40}$ [476,477]	$1.5-7 \times 10^{-9}$	250−400
$Nb_{17}Ti_{42}Ni_{41}$ [477,478]	$1.1-6 \times 10^{-9}$	250−400
$Nb_{10}Ti_{50}Ni_{40}$ [477,478]	$0.55-4.5 \times 10^{-9}$	250−400
$Nb_{39}Ti_{31}Ni_{30}$ [477,478]	$0.3-2 \times 10^{-8}$	250−400
$Nb_{28}Ti_{42}Ni_{30}$ [477,478]	$0.3-1 \times 10^{-8}$	250−400
$Nb_{21}Ti_{50}Ni_{29}$ [477,478]	$0.09-2 \times 10^{-8}$	250−400
$V_{90}Ti_{10}$ [81]	2.7×10^{-7}	400
$V_{85}Ti_{15}$ [81]	3.6×10^{-7}	435
$V_{85}Ni_{15}$ [81]	3×10^{-8}	400
$V_{90}Co_{10}$ [81]	1.2×10^{-7}	400
$V_{85}Al_{15}$ [81]	6×10^{-8}	435
α-$Zr_{36}Ni_{64}$ [47,478]	1.2×10^{-9}	350
$(Zr_{36}Ni_{64})_{1-\alpha}(Ti_{39}Ni_{61})_\alpha$ [68]	$0.1-3.5 \times 10^{-9}$	200−400
$(Zr_{36}Ni_{64})_{1-\alpha}(Ti_{36}Ni_{64})_\alpha$ [68]	$0.15-3.5 \times 10^{-9}$	200−400
$Zr_{36-x}Hf_xNi_{64}$ [66]	$0.6-3 \times 10^{-9}$	200−400
$Ni_{65}Nb_{25}Zr_{10}$ [110]	$\sim 5 \times 10^{-9}$	400
$Ni_{45}Nb_{45}Zr_{10}$ [110]	$\sim 3 \times 10^{-9}$	400
$Ni_{50}Nb_{50}$ 110	$\sim 2 \times 10^{-9}$	400

[a] For unit conversions, please see p 19 of ref 46.

Scheme 1. Namboodhiri's[469] Taxonomy of H_2 Damage in Solids

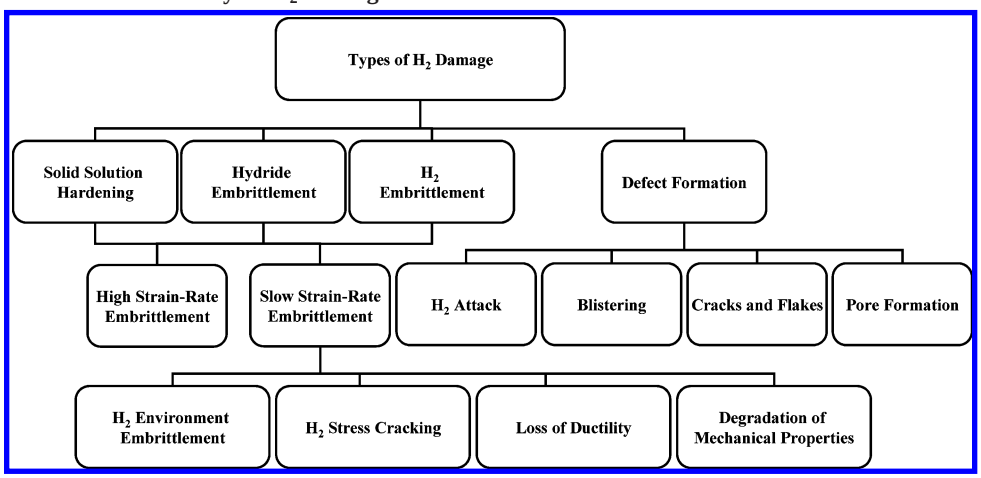

span a wide variety of properties, from H_2 diffusivity, solubility, and adsorption/desorption, to alloying and H_2 exposure effects on thermal and mechanical stability, and mechanisms of H_2 damage (Scheme 1). The transport and separation of H_2 is governed purely by the absorption, diffusion, and desorption energies[91] and by the enthalpy of hydride formation for a given alloy. Theoretical models which account for variations in the amorphous structure are useful for describing H_2 occupancies and distributions in an amorphous alloy.[23,91,118,119] Direct measurements of hydrogen vibrations within an alloy lattice have demonstrated that topological changes are insignificant in amorphous alloys and that specific polyhedral sites are preferentially occupied by hydrogen atoms.[120] This direct observation is further supported by models using Fermi−Dirac statistics which successfully describe the hydrogen distribution throughout a predefined energy landscape or density of site energies.[117,121] According to Dos Santos and co-workers,[122] at lower concentrations, the hydrogen atoms occupying high-energy sites have restricted mobility, but as the concentration increases, the low-energy sites become increasingly populated, which increases mobility and diffusivity, thus raising permeability and flux values. This provides a realistic model which can be used to evaluate potential membrane candidates from a variety of alloys. Hydrogen trapping, short range ordering, and structural and chemical defects are additional factors which affect hydrogen diffusivity in amorphous alloys.[123]

H_2 permeability through a metallic membrane (crystalline or amorphous) is fundamentally governed by the solubility of hydrogen within that particular metal or alloy. This solubility depends on both the solution activation energy and the operating temperature.[26,27] Hydrogen absorption capacities are the major method by which H_2 solubilities are quantified. Typically, larger values (for example amorphous $Ni_{64}Zr_{36}$ has a H/M solubility of 0.4 H/M) are reported for amorphous alloys than for their crystalline counterparts,[26,116,120,124,125,126] and this is commonly attributed to the "matrix of defects" within a specific amorphous alloy. This provides a considerable density of defects (a distribution of high energy sorptive sites) which can be occupied by the hydrogen over a wide range of potential energy levels. However, depending on the mechanism by H_2 dissolution, the hydrogen solubilities can vary considerably. Although there is a definitive dependence of H_2 permeability on solubility, it is also heavily dependent upon the hydrogen diffusivity, which is directly correlated to the membrane's crystalline or amorphous nature. For example, amorphous alloys exhibit higher H_2 permeation rates, but this may be significantly offset by their slower diffusivities. Conversely, crystalline alloys have lower H_2 permeation rates, but this is offset by their faster diffusion rates.

Hydrogen diffusivity in amorphous metals and alloys increases with the absorption of increasing amounts of hydrogen. According to Wu et al.,[123] this is due to weakening of metal−metal bonds. However, this also corresponded with an increasing population of low-energy sites and increased hydrogen mobility, which ultimately translates to higher diffusivities. Generally, greater mobilities and smaller average activation energies have been observed for hydrogen in amorphous metals and alloys.[116,117,124,127,128] In contrast to this work, Dos Santos et al.[122,126] have argued that hydrogen diffusivities decrease in amorphous metals and alloys as compared to the crystalline structure. This is due to a higher density of defects, which is heavily dependent on the method of preparation. Although highly dependent on composition and structure, the hydrogen diffusivities of an amorphous or crystalline metal can easily be distinguished from the standard Arrhenius behavior in amorphous metals, which is linked to the temperature dependence of hydrogen diffusion on the short-range order.[129]

Optimal structures for maximum diffusivity in amorphous metals remain to be established, and modeling the hydrogen distribution and diffusion in amorphous alloys has proved to be more complicated than for crystalline alloys.[124] Recent Monte Carlo simulations have provided a useful model which can predict hydrogen diffusion in amorphous metals based on the dispersion of interstitial sites and a distribution of their sizes.[130] Since they are thermodynamically metastable,[75] amorphous alloys have the distinct disadvantage that they have a tendency to crystallize when heated to temperatures > 500 °C (dependent on time, temperature, and composition). This limits the operating conditions (low temperature) and subsequent applications where this class of membrane can be used. Unfortunately, since hydrogen permeation is slower at lower temperatures, the fluxes are not sufficient to be industrially attractive.

Other factors influence permeation in amorphous metals. First, amorphous metals exhibit exothermic enthalpies of H_2 absorption, which has the potential to generate sufficient energy to crystallize, decompose, or change the local structure near the absorption site.[131] The physical differences between amorphous and crystalline metals of similar chemical composition for application as H_2 separation membranes

Table 6. Distinctions between Crystalline and Amorphous Metallic Membranes with Comparable Compositions

crystalline	amorphous
plateau in P_{H_2} vs $[H_2]$ isotherm	no plateau in P_{H_2} vs $[H_2]$ isotherm
Sieverts' law obeyed at elevated $[H_2]$	positive deviation from Sieverts' law
Arrhenius H_2 diffusion behavior	no−Arrhenius H_2 diffusion behavior
H_2 embrittlement from dislocation	H_2 embrittlement from free volume filling
constant diffusivity with dissolved $[H_2]$	no constant diffusivity with dissolved $[H_2]$
stable at high temperatures	potential crystallization at high temperatures
mechanically weak	mechanically strong

are summarized in Table 6. Second is the presence (crystalline) or absence (amorphous) of a plateau in the pressure−concentration isotherm. This lack of a plateau in the amorphous isotherm suggests that no plastic deformation accompanies hydride formation.[132] However, hydrogenation of amorphous and crystalline metals and alloys usually leads to a significant volume expansion of similar magnitude.[122]

Somewhat paradoxically, there are no differences in the enthalpies of solution as hydrogen concentrations are increased in either the crystalline or amorphous materials. While H_2 embrittlement is observed for both types of metallic membrane, it is less substantial in amorphous than crystalline metals because the mechanisms which cause the embrittlement are slightly different.[133] That is, dislocation transport is thought to be the major H_2 embrittlement pathway in crystalline membranes while filling of free volumes is the mechanism believed to cause H_2 embrittlement in amorphous membranes.[117]

2.4. Membrane Fabrication and Processing

New and novel alloys are being produced by sputtering, thermal evaporation, arc-melting,[71] die-casting techniques,[134] and electrodeposition. However, the most commonly employed methods for preparing novel alloys of variable structure and diverse composition are from melt-spinning[47] and arc-melting.[71] Ni-based alloys,[106,124,135,136] Ti-based alloys,[137] Zr-based alloys,[138] and, to a lesser extent, Cu-based alloys[139,140] have all been developed as bulk metallic glasses (BMGs) and BMG matrix composites.[134] To enhance the utility of grain boundaries, biphasic or multiphase alloys could be developed (where the presence of a bcc structure may or may not be required) to promote specific types of grain boundary conditions. Such alloys may include nanocrystalline alloys or those designed with mixed crystallites of variable sizes and structure. Nanocrystalline alloys are particularly attractive because of their high resilience to degradation[37] and their preparation through a variety of techniques, such as melt-quenching,[141] devitrification,[142,143] or, more traditionally, high-energy ball milling, electrodeposition,[37] and laser ablation. The range of nanocrystalline alloys formed following the devitrification pathway is less studied than bulk metallic glasses (BMGs).

To date, no established methodology has been formulated for the formation of a nanocrystalline structure. However, the methods generally include (1) a multistage crystallization process, (2) high nucleation frequency, (3) slow growth rate, and (4) thermal stabilization of the remaining amorphous phase by the solute element redistributing along the nanocrystal/amorphous interface.[144] Other authors have cited the need for high rates of homogeneous nucleation, normally associated with stoichiometric compositions and governed by atomic diffusion.[139] The applied cooling rate should remain not only high enough to prevent bulk grain growth but also lower than that required to form a glass in order to retain a nanocrystalline state.

An important aspect of the formation of nanocrystalline metals is the role of minor alloying additions. It has been demonstrated that adding a small amount of elements with nearly zero or positive heat of mixing to alloy components based on Zr and Hf (e.g. Ag, Pd, Au, Pt, Ir, Re, Zn, Mo, V, Nb, Ta, and Cr) causes the precipitation of a primary nanoscale icosahedral phase,[145,146] resulting in the formation of homogeneously distributed nano-quasi-crystalline (nq) particles within the bulk glassy alloy. However, the addition of an element with an extremely negative heat of mixing to a Zr-based amorphous alloy may result in the production of a nanocrystalline alloy where the nanocrystalline particles are dispersed throughout the glassy phase.[140]

2.5. Modeling/Simulation and Characterization

Modeling is becoming an acceptable method for identifying candidates for metal membranes. In particular, many recent efforts have focused on predictive modeling of candidate metallic alloys from first principles. Ideally, specific performance features such as hydrogen permeability, hydrogen embrittlement, and possibly thermal and chemical stabilities are modeled as a function of metal composition or structure. A recent strategy to predict the hydrogen flux through various metal alloys was based on density functional theory (DFT) *ab initio* calculations and coarse grain modeling.[147−150] An alternative method for predicting metal candidates may be based on the enthalpy of solution of hydrogen within a material such as disordered transition-metal alloys. For these metals, the enthalpy of solution has been predicted using a semiempirical embedded-cluster model and is based on the local band structure model, which incorporates a coupling between local-site volumes and the average site volume in the alloy.[151]

In combination with predictive structural models, it is useful to have experimental techniques to characterize or confirm their structure. For instance, energy selective electron diffraction can provide diffraction data of amorphous metals subsequently used to refine models based on molecular dynamics simulations.[152] One recently developed experimental technique, fluctuation electron microscopy (FEM), can verify the medium-range order of amorphous alloys predicted by mathematical models such as that proposed by Miracle et al.[153] The "medium-range order" of amorphous alloys is not easily determined through traditional scattering methods because its pair correlations have a relatively small contribution.[154] The advantage of FEM is that it is quite sensitive to spatial variations in the scattered intensity which are caused by the "medium-range order".[155] As a consequence, it is receptive to higher-order correlations such as the more common triple (three atom) and pair−pair (four atom) correlations which have been observed in amorphous metals.

Numerous other general material design strategies exist which have not yet been extended to the design of novel metallic membranes for H_2 separation. These include the utilization of trained neural network models which have led to optimization of Ni-based polycrystalline superalloys by using composition iterations to predict tensile properties as a function of temperature.[156,157] However, the use of neural networks to predict H_2 permeability or durability as a

function of composition has not yet been reported in the open literature. Alternatively, recent application of combinatorial materials screening and synthetic methods for accelerating the process of technology discovery and application could play a significant role in the rapid development of H_2 separation membranes.[158−161] Notably, combinatorial materials preparation has already been used to produce continuous phase diagrams useful for describing structure−property relationships of well established $Ni_{1-x}Fe_x$ alloys.[162,163] The challenge of using the combinatorial method lies in determining the H_2 permeabilities and operating durabilities of the metals on such small scales. This is an essential component of screening the candidates as a function of composition, structure, and H_2 interaction characteristics. Significant advances have been made in utilizing thin-film deposition and masking techniques, such as molecular beam epitaxy (MBE), to incorporate spatially variable or selective deposition, needed in making combinatorial databases and wide composition candidates.[156,164]

Compositional libraries can also be created from "diffusion multiples", an assembly of three or more metal blocks, which undergo high temperature interdiffusion to generate complete phase diagrams, as has been done for Ni-based alloys.[165] Compositional databases are generated by solution-based combinatorial synthetic methods using simple and cost effective multicomponent inkjet delivery systems, which have many obvious advantages over the thermal interdiffusion methods.[166] Property characterization of samples generated by the combinatorial approach requires highly sensitive, sophisticated, and typically nondestructive equipment. For example, scanning microwave microscopy (SMM) can characterize and map conducting and electromagnetic materials,[156,167] while electron probe microanalysis (EPM) can be used for compositional mapping.[168] Electron backscatter diffraction (EBD) can provide crystal structure analyses, while nanoindentation determines some of the mechanical properties. As the amount of information describing novel bulk metallic glasses, crystalline metals, and nanocrystalline metals increases, new databases are developed to allow more systematic comparisons to inform future alloy design directions and eventually develop methods for rational alloy design.[169] Although currently in its infancy, rational alloy design is now starting to be achieved through prediction of bulk composition ranges using a range of thermodynamic models such as Miedema's semiempirical model, quasichemical models, or kinetic models (e.g., phase field model).[151,170,171]

Having established a list of useful candidates with high performance characteristics, methods for large-scale processing, production, and fabrication of industrial membranes can then be addressed. Alloy compositions are selected and designed such that they can be manufactured from more conventional casting or high-pressure die casting techniques to ease large-scale membrane production. However, if these fabrication and production methods are underdeveloped or unavailable for utilization, this will further delay the process and ultimately make complete assessments unavailable for commercially promising membranes. Furthermore, *in situ* membrane repair and regeneration costs must also be considered during membrane development before implementing large-scale fabrication methods.

2.6. Membrane Fabrication

Metals are being deposited as thin layers on various supports (e.g., glasses, ceramics, or other metals), in an effort to increase H_2 flux while maintaining mechanical strength, thermal stability, and reliability. The current deposition methods used are electroless plating,[172] electrodeposition, spray pyrolysis, sol−gel dip coating, physical and chemical vapor deposition (PVD/CVD), or sputtering.[173,37] While CVD offers a thin layer with more efficient hydrogen permeation compared to that prepared by electroless plating, this technique is less industrially attractive.[174] Reports in the literature show CVD layers having higher H_2 permeability because hydrogen transported through the membrane via a surface diffusion mechanism rather than the traditional solution diffusion (i.e., bulk diffusion) mechanism of dense metals, as observed for Pt electroless layers.[65] However, researchers have reported that electroless coated amorphous Ni−B alloys exhibit a Knudsen diffusion mechanism (i.e., the mean free path of the diffusing H_2 molecule is much larger than the pore size) for hydrogen and speculate that a surface diffusion mechanism may also be operating here rather than a solution diffusion mechanism.[175]

Thin layer metallic coatings have been classified into four types:[29] (1) a thin metal layer (dense or porous) is formed on the surface and extraneous to the support; (2) a thin metal layer is formed on the walls within a porous support; (3) a microporous ceramic layer is formed on the supporting layer by finely distributing metal particles within the pores of the support; and (4) a microporous ceramic layer is formed on the supporting layer by sintering metal-coated particles onto the surface. For thin metal membranes, the permeability behavior may differ significantly from that of bulk metals of similar composition. This is due to the increase in the dominance of surface phenomena, defects, grain boundaries, thermal dilatation, and lattice defects on the permeability behavior (for instance, have been observed in Pd).[74] This divergence emphasizes how critical it is to characterize the permeability behavior for thin metal structures as opposed to mere inference from bulk metal behavior.

2.7. Catalytic Surface Coatings

Aside from Pd-based supported thin films, electroless and electrolytically deposited films of alternative compositions, such as Ni-based alloy films, have been reported.[172] It is expected that Ni-based films will be useful for catalyzing the dissociation and reassociation reactions of H_2, since they have already been shown to catalyze the hydrogen evolution reaction.[176] Typically, amorphous alloys have the premier catalytic activity. In particular, high catalytic activity has been found for Ni with S, P, and B existing as amorphous alloys with some pure Ni nanocrystals.[177] Initial results indicate that Ni−P alloys are also very efficient for separating H_2 due to permeation via both surface diffusion and Knudsen diffusion mechanisms. Both mechanisms are available because of the NiP "cluster" structure and the amount of interstitial space available for diffusion.[72] While Ni−P films, particularly electroless deposited films, are relatively easy to synthesize and do not require special equipment for preparation or pretreatment for surface catalytic activity, they do have a few drawbacks. Namely, H_2 separation must be performed at low temperatures (<10 °C); otherwise, the structures may crystallize. In addition, the surface area of the alloys can be quite small, and the storage of the amorphous alloys can be difficult, since certain compositions are sensitive to oxidation.[178]

Catalytic thin-film layers (e.g., Pd) can be applied by vapor deposition,[59,74] by electro- and electroless-plating,[56] or by roll

Table 7.

metal (indices)	M−H bond energy (kJ/mol)	M−CO bond energy (kJ/mol)
Ag(111)	218	25
Pt(100)	247	134
Pt(111)	247	126
Co(0001)	251	105
Co(1010)	251	
Cu(111)	251	70
Ni(110)	259	
Ni(100)	263	109
Ni(111)	263	109
Pd(111)	259	142
Pd(100)	268	151
Pd(110)	268	
Fe(100)	265	105
Fe(110)	273	
Nb(100)	273	
Mo(110)	273	
Mo(100)	277	

cladding. This has been effective for bcc materials such as V, Nb, and Ta[57,59] and for Ni−Zr-based amorphous alloys.[64] The addition of surface layers or treatment of the metal membrane surface is becoming increasingly common to improve the catalytic activity (for dissociation and reassociation of hydrogen) and chemical stability of the metal membrane in use. Dissociation and reassociation of H_2 on the metal membrane surface can be accomplished by several means, including the inherent catalytic nature of the metal itself, the addition of a catalytic layer, or electrochemical reactions. This process is directly controlled by the atomic-scale tomography of the surface, the quantity and distribution of impurity species, and any one of these steps can be kinetically controlled. A single material can be effective at catalyzing the dissociation/reassociation processes in addition to having high bulk diffusivity, as is the case for Pd and Pd alloys such as Pd−Cu and Pd−Ag and Ni−P.[72] Other candidate membrane alloys, for example amorphous Ni−Zr, could be activated by exposure to H_2 at elevated temperatures.[64] Alloys containing one of the following elements, Fe, Ru, Rh, W, Mo, Pt, Co, or Ni, can also be sufficient to act as a catalyst to dissociate the hydrogen.[78] Alternatively, catalytic layers could be applied to the surfaces of metals which readily diffuses hydrogen ions but have inadequate catalytic properties.

There is considerable room for developing non-Pd alternatives for catalytic layers, with numerous transition-metal-based catalysts having already been tried, e.g., Pt, Ir, Co, Co−Mo, Fe, magnetite (Fe_3O_4), La−Sr−Co−O, WS_2, or MoS_2.[78] The main requirements for such catalytic surface coatings are that reactive surface sites should be sufficiently close and concentrated to assist the dissociative adsorption of hydrogen and are not readily blocked by the adsorption of contaminants such as S, CO, or other adsorbates. When hydrogen reassociates to leave the surface of the metal having passed through the membrane, the surface of a metal with the lowest possible desorption energy will favor the process. Table 7 provides a list of the adsorption/desorption energies for H_2 and CO onto the crystal face of a pure metal. Despite the fact that the energies depend on the crystal surface indices, if the metal is alloyed with Ag or Pt, then H_2 will more readily desorb than the pure metal, particularly if Ag segregates to the surface. On the other hand, if a contaminant such as CO has a high binding energy, it will most likely persist and interfere with H_2 surface dissociation. Thus, Pd and Pt are the most susceptible to CO contamination (see Table 7), while Ag and Pt have the lowest adsorption energies. In addition, a substantial amount of work has investigated and modeled surface segregation in multicomponent systems for the purpose of designing catalytic layers with seemingly contradictory properties but that are optimal for a specific application.[179−181]

Table 8.

metal (indices)	specific site	binding energy (eV)
V(110)	3-fold	−3.29
Ta(110)	3-fold	−3.24
W(110)	3-fold	−3.15
Mo(110)	3-fold	−3.05
Fe(110)	3-fold	−2.99
Ru(0001)	fcc	−2.97
Ni(111)	fcc	−2.89
Co(0001)	fcc	−2.89
Pd(111)	fcc	−2.88
Rh(111)	fcc	−2.81
Ir(111)	fcc	−2.74
Pt(111)	fcc	−2.72

Near surface alloys (i.e., alloys that have a different surface solute metal concentration from that of the bulk) have presented themselves useful for providing a surface that simultaneously allows both weak hydrogen binding and low hydrogen dissociation barriers.[182] According to Table 8, metals with high binding energies such as V (−3.29 eV) and Ta (−3.24 eV) can be alloyed with Pt, for example, to yield surfaces with low H_2 dissociative transition state energies, calculated to be around about 0.5 and 0.6 eV, respectively.[183] However, under certain conditions, such as strong oxidizing conditions, inverse segregation occurs depending on the relative affinities of the alloy components for gaseous oxygen.[184] Oxide layer formation on the alloy surface may inhibit the catalytic advantages of the surface.

3. Silica Membranes

Due to some of the inherent limitations of metal membranes, research is underway for alternative membrane materials for H_2-based applications. Silica membranes are one of the candidates for hydrogen separation due to their ease of fabrication, low cost of production, and scalability. Because of their porosity and composition, silica membranes are also less expensive than metals (due to the lack of precious elements) and not susceptible to H_2 embrittlement. They are inorganic membranes that have a network of connected micropores of approximately 0.5 nm diameter and can accommodate the separations of small molecules such as H_2, He, CO_2, CO, N_2, and O_2. In fact, these membranes have yielded exceptional H_2 selectivities, with reported H_2/N_2 values exceeding 10,000.[185−187,199] Summaries of the preparation of inorganic membranes have been presented by many research groups, including those of Morooka and Kusakabe,[188] Tsapatsis and Gavalas,[189] Omaya,[190] and Verweij.[191] Contrary to dense metal, alloy, and ceramic membranes, microporous silica membranes are not 100% selective for one component. Their separation of molecular mixtures is based on a competitive process in which individual molecules move by site-hopping diffusion in the connected micropore network. A full description is found in ref 191.

Silica membranes are generally comprised of three layers: (3.1) a membrane layer, (3.2) an intermediate layer, and (3.3) a support. Much research has focused on each component to determine the structure/property relationship between material and light gas permeation ability. Each of

the three layers that comprise a silica membrane will be more fully explained below.

3.1. Membrane Layer Synthesis

Silica membranes are synthesized primarily through two different methods: sol−gel modification[192−198] and chemical vapor deposition (CVD).[188,199−210] Sol−gel modification provides good selectivity and permeability, as opposed to CVD methods, where there is an attendant loss of permeability, though the selectivity is enhanced. The sol−gel method, however, suffers from a lack of reproducibility. CVD methods usually require substantial capital investment and controlled conditions of deposition. More detailed descriptions of each method are given below.

3.1.1. Sol–Gel Processing of a Membrane Layer

Sol−gel processing can be done via three different synthetic methods: the *silica polymers*, *particulate-sol*, and *template* methods.[221] The *silica polymers* route involves the hydrolysis and condensation of alkoxysilane precursors, such as tetraethyloxosilane (TEOS), under controlled conditions.[211−214] Furthermore, de Lange showed ultrathin 60 nm microporous membranes with pores of 0.5−0.7 nm. Gas transport was activated for H_2 (E_{act} = 21.7 kJ/mol) and molecular sieve-like separation factors of 200 for mixtures of H_2/C_3H_6 at 260 °C.[195] The *particulate-sol* route is based on the packing of nanoparticles to make a highly porous structure.[215−217] Silica particles of different sizes are packed into the support substrate to process membranes with different pores sizes. Added binder material or hierarchical size packing aids in packing the particles to avoid defects. The *template* route uses organic molecules as templates in the sol matrix that are burned out upon calcination. The organic molecule's size and shape can be imprinted in the sol for a tuned porosity. Surfactants, organic ligands, and polymers have been reported as templates (Figure 3).[218−221]

Silica membranes by sol−gel deposition are made by dip-coating an aqueous silica polymer sol on a mesoporous support surface, followed by drying and calcination at 400 < T < 800 °C.[222] The silica polymers are formed by acid-catalyzed hydrolysis and polymerization at p_H < 7 of TEOS and MTES.[275] Reaction parameters such as time, temperature, pH, and mixing must be closely controlled in all stages of the process.[223] However, the effect of these parameters on the final microporous structure is limited. The micropores in sol−gel silica are likely formed around original solvent molecules such as H_2O and C_2H_5OH. Examples of predesigned templating have been reported with other alcohols,[224] HTEAB,[225] and methacryl oxypropyl trimethoxy silane.[226] Amorphous silica contains many "nonbridging" Si−O bonds that surround the micropores. These are normally terminated with protons to form Si−OH, but introduction of MTES before hydrolysis results in the formation of Si-CH_3-terminated groups.[227] The latter makes the structure more stable and more open. The terminal groups gradually disappear upon heating by condensation and carbonization below 600 °C, and a "dense" silica structure is formed at 800 °C. In ref 228 an alternative to the sol−gel method is reported, where polysilazane was spin coated, cross-linked in N_2 at 270 °C, and pyrolyzed in air at 600 °C.

3.1.2. Chemical Vapor Deposition (CVD) of a Membrane Layer

CVD methods to prepare a membrane on a porous substrate are classified into two types, based on the supplying configuration of the precursors.[197,198] In the first type, the precursors are provided from one side of the substrate[188,201] while the other side of the substrate is usually vacuumed to obtain a pinhole-free membrane.[205] Prabhu and Oyama[187,190] reported that a stable silica membrane was prepared by CVD treatment at 600 °C. However, hydrogen permeance was less than 1.8×10^{-8} mol/(m^2 s Pa).

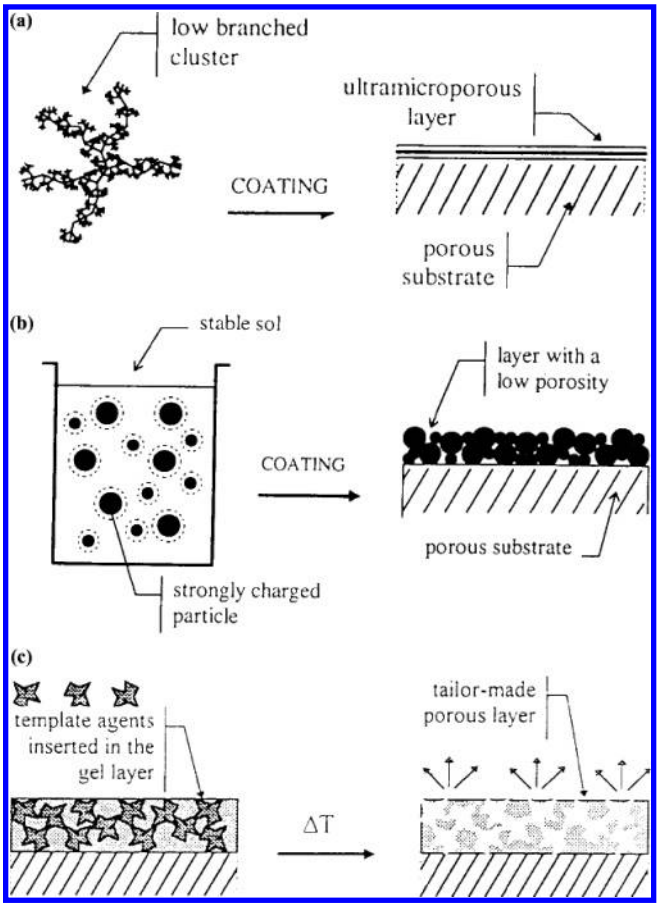

Figure 3. Schematic of the three important sol−gel routes used for preparation of microporous membranes.[246,299] (Reprinted with permission from ref 246. Copyright 2002 Taylor & Francis Group, LLC, http://www.taylorandfrancis.com.)

The second method is counterdiffusion CVD, where two kinds of reactants are supplied from the opposite sides of the substrates.[197,200−202,206] Pore sizes and effective membrane thickness can be controlled by changing reactants and reaction conditions. One of the first gas-phase methods to be developed was generation of a silica-modified membrane by a high temperature atmospheric CVD process on Vycor glass.[188,247] The new membrane (Nanosil) showed unprecedented selectivity to hydrogen (100%), without loss of permeability compared to the porous Vycor precursor. The membrane also showed high stability under hydrothermal conditions over prolonged times. Contrary to various other silica membranes, this Vycor membrane showed high stability under hydrothermal conditions over prolonged times. In particular, the membrane was used in a catalytic reactor with 1% Rh/Al_2O_3 for the dry reforming of methane. Conversions were higher than those in the bulk packed-bed reactor. The incorporation of the inorganic membrane into the catalytic process resulted in the circumventing of thermodynamic limitations normally found in the bulk process.

Other CVD methods use simple thermal decomposition[186] or oxidation of the precursor with oxygen or ozone within similar temperature ranges.[229]

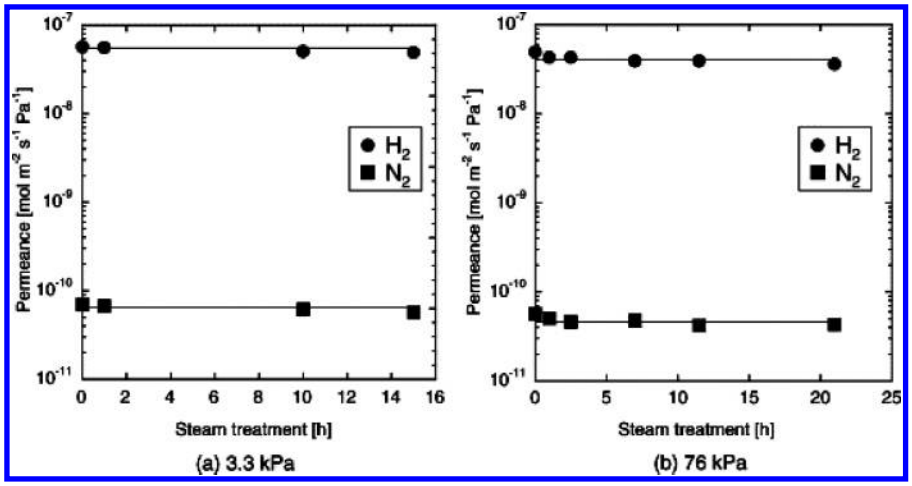

Figure 4. Steam stability for a silica membrane prepared at 600 °C.[199] (Reprinted from ref 199, copyright 2005, with permission from Elsevier.)

Nakao et al. reported silica membranes having an excellent H_2/N_2 permeance ratio (about 1000).[231] They were obtained on porous γ-alumina substrates by the counterdiffusion CVD method using a TMOS/O_2 system at 600 °C. This membrane was stable under 76 kPa of steam vapor at 500 °C for 21 h without any reduction in the H_2/N_2 permeance ratio. This membrane can be applied for H_2 production from the steam reforming of methane, because 76 kPa of steam vapor at 500 °C is one of the target conditions for the H permselective membrane reactors of the reaction (Figure 4). The reaction species at 500 °C of the counterdiffusion CVD method was confirmed as TMOS/O_2 by comparing the permeation results of thermal decomposition of TMOS, the TMOS/O_2 system, and the TMOS/O_3 system. The activation energy of H_2 was ~20 kJ/mol through the membrane. The H_2 permeance of the 600 °C permeation test was 1.5×10^{-10} mol/(m^2 s kPa). The H_2/N_2 permeance ratio was kept for 21 h under the typical steam-reforming conditions of methane for a membrane reactor (76 kPa of steam at 500 °C). The silica membrane was damaged by the heat treatment at higher than the deposition temperature. The membrane should be prepared at higher temperature than the application temperature.

3.2. Preparation

There are a variety of coating methods commonly used and continuously optimized for making thin films of silica membranes. For an overview, see ref 6. In *dip-coating*, a support is contacted briefly with a sol or dispersion. Film formation occurs by two mechanisms: slip-casting and film-casting. In *slip-casting*, the dispersion liquid penetrates into the support under the action of capillary forces. The dispersed particles (polymers) form a dense-packed film on the surface while dissolved additives disappear into the support. In *film-coating*, a dispersion layer is formed on the slip cast layer and maintained by surface tension. To avoid the frequently present defects in *dip-coating*, researchers need to avoid airborne contamination, agglomeration, and particulate contamination *during* synthesis, and microbubbles by controlling shear, ultrasonic treatment, and additives. Finally, particulate contamination needs to be removed after synthesis by screening or centrifugation.

The effect of connected coating defects is often diminished by application of two or more coatings. This approach, however, does not work for surface defects in the support, and it may affect the operational lifetime due to excessive layer thickness and delamination. The silica membranes are repaired by impregnation with TEOS ethanol, followed by thermolysis.[230] CVD methods have also been proposed to repair residual connected defects in wet-chemical layers.[231]

3.3. Intermediate Layers

Intermediate layers are prepared by dip coating of nanoparticle dispersions, followed by drying and calcination. Typical compositions include transition aluminas, silica, and zirconia. Precursor particles are made by precipitation from simple salt solutions or hydrolysis of organo-metal reagents. To obtain homogeneously packed layers with little shrinkage, it is important to control particle agglomeration during synthesis and to remove any agglomeration after synthesis. A well-known synthesis of γ-alumina layers starts with hydrolysis of ATSB at 90 °C, followed by HNO_3 addition, resulting in the partial dissolution of the Boehmite precipitate and redispersion of agglomerates.[230] The HNO_3 addition also ensures colloidal charge stabilization by preferential proton sorption. The hydrolysis/peptization method has a favorable yield but suffers from the presence of residual agglomerates. The agglomerates can be removed by high-*g* centrifugation,[232] which leads to stable and homogeneous layers. Sonochemical and modified emulsion precipitation methods help avoid formation of the agglomerates. More recently, methods were developed in which agglomeration is completely avoided up-front, such as sonochemical and modified emulsion precipitation.[233,234] Intermediate layer formation from a nanoparticle dispersion is often assisted by additions of linear chain polymers such as PVA to the dispersion or by pretreatment of the support with polymers to minimize penetration. An example includes the repair of a commercial supported γ-alumina membrane by dip-coating with a Boehmite precursor nanoparticle dispersion.[235]

3.4. Support

A variety of methods for fabricating support layers have been employed. One common method is the dip-coating of agglomerate-free submicron particle dispersions, made from commercially available α-Al_2O_3 powers. Colloidal stabilization can be adjusted such that coherent dense-packed layers are formed with 25 nm surface roughness after slight sintering at temperatures around 1000 °C.[222] Other methods result in thicker support layers and include colloidal filtra-

tion[222] and centrifugal casting,[236] resulting in high strength, excellent surface properties, and roundness of the tubes. These structures can also be considered for applications where $f^{K_n}_{H_2,l} < 10^{-8}$ mol/(m^2 s kPa) is acceptable.

Carrier structures are generally made with conventional ceramic forming methods using commercially available, coarse α-Al_2O_3 powders. *Dry-pressing* is used to make small disks for research purposes. *Extrusion* is used for tubes and multichannel honeycomb structures.[237,238] These forming methods are very suitable for fairly cheap mass-scale production but have limited near-net-shape capabilities. Nonroundness and other dimensional limitations may result in sealing and construction problems in high-temperature membrane reactors. It is for this reason that gel-casting methods[239] are also considered. Such methods allow for a higher initial solid load, better control of overall homogeneity during forming, and, hence, better dimensional specifications. The large pore diameter requires very high sintering temperatures and may result in poor mechanical strength and reliability. This problem might be addressed by application of wet-chemical techniques such as phosphate bonding,[240] which provides thermochemical stability up to 900 °C.

3.5. Modification

An extension of the silica membranes work is the metal-coated silica systems.[208] Al-coated SiO_2 permselective membranes have been studied and reported.[188] They are prepared by chemical vapor deposition of a thin SiO_2 layer on a porous alumina substrate, resulting in a noncontinuous network of solubility sites. The submicron thick silica-on-alumina composite membranes utilize size gradation in their layering, allowing for enhanced permeability for hydrogen over CO_2, N_2, CO, and CH_4. However, silica modified membranes developed by several researchers suffer from loss of permeability (as much as 50% or greater in the first 12 h) on exposure to moisture. This has been attributed to the removal of Si−OH groups leading to the formation of Si−O−Si bonds which close pore channels.[241] This phenomenon is termed densification. Moisture catalyzes this reaction, particularly at higher temperatures.[242] Densification not only leads to lower permeability but also causes embrittlement of the silica film that compromises selectivity.

3.5.1. Silica Membrane Modification

In order to improve the stability of silica membranes in steam, inorganic oxides, such as TiO_2, ZrO_2, Fe_2O_3, Al_2O_3, NiO, etc., were added to silica.[239,243,244] Aseada et al. have shown the Ni-doped silica membranes exhibited relatively high H_2-permeance and high stability against water vapor at 35−300 °C,[242] suggesting the effectiveness of the addition of nickel oxides to silica for the membrane stability against steam at higher temperatures. The Ni-doped silica membranes[242] were fabricated in this work by the sol−gel techniques under various conditions of Ni contents and firing temperatures. The H_2-selective permeation characteristics and hydrothermal stability of the membranes were tested in steam at 500. The hydrothermal treatments of the membranes before exposure to H_2 were quite effective to prevent the further densification of Ni-doped amorphous silica networks. This is due to reduction in H_2 and sintering in steam (500 °C, 70 kPa). Ni-doped silica membranes (Si/Ni = 2/1) fired in the steamed atmosphere (partial pressure: 90 kPa) at 650 °C, for example, were found to show an asymptotic steady

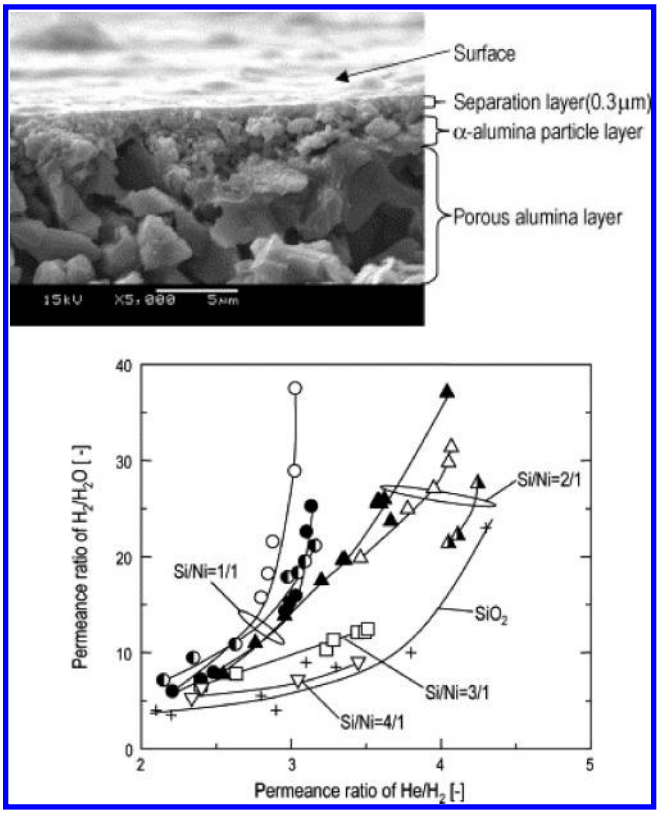

Figure 5. (a) Cross section of a Ni-doped silica membrane (Si/Ni = 2/1). (b) Observed permeance ratio of H_2/H_2O vs the permeance ratio of He/H_2 for nine membranes (Si/Ni = 0−1/1) at 500 °C. (Reprinted from ref 244, copyright 2006, Elsevier.)

Table 9. Reported Values of High-temperature Hydrogen Permeation and Separation through Silica Membranes[237]

prep method	measurement temp (°C)	H_2 permeation (mol/m^2·s·kPa)	separation	ref
CVD	400	4×10^{-10}	$H_2/HBr = 1000$	480
CVD	427	6×10^{-10}	$H_2/N_2 = 160$	480
CVD	600	1.8×10^{-10}	$H_2/CH_4 = 4200$	187
sol−gel	300	1.3×10^{-9}	$H_2/CH_4 = 150$	217
sol−gel	350	2.2×10^{-9}	$H_2/CH_4 = 35$	481
sol−gel	600	2.5×10^{-9}	$H_2/C_3H_8 = 75$	482
sol−gel	500	2.6×10^{-10}	$H_2/N_2 = 87$	483
CVD	500	1.3×10^{-10}	$H_2/N_2 = 2300$	199

permeance for He and for H_2 with a high selectivity of 1450 (He/N_2) and 400 (H_2/N_2) even after being kept in steam (steam: 90 kPa) at 500 °C for about 6 days. The permeance ratio of H_2/H_2O was found to be dependent not only on the permeance ratio of He/H_2 (Figure 5) but also on the Ni content, while the maximum permeance ratio observed at 37 for a Ni-doped silica membrane (Si/Ni = 1/1).

The silica membranes shown in Table 9[237] have excellent separation performance for hydrogen and helium in dry conditions in a wide temperature range, 50−600 °C. Their stability against water or water vapor, however, is rather poor at high temperatures or even at room temperature.[188,221,226,241,245,246] Separate measurements have shown that H_2 gas permeation available with the present silica membrane system has a maximum value of 5×10^{-9} mol/(m^2 s kPa). This value was around 50% of the H_2 permeation of the γ-alumina membrane layer under the same measurement conditions. The permeation through the support substrate was therefore considered as the major resistance for gas permeation. An increase in gas permeation of the substrate by increasing the porosity or by reducing the thickness of the

substrate should not be difficult. Yet, retaining the strength of the support substrate is important for membrane reactor applications, where a thermal gradient exists between the inlet and other parts of the reformer.

3.5.2. Membrane Structure Modification

The most popular configuration of these membrane systems is a three-layer asymmetrical structure[247] with an α-alumina-based substrate and a γ-alumina-based intermediate layer as supports for the top coated silica microporous layer. Though the structure is simple, the smaller particle size of γ-alumina mostly limits the pore size of the alumina substrate. The resultant permeation of the system is limited due to the large resistance of the support substrate.

Nair in ref 237 recently reported a four-layer membrane; the thickness of the γ-alumina membrane could also be reduced because of the better surface smoothness of the dip coated α-alumina intermediate layer compared to the extruded substrate, which normally supports the γ-alumina layer in the three-layer configuration. In this configuration, the intermediate support layer was made from α-alumina particles of average size 300 nm. These alumina particles were made into a water-based slurry. Alumina tubular substrates were dip-coated with this slurry and sintered at 1077 °C to make intermediate layers. The slurry was also dried (and in some cases powdered and pressed into pellet form) and heat-treated to make samples for characterization of pore size, porosity, and thermal expansion properties. They conclude that the pore size of the membrane is probably the easiest and most trouble-free way of improving the gas permeation of the substrate while retaining its strength, stability, and durability.

3.6. Operational Stability

The microporous silicas are very promising due to their low cost, high stability, and high permeance.[226] Systematic studies of the operational stability of supported membranes with good zero hour properties are scarce. The micro- and mesoporous structures used for the membranes and intermediate layers have a very high surface area, which means that further densification, phase transformations, and structural disintegration may occur at elevated temperatures and steam pressures. Rapid pressure fluctuations may lead to disruptive tensile stresses in the interfaces between the layers.[247]

In a recent review by Verweij et al.,[247] different studies were described regarding optimization of silica membranes for enhanced operational stability.[248] Supported silica membranes are affected by the delamination and structural instability of the intermediate layer. As described in ref 252, the formation of macrodefects in the γ-alumina layer was found after 23 h at 475 °C and a partial pressure of H_2O of 40 kPa. Further studies showed partial delamination of γ-alumina after a 100 h steam reforming treatment.[227] The instability of the γ-alumina layers is ascribed to poor adhesion in combination with structural densification. The latter, in turn, is caused by γ-alumina packing defects and sintering. These phenomena are confirmed in a recent study of the stability of a tubular four-layer structure.[237] It was also shown that these problems can be addressed by improving adhesion by phosphate bonding and γ-alumina surface modification with La_2O_3. Improvements in the γ-alumina packing homogeneity as demonstrated in ref 236 are also expected to result in less shrinkage and better adhesion. In refs 249 and 252, the stability is reported on sol−gel silica membranes in synthetic reformate: H_2O:H_2:N_2:CO_2:CO = 34:28:24:8:6 at 200 °C and a total pressure of 200 kPa. These fairly mild conditions likely did not lead to any significant intermediate layer degradation. It was found that membranes made with HTEAB (hexyl triethylammonium bromide) templating were more stable than conventional sol−gel membranes. They exhibited a gradual decline of total flux for H_2, but that effect could be undone by regeneration at 500 °C in air. The conventional sol−gel membranes showed a similar decline but could not be regenerated.

Amorphous silica is emerging as a valuable material for H_2 production membranes as long as the operational stability can be optimized. The thermochemical stability of the membrane and the intermediate layers is probably best if their thickness remains well below 1 μm. This limits the build up of stresses due to (dynamic) thermal expansion differences. The current cost price of lab prototypes indicates that dramatic cost reductions are needed to realize viable membrane designs. These reductions might be realized by replacing conventional synthesis and ceramic firing by rapid processing methods, instead of sintering for support and carrier structures. Wet-chemical deposition of films provides favorable cycle times but requires supports with excellent surface quality. The occurrence of structural defects remains a major source of irreproducibility and poor performance. Further defect minimization requires characterization of the overall *and* local defect population by any of the application methods.

Amorphous silica shows primarily a structural densification that is determined by the presence of terminating groups and temperature, as discussed before. There is little evidence that this process is influenced by modest steam pressures. Optimization of the industrial processes to lower pressures, plus taking into account the chemical stability of the amorphous silica, will enable widespread industrial use of these materials as membranes.

4. Zeolite Membranes

Much effort has recently been devoted to the synthesis and potential application of inorganic membranes in the domains of gas separation, pervaporation, and reverse osmosis or in the development of chemical sensors and catalytic membranes. Inorganic membranes, which have good thermal stability and chemical inertness, have advantages over polymer membranes for many industrial applications. Improved membrane integrity and manufacturing costs are constant factors which are the focus of many research efforts. Zeolite membranes, in particular, combine pore size and shape selectivity with the inherent mechanical, thermal, and chemical stability necessary for continuous long-term separation processes. The effective pore size distribution of the zeolite membrane, and hence its separation performance, is intrinsically governed by the choice of the zeolitic phase(s). This applies when molecular size exclusion sieving is the dominant mechanism and no other diffusion pathways bypass the network of well-defined zeolitic pores/channels; otherwise, viscous flow through grain boundaries prevails. The optimum thickness of the zeolite film is always a compromise between separation performance and overall trans-membrane flux and is often tailored to the specific needs of the envisioned application.

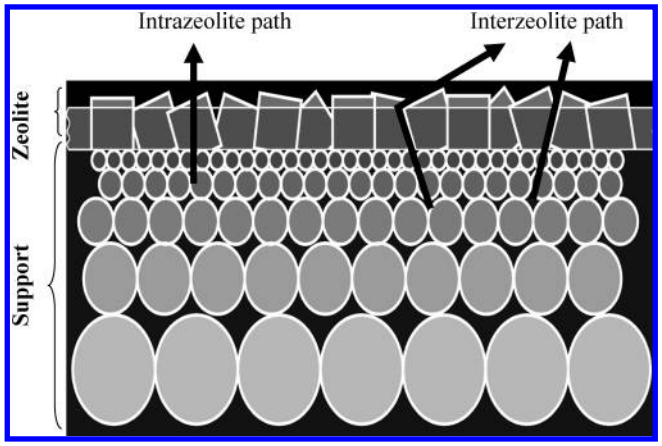

Figure 6. Not-to-scale representation of a zeolite membrane on a nonselective oxide support (ie., Al_2O_3), showing possible permeation pathways, either interzeolite crystals or intrazeolite crystals.

Zeolites are crystalline inorganic framework structures that have uniform, molecular-sized pores. They have been used extensively as bulk catalysts and adsorbents. The zeolite structure is made up of TO_2 units, with T = a tetrahedral framework atom (Si, Al, B, Ge, etc.). In all cases other than neutral silica zeolite frameworks, the net overall charge of the framework is negative and is charge balanced by cations (either inorganic or organic). The cations reside in the pores of the framework; the size of the pore is catagorized by the number of T atoms in that ring. Small-pore zeolites include those structures made up of eight-member oxygen rings, medium-pore zeolites have 10-member rings, and large-pore zeolites have 12-member rings.[250] More recently, membranes of continuous polycrystalline zeolite layers have been deposited on porous supports. The first zeolite membranes were reported in 1987,[251] and since then, significant progress has been made to expand the types of zeolites utilized in membranes, improve membrane quality, and widen their range of applications. Today, more than 14 zeolite structures, including MFI,[252−260] LTA,[261−263] MOR,[264−266] and FAU,[267−270] have been employed as H_2 selective separation membranes. The MFI structure is typically used in zeolite membranes because of its pore size and ease of preparation, and this structure includes silicalite-1 and ZSM-5. Silicalite-1 is made up of pure silica, and ZSM-5 has Al substituted for some of the Si atoms.

Significant progress has been made in developing new membranes, optimizing their synthetic preparation, and understanding transport and separation fundamentals over the past decade. Several reviews of zeolite membranes[243,246,250,271−282] have focused mainly on membrane synthesis and gas separation applications. This progress suggests that many applications of zeolite membranes in commercially valuable enterprises, such as separations, are promising. Gas and liquid separation on zeolite membranes is primarily governed by competitive adsorption and diffusion mechanisms. When the zeolite pore size distribution falls between the molecular sizes of the feed components, a size exclusion mechanism can dominate the separation process.[225,283] However, one of the main challenges in zeolite membrane development is the minimization of intercrystal pores formed inherently in polycrystalline zeolite films (see Figure 6). The existence of intercrystal pores with sizes larger than the zeolitic pores is the major cause for decline in molecular separation efficiency.[231] The elimination of intercrystalline pores is essential for having high separation selectivity viable for industrial applications. Currently, research is ongoing to resolve the intercrystalline diffusion path issue by using mixed matrix membranes. Readers are directed to refs 284 and 285 for further information on this area.

4.1. Membrane Growth Methods

Syntheses of zeolite membranes, described recently, can be broadly classified into two categories: *in situ* and secondary (or seeded) growth.[286,287] In the *in situ* technique, the support surface is directly contacted with an alkaline solution containing the zeolite precursors and subjected to hydrothermal conditions. Under appropriate conditions, zeolite crystals nucleate on the support and grow to form a continuous zeolite layer. At the same time, reactions occurring in the solution lead to deposition of nuclei and crystals on the surface followed by their incorporation into the membrane, thus minimizing intercrystal pore contributions. MFI films grown *in situ* may exhibit a preferred orientation that depends on the synthetic protocol and associated interplay of nucleation and growth phenomena.[286] However, because of the insufficient understanding of nucleation and growth processes in hydrothermal systems, the success of *in situ* methods in yielding uniformly oriented MFI films is limited.

In the secondary (or seeded) growth technique, zeolite nucleation is largely decoupled from zeolite growth by depositing a layer of zeolite seed crystals on the support surface prior to membrane growth. The layer of seed crystals can be deposited with precise control over which crystallographic axis is oriented perpendicular to the support (see Figure 7).[225] The seeded surface is then exposed to the membrane growth solution and hydrothermal conditions, whereupon the seed crystals grow into a continuous film. Although this method offers greater flexibility in controlling the orientation of the zeolite crystals and the microstructure of the zeolite membrane (since it decouples nucleation from growth), it is done so at the expense of additional processing steps. In principle, the orientation and morphology of the membrane can be manipulated by changing the morphology and orientation of the deposited seed layer and then performing secondary growth under appropriate conditions.

4.2. Permeation and Gas Transport

The following five-step model can be used to describe the gas-molecule transport through a zeolite membrane:[288,289] (1) adsorption from the bulk phase to the zeolite external surface; (2) diffusion from the surface to the inside of the zeolite channels; (3) diffusion inside the zeolite channels; (4) diffusion from the zeolite channel to the external surface; and (5) desorption from the external surface to the gas phase. The actual mechanism of gas permeation through an MFI-type zeolite membrane depends on the gas adsorption properties on the zeolite. For nonadsorbing gases, molecules may directly enter the zeolite pores from the gas phase. The separation factor of a nonadsorbing gas mixture is determined by the mobility of the molecules inside the zeolite pores and the probability of the molecules entering the zeolitic pores.[256] Gas molecules with small size and high mobility tend to permeate through the zeolite membrane, while those with larger size and lower mobility tend not to permeate. For strongly adsorbing gases, permeation through an MFI membrane is controlled by either adsorption or activated diffusion, or both, depending on the operation conditions

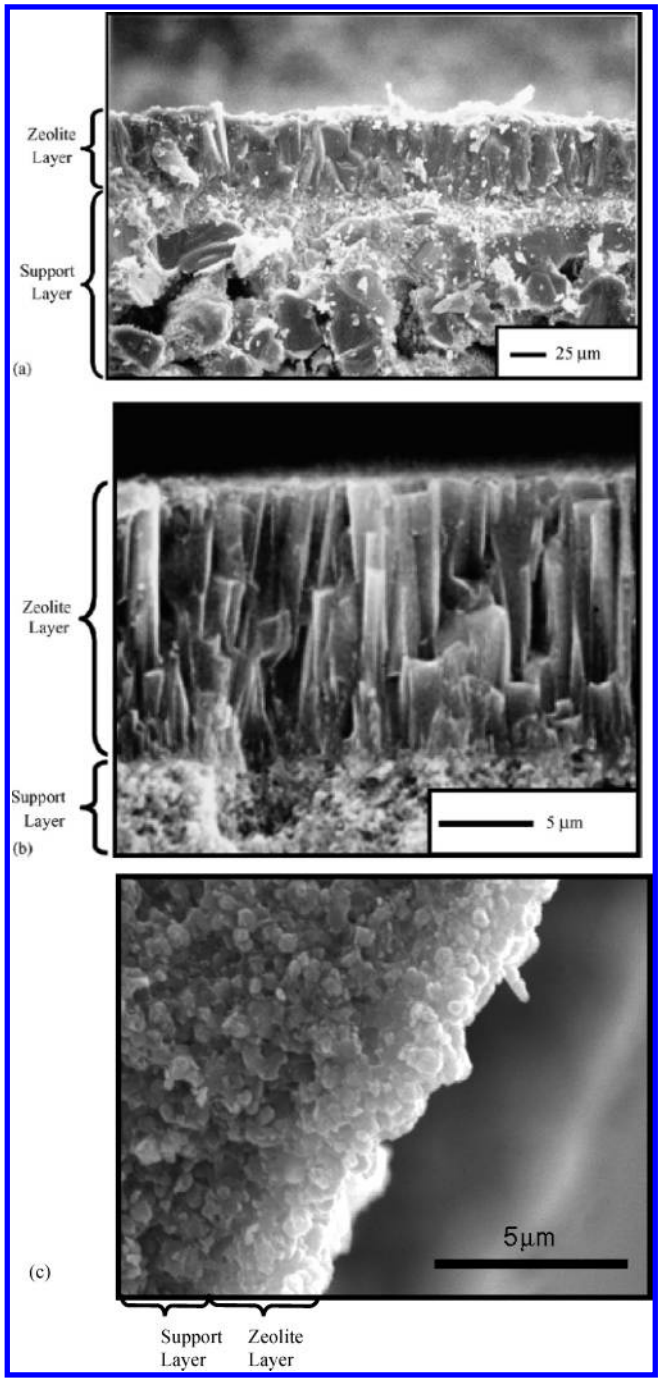

Figure 7. Cross-sectional SEM photographs of (a) a nonoriented B-ZSM-5 zeolite membrane on an α-Al_2O_3 coated SiC porous support;[192] (b) an oriented silicalite-1 membrane on a silica coated α-Al_2O_3 porous support[223] (Part b is from ref 225 (http://www-.sciencemag.org). Reprinted with permission from AAAS.); and (c) a nonoriented silicalite-1 MFI membrane on tubular α-Al_2O_3 substrates (Pall Corp., New York).[241]

(temperature and pressure) on both sides of the membrane. The maximum value of flux with respect to temperature can be observed for strongly adsorbing gases, because the apparent activation energy is the sum of adsorption heat (negative) and diffusion activation energy (positive).[257,289] The temperature of maximum flux increases with the adsorption strength of the substance.[252] For permeation of binary gas mixtures, when both components are nonadsorbing, the separation factor is α:

$$\alpha = \frac{(y_1/y_2)_p}{(y_1/y_2)_f} \quad (5)$$

The separation selectivity, α, is defined as the enrichment factor of one component in the permeate as compared to the feed composition ratio, where y_1 and y_2 are the mole fractions of components 1 and 2, respectively, and the subscripts p and f refer to the permeate side and feed side, respectively.[289] When one or two strongly adsorbing components are involved, there is no correlation between the permselectivity and the separation factor. For gas mixtures containing strongly adsorbing components, the separation factor strongly depends on the operation conditions, that is, temperature and pressure.[289] Molecular simulations and Maxwell−Stefan (M−S) modeling of multicomponent diffusion through zeolite pores indicate that, in some mixtures, slower larger molecules inhibit the diffusion of faster smaller molecules.[290,291] In addition, detailed studies by several groups have been reported over the last 5 years[292−296] and reviewed by Sholl last year.[297]

4.3. Defect Site Diffusion/Nonzeolitic Pores

Polycrystalline zeolite membranes contain transport pathways within the intercrystalline regions, or nonzeolite pores. The synthesis procedure, the type of zeolite, and the calcination conditions affect the number and size of the nonzeolite pores. Molecules which interact with nonzeolite pores have different adsorption and diffusion properties from those in zeolite pores. The differences, however, are difficult to quantify because of the irregularities in both shape and size of the nonzeolite pores. Usually, only nonzeolite pores that are larger than the zeolite pores are considered, but nonzeolite pores have a size distribution and pores smaller than the zeolite pores may also affect flux and selectivity.[254] Transport through nonzeolite pores that are larger than zeolite pores has contributions from both surface diffusion and Knudsen diffusion, and it might also have viscous flow contributions. Knudsen diffusion requires that the pores are smaller than the mean free path of the diffusing molecules.[298] Viscous flow requires a pressure gradient across the membrane and sufficient interactions between diffusing molecules that their motions are driven by the pressure gradient.[299]

4.4. Thin Films

Recent advances in preparing thin zeolite membranes have dramatically increased gas permeation fluxes while maintaining good selectivities. Recently, ultrathin silicalite-1 membranes with a thickness of 0.5 μm were made, and they had light gas fluxes that are 1 to 2 orders of magnitude higher than those of other silicalite-1 membranes reported in the literature.[253] In another report, Lai et al.[225] prepared 1 μm thick oriented silicalite-1 membranes that performed significantly better for xylene isomer gas-phase separations than previously reported membranes. They obtained *p*-/*o*-xylene separation factors as high as 500 with a permeance of 2×10^{-7} mol/(m^2 s Pa) at 200 °C.

4.5. Zeolite Membrane Modification

In an effort to further improve zeolite membranes, surface modification techniques have been developed by a number of research groups.[71] The majority of the techniques are post-

treatment methods that include inorganic silylation to decrease pore size[300] and to increase hydrophobicity[301,302] and defect treatments to fill nonzeolite pores by chemical vapor deposition (CVD),[283] atomic layer deposition (ALD),[303] or coking.[304,305] Recently, we (Nenoff et al.) reported on a new method of online membrane modification by carbonization of 1,3,5-triisopropylbenzene in the feed stream, which was found to be effective for reducing the MFI intercrystalline pores and improving the P_X separation (see Figure 7c).[306] For an eight-component mixture containing hydrogen, methane, benzene, toluene, ethylbenzene (EB), P_X, M_X, and O_X, a $P_X/(M_X + O_X)$ selectivity of 7.71 with a P_X flux of 6.8×10^{-6} mol/(m^2 s) was obtained at 250 °C and atmospheric feed pressure (87 kPa).

The silylation method of modifying the effective pore opening of a zeolite was first reported by Masuda et al.[300] In this method, methyldiethoxysilane (MDES) compounds are preadsorbed on active sites within the MFI zeolite, and then they are catalytically cracked, leaving coke that contains Si atoms on the active sites. After calcination, mono-SiO_2 units are formed on active sites, thereby reducing the size of the pores. After the silation modification of the membrane, a mixture of varying gas ratios of H_2/N_2 was tested (fraction of H_2 in retentate gas: $H_2/(H_2 + N_2) = 0.2-0.8$; 110 °C, 101.9 kPa steady-state pressure). The separation factor of H_2 was calculated at 90−140 for the treated membrane. This is about 50 times larger than that of the fresh membrane (1.5−4.5). Similar results were obtained for mixture gases of H_2 and O_2 (separation factor = 110−120).[300]

This method was borrowed and applied[307] to modification of B-ZSM-5 and SAPO-34, whose pores are approximately 0.4 nm and, thus, too small for the silyation compound to penetrate. The MDES reacted in the B-ZSM-5 pores and reduced their effective pore diameter, and their H_2 selectivity greatly increased. The H_2/CO_2 separation selectivity at 473 K increased from 1.4 to 37, whereas the H_2/CH_4 separation selectivity increased from 1.6 to 33. Though silylation decreased the H_2 permeances in the B-ZSM-5 membranes, at 673 K, the H_2 permeance increases and the H_2/CO_2 separation selectivity was 47. In contrast, MDES does not fit into SAPO-34 pores, but silylation apparently decreased the pore size of the nonzeolite pores in the SAPO-34 membranes. After silylation, the H_2 permeances and H_2/CO_2 and H_2/N_2 separation selectivities were almost unchanged in the SAPO-34 membranes because H_2, CO_2, and N_2 permeate mainly through SAPO-34 pores. In contrast, the H_2/CH_4 separation selectivity increased from 35 to 59, and the CO_2/CH_4 separation selectivity increased from 73 to 110, apparently because CH_4 permeates mainly through non-SAPO-34 pores.

The synthesis of small-pore zeolite membranes has also been pursued for the separation of small light gas molecules. Zeolite A membranes have shown H_2 permeances ranging from 10^{-10} to $<10^{-11}$ mol/(m^2 s kPa), with a maximum of H_2/N_2 separation selectivity of 4.8 between 35 and 125 °C.[262] Changes in the charge balancing cation result in changes in the H_2 permeance and followed the order of K < Na < Ca, which is consistent with the order of the pore size of the A zeolite.[308] The highest H_2/N_2 separation selectivity of 9.9 was obtained for a KA membrane. For $AlPO_4$-5 membranes (pore size of 0.73 nm), the H_2 permeance was 2×10^{-10} mol/(m^2 s kPa) at 35 °C.[309] The H_2/CO_2 ideal selectivity (α_{H_2}, CO_2) was 24, and the separation selectivity for an equimolar H_2/CO_2 mixture was 9.7 at 35 °C.

More recently, we (Nenoff et al.) explored using zeolite membranes for the separation of hydrogen from multicomponent reforming streams.[310−312] Using methods developed by Dong et al.,[185] we synthesized silicalite-1 membranes and tested their H_2 separation abilities with varying temperatures (70−300 °C) and feed compositions.[313] The composition of the dry stream was H_2, CO_2, CO, CH_4, and H_2S in the ratio 70.8:8.7:5.79:14.69:0.03; the wet stream was H_2, CO_2, CO, CH_4, H_2S, and H_2O in the ratio 50:10:6:4:0.02:30. At lower temperatures in both experiments, H_2 had low permeation due to pore blockage by adsorbing components such as H_2O, CO_2, CH_4, and CO. H_2 permeance increased with temperature throughout the range 70−300 °C with a separation factor varying from 0.13 to 0.4. However, the H_2 separation value for the five-component stream increases to 2 when water is not included, with permeances around 3×10^{-11} mol/(m^2 s kPa).

4.6. CO_2 Sequestration in H_2 Separations

CO_2 separation is one of the most studied applications for FAU-type zeolite membranes[314,315] due to its significance, such as CO_2 capture for carbon sequestration, natural gas purification, and separation of product streams from water-gas-shift (WGS) reactions for hydrogen production, to name a few. We (Dong and Nenoff et al.) investigated FAU membranes for the purification of CO_2 from 50/50 mixtures of CO_2/N_2 under dry and moist conditions in the temperature range 23−200 °C at atmospheric pressure.[316] At room temperature, the CO_2 selectivity was about 31.2 for the CO_2/N_2 dry gas mixture with a CO_2 permeance of 2.1×10^{-11} mol/(m^2 s kPa). The addition of water to the stream significantly enhanced the CO_2 selectivity at 110−200 °C but drastically lowered the CO_2 selectivity below 80 °C. At 200 °C, with increasing water partial pressure, the CO_2 selectivity increased and then decreased after reaching a maximum of 4.6 at a water partial pressure of 12.3 kPa.

In another study, Noble and Falconer have shown that their silica/aluminophosphate (SAPO-4) zeolite membranes can be made and used to separate CO_2 from CH_4 under a variety of pressures and temperatures, with high selectivities at 3.04 MPa and 50 °C.[317] Permselectivity for H_2 by zeolite membranes from more complex eight-component simulated refinery gas steam has also been reported.[185] The steam included hydrogen (≈84 mol %) and light hydrocarbons (C_1-C_4, 7.5−0.3 mol %). An α-alumina-supported polycrystalline MFI zeolite membrane was tested between 25 and 500 °C and at feed pressures of 0.1−0.4 MPa. The zeolite membrane showed excellent separation properties for rejection of hydrogen from the hydrogen/hydrocarbon mixture at <100 °C. At room temperature and atmospheric pressure on both feed and permeate sides, the hydrogen permeation rate is almost zero, while the hydrocarbon permeation rate is $2-4 \times 10^{-7}$ mol/(m^2 s kPa). At 500 °C, the zeolite membrane becomes permselective for hydrogen over hydrogen (C_1-C_4), with a separation factor over 3.

4.7 Manufacturing

Zeolite membrane manufacturing is still an industry in the making. Most membranes are still fabricated in lab scale sizes and quantities. Furthermore, the technology needs to be able to commercialize large-scale continuous films without in-

tercrystalline pores for successful high separation selectivity. However, recently, there has been a big leap forward in the commercialization of this technology. Currently, only Mitsui Engineering and Shipbuilding Company in Japan has commercialized a process using zeolite membranes.[282] It is a pervaporation process using NaA zeolite membranes for organic dehydration. The membranes are 20−30 μm thick on porous, tubular ceramic supports. The plant processes alcohols up to 530 L/h with separation factors up to 10,000. Manufacturers of zeolite membranes listed by Bowen et al.[282] include Smart Chemical Co., Ltd and Christison Scientific, both in the U.K., and Artisan Industries Inc., USA.

Current estimated costs per zeolite membrane gas separation module have been approximated around \$400/ft^2. Though this is an estimate, it compares favorably with metal membranes and modules ($\approx$ \$1500/ft^2).[318] It is safe to assume that, once in mass use and production, those costs will decline significantly to about \$100/ft^2, allowing zeolite membranes to compete both in economics and on performance.

Significant progress has been made in the synthesis or various types of crystalline zeolite membranes. Good quality zeolite membranes can be prepared by several methods, including *in situ* synthesis, secondary growth, and vapor-phase transportation. To be considered useful for gas separations applications, these membranes will have to be synthesized without macropore-sized defects or pinholes. Furthermore, the ability to surface modify zeolite membranes (both internal pore surfaces and external surfaces) through silation or carbonization allows for the fine-tuning in selectivity. Gas separations[246] through the membranes are governed by mechanisms of preferential adsorption, selectively configurational diffusion, or molecular sieving. Gas permeation through these microporous inorganic membranes is an activated process that can be predicted through gas diffusion theories (i.e., Maxwell−Stephans equations that govern gas permeation and separation).

Zeolite membranes have chemical, mechanical, and thermal stability not observed in many types of membranes. The trends in zeolite membrane research show clearly the improvements in selectivity, fabrication methodology, and energy-production applications. In the near future, the ability to inexpensively fabricate these membranes for tuned selectivity will put them at the forefront of separations technology. For the time being, their stability at high temperatures and their ability to be regenerated without loss to performance make them interesting candidates for streamlined hydrogen production via natural gas reformation.

5. Carbon-Based Membranes

Hydrogen rejection and contaminate permeation is yet another method which is being intensely explored as a new approach for H_2 purification, primarily using carbon-based membranes. Because of hydrogen's low critical temperature and small kinetic diameter, a rejective membrane process allows for H_2 purification via contaminant permeation with respect to H_2. Such rejective membranes have the very distinct economic advantage that maintaining/collecting H_2 in the retentate reduces the need for costly H_2 recompression steps, though it potentially adds a CO_2 compression step. Therefore, this may only find limited utility in certain applications, such as refinery use of H_2, where only medium or low pressure hydrogen is required. Furthermore, in 2003 a project was started by the United States Department of Energy, called FutureGen, which proposed that large amounts of CO_2 could be sequestered and ultimately removed (presumably through recompression) from coal gasification products to prevent its escape into the atmosphere.[319−321] This process would require a rejective type H_2 membrane which, unlike the selective membranes, must possess decreased H_2 diffusion but increased solubility and selectivities (Table 14).

Nonpolymer carbon-based membranes are rejective H_2 membranes that can be categorized into three classes: carbon membranes, carbon molecular sieve membranes (CMSMs), and carbon nanotubes (CNTs). The separation ability of each class of material is dependent both on the chemistry of the material and on the fabrication/implementation (ie., module design). As a result, there are serious advantages and disadvantages to each.

When compared to polymeric membranes, the cost of carbon-based membranes is 1 to 3 orders of magnitude greater per unit area. Only when they achieve higher performance than polymeric membranes is the high investment cost justified. The most popular precursor for carbon membranes is currently polyimide, which contributes largely to the high manufacturing cost. Therefore, attempts have been made to use less expensive starting materials, such as polyacrylonitrile. However, the performance of these membranes still remains inferior.[322]

Carbon membranes have been prepared in both unsupported and supported forms of materials. Typical precursors are organic polymers that are converted to pure carbon materials by treatment at high temperature in an inert atmosphere (carbonization). Among the unsupported membranes, capillary tubes or hollow fibers and flat membranes have been prepared. Supported membranes are flat or tubular and are grafted onto macroporous materials.[323] The major disadvantage with both types is that they suffer from mechanical performance problems, specifically brittleness. Brittleness presents a problem for unsupported membranes, whereas multiple polymer deposition and carbonization cycles must be repeated to obtain crack-free supported membranes. The complexity of the latter procedure presents an impediment to practical applications.

Different configurations exist for unsupported and supported carbon membranes. Unsupported membranes have three different configurations: flat (film), hollow fiber, and capillary. Supported membranes can adopt two configurations: flat and tube. Detailed descriptions of these two categories can be found in Ismail and David's review.[324] In most cases, supported polymeric membranes are produced because of the poor mechanical stability (i.e., brittleness) of unsupported carbon membranes. In making the supported carbon membranes, various options are available for coating the supports with thin polymeric films, such as ultrasonic deposition,[325,326] dip coating,[327] vapor deposition,[328] spin coating,[329] and spray coating.[330]

The six major steps in carbon-based membrane fabrication are briefly detailed in this section of the review but are more fully described elsewhere.[324] These six steps are precursor selection, polymeric membrane preparation, pretreatment of the precursor, pyrolysis process, post-treatment of pyrolyzed membranes, and module construction. The manipulation of the pretreatment variables, pyrolysis process parameters, and post-treatment conditions was shown to provide an opportunity to enhance the separation performance of carbon membranes in the future.

5.1. Carbon Membrane Preparations

Carbon membranes can be produced through the carbonization or pyrolysis process of suitable *precursor* carbon containing materials, such as thermosetting resin, graphite, coal, pitch, and plants, under inert atmosphere or vacuum.[331] Numerous synthetic precursors have been used to form carbon membranes, such as polyimide and derivatives, polyacrylonitrile (PAN), phenolic resin, polyfurfuryl alcohol (PFA), polyvinylidenechloride−acrylate terpolymer (PVDC−AC), phenolformaldehyde, cellulose, and others. A thermosetting polymer can often withstand high temperatures[332] and neither liquefies nor softens during any stage of pyrolysis. Suitable precursor materials for carbon membrane production will not cause any pore-holes or cracks to appear after the pyrolysis step.[333]

Pretreatment methods can be divided into physical and chemical methods. The *polymer membrane preparation* involves the physical pretreatments of stretching or drawing hollow fiber membranes prior to pyrolytic processing. In contrast, chemical pretreatments involve chemical reagents, which are applied to the *polymeric precursor* to alter its properties or behavior. Sometimes the precursor is subjected to repeated and varied pretreatment methods to achieve the desired properties in a carbon membrane. Perhaps the most important and popular pretreatment method employed has been the oxidation treatment.[324]

Pyrolysis, the process in which a suitable carbon precursor is heated in a controlled atmosphere to its pyrolysis temperature, is conventionally used for the production of porous carbon fibers, and it causes the product to have a microporous structure. Control over the molecular dimensions of these micropores and the subsequent molecular sieving properties is one of the primary methods being actively researched.[334] The pores vary in size, shape, and degree of connectivity, depending on the morphology of the organic precursor and the chemistry of its pyrolysis. The pore structure is essentially retained and can be controlled selectively by adjusting the various process parameters (i.e., chemical pretreatment, precursor identity, etc.).[334] While pyrolytic treatment methods do have a definitive effect on the performance behaviors of carbon membranes, the temperature is almost always between 500 and 1000 °C.[335,336]

5.2. Carbon Membrane Post-treatment

As a result of pyrolytic processing, polymeric membranes are transformed into carbon membranes with varying degrees of porosity, structure, and separation properties that depend to an extent on the carbonization conditions employed. In most cases, it is found to be an advantage that the pore dimensions and distribution in the carbon membrane can be finely adjusted by simple thermochemical treatment(s) to meet different separation needs and objectives.[331] The various post-treatment methods include postoxidation, chemical vapor deposition (CVD), postpyrolysis, and coating. These post-treatments can also repair the defects and cracks that exist in the carbon membrane.

5.3. Carbon Membrane Module Construction

The geometry and installation of a membrane in a suitable device (i.e., a module) are also important[337] to its separation abilities. The selection of a membrane module is mainly determined by economic considerations, including all the cost factors plus the cost of the module.[338] For commercial applications of membranes, it is preferable to fabricate a module with an asymmetric structure and capillary or hollow fiber configurations in order to increase the rate of permeation of the products.[339] In general, the characteristics of modules must be considered in all system designs.

5.4. Selective Surface Flow Membranes

Rao and Sircar introduced new membranes in 1993 for the separation of gas mixtures that they called selective surface flow membranes (SSF).[340−342] These membranes were synthesized by coating a macroporous graphite disk with layers of polyvinylidene chloride−acrylate terpolymer latex which contained 0.1 mm polymer beads in aqueous solution. After deposition of each layer, the disk is dried and heated to 1000 °C, which produces a porous carbon membrane through sequential cross-linking and carbonization of the underlying polymer. The resulting thickness of each layer was ∼0.5 mm, and between two and five layers were applied, to yield a complete module between 1.0 and 2.5 mm. The permeability for H_2 in a mixture with hydrocarbons was reduced by several orders of magnitude over that of pure hydrogen. These membranes became promising for H_2 separation because the hydrocarbon selective adsorption hindered pore diffusion by hydrogen.

Further fine-tuning of the pore structure can be facilitated through various synthetic methods. They include an increase in the oxidation time and temperature, allowing for controlled increase of the pore size and permeabilities of all components, and a variation in the kinetic selectivity.[343] Excessive oxidation, however, may render the pores too large to be selective.

Optimization of these membranes has led to even further gas separation advantages, such as hydrogen gas purification. However, this process works opposite to other inorganic membranes. Since adsorption occurs on the high pressure side, the partial pressure of the component to be adsorbed can be low. The partial pressure gradient across the membrane does not need to be high to attain separation, since the driving force for mass transfer across the membrane is the difference in the concentration of the adsorbed species (i.e., concentration gradient). It should also be noted that the activation energy for surface diffusion is typically lower than that for transport across the membrane. Furthermore, adsorption decreases the effective pore volume, hindering the Knudsen diffusion mechanism of nonadsorbed molecules, which would ultimately diminish the degree of separation. Separation processes utilizing SSF membranes are based on the adsorption properties of the component(s), and larger or more polar species can be separated from the mixture. For example, in the methane reforming process, hydrogen remains on the high-pressure side of the membrane while unwanted species are passed through, eliminating subsequent compression of the H_2 gas for many applications. A further advantage of the technique lies in the fact that adsorption capacity and selectivity increase with decreasing temperature, reducing operational cost. This is the reverse of molecular sieving.[342]

Furthermore, the pressure swing adsorption (PSA) process has been integrated with SSF membranes for enhanced performance in the extraction of hydrogen from steam-methane reformer gas.[344] In the commercial production of hydrogen, this reformer gas is subjected to water gas shift (WGS) reactions followed by hydrogen purification by PSA. Typical PSA cycles consist of alternating pressurization and

depressurization of feed gas and hydrogen enriched gas to augment hydrogen recovery. If a SSF membrane is used for purification of the waste gas of the PSA process, hydrogen recovery can be increased from 78% to 85% in the integrated process. Due to a reduction in the compression duty and the membrane area, the process is particularly economic when the PSA waste gas is first fractionated, and only the hydrogen rich portion is used as feed for the SSF membrane.[344]

Viera-Linhares and Seaton used molecular dynamics calculations[343] and critical path analysis[345] to model the separation process in selective surface flow membranes for methane/hydrogen mixtures. They showed that pore width is critical for the separation process, since it controls adsorption capacity and transport properties through the material. They defined three distinct regions, characterized by pore size. If the size is smaller than 6 Å, a sieving effect results and separation occurs solely based on molecular size. Between 6 and 10 Å, selective adsorption of methane occurred with very little dependence on pressure, due to the pores being filled almost to capacity. Maximum selectivity was achieved at 7−8 Å, while permeability was optimal at 9 Å. Larger pore sizes gave rise to a regime in which methane was preferentially adsorbed on the pore walls and hydrogen occupied the center of the pore. It is less effective for H_2 purification, as the hydrogen can diffuse through the low-density region of the porous network. Further research showed that, for the separation of methane from hydrogen,[345] both species pass through distinct pore subnetworks of the membranes, with methane populating the larger pores. The importance of this work lies in the fact that a selective blockage of smaller pores would reduce the permeability to hydrogen and enhance the effectiveness of the separation.

5.5. Disadvantages of Carbon Membranes

Though carbon-based membranes show much promise in the area of light gas separations, they still possess problems that influence their introduction to market. First, they are very brittle and fragile. Therefore, they require more careful handling.[324,331,346,374,] This may be avoided to a certain degree by optimizing precursors and preparation methods.[331] Second, their difficulty to process results in high expenses to fabricate.[374] Carbon membranes require a prepurifier for removing traces of strongly adsorbing vapors, which can clog up the pores due to the transport being through a pore system rather than through the bulk system. This is typical of many industrial adsorption separators. This problem may be avoided by operating at sufficiently high temperatures.[346] Third, they only demonstrated high selectivities for certain gas mixtures, with gases of molecular sizes smaller than 4.0−4.5 Å. Carbon membranes are not suitable to separate certain industrially relevant gas mixtures, such as branched pentanes versus linear hydrocarbon molecules or gas−vapor mixtures (i.e., H_2/hydrocarbon).[374]

5.6. Molecular Sieving Carbon Membranes

Molecular sieving carbon membranes (MSCMs) are the second class of carbon-based membranes on which we will focus. These membranes are able to achieve both capacity and selectivity, primarily due to having pore openings of optimal molecular dimensions and high pore volume(s). The broad variety of carbonaceous precursors and different processing procedures allow for a wide range of variability. The development of porosity begins in the pyrolysis process. Subsequent mild oxidation, known as activation, may enhance the development of new pores and the widening of existing ones.[347] It is possible to interrupt the pore development process when the pore widths have reached molecular dimensions. Under these conditions, however, the capacities are generally low, as the overall pore dimension remains low. Another problem may be the low degree of carbonization. Alternatively, carbon molecular sieves can be prepared from activated carbons with high adsorption capacities. Tuning of pore opening sizes is possible through chemical vapor deposition (CVD) processing of certain organic compounds, thus increasing the selectivity. Nevertheless, the deposition control at pore mouths is difficult to achieve, and often the process results in a shift of the pore size distribution to overall smaller values.[347]

MSCMs produced through pyrolysis of polymeric materials have proved very effective for gas separation in adsorption applications.[348−351] Molecular sieving carbon can be obtained by pyrolysis of many thermosetting polymers, such as poly(vinylidene chloride) (PVDC), poly(furfuryl alcohol) (PFA), cellulose, cellulose triacetate, saran copolymer, polyacrylonitrile (PAN), and phenol formaldehyde, and various coals, such as coconut shell.[348] The pore dimensions of carbon depend on the morphology of the organic precursor and the chemistry of pyrolysis. In particular, nongraphitizing carbons were extremely specific and adjustable by mild activation and sintering steps to the discrimination range 2.8−5.2 Å.[352,353] Pyrolysis of thermosetting polymers typically yielded an exact mimic of the morphology of the parent material without proceeding through a melt or softening during any stage of the pyrolysis process.[352] Koresh and Soffer[346,352,353] successfully prepared crack-free molecular sieving hollow fiber membranes by carbonizing cellulose hollow fibers. They have shown the dependence of permeabilities and selectivities on temperature, pressure, and extent of pore for both adsorbing and nonadsorbing permeates.[352,353] They recognized that the adsorption followed a sequence of $CO_2 > H_2 > N_2 > Xe > SF_6$ for the molecules studied and that hydrogen and methane permeabilities exhibited a maxima between 600 and 700 °C, which they attribute to a molecular-sieving permeation mechanism. However, those membranes would lack sufficient mechanical strength and durability for practical applications.

Fuertes and Centeno[323] reported in 1998 the preparation of a flat, asymmetric carbon membrane supported on a macroporous carbon support, made by carbonization of agglomerated graphite particles blended with a phenolic resin.[340] The support had a porosity of 30% and a mean pore diameter of 1 mm. In an effort to stop translation of support cracks to the membranes, the support was coated with an intermediate carbon layer made from fine graphite particles blended with a polyamide-imide resin. The disk was then carbonized and polished before deposition of the polymeric membrane with an asymmetric structure through a polyamic acid precursor. Gelling of the polymer film, drying, and subsequent thermal treatment led to carbonization. The resulting membrane had better permselectivities for carbon dioxide and methane than the multilayer SSF.[323,340−342] However, the permeabilities of the pure gases decreased, and no data on hydrogen have yet been reported.

In a recent study by Hatori,[354] H_2 and CO_2 data were reported for their polyimide molecular sieving membranes. Precise pore size and structure control were reportedly achieved by adjusting the heat-treatment temperature for

carbonization. They used commercially available polyimide films that were subsequently carbonized under a flow of dry argon. Their data showed that, with increasing carbonization temperatures, the micropores' size of their membranes decreased. After treatment at 1000 °C, the H_2/CO selectivity increased to above 1000. Above 1000 °C, an obvious decrease in CO_2 adsorption was observed due to the decrease in pore size to below that of a CO_2 molecule. The authors concluded that a surface diffusion mechanism was responsible for the achieved separation.

The commercial availability of activated polyaramid carbon fibers led Villar-Rodil et al.[347] to investigate their gas separation properties. These fibers have narrow pore size distributions. After chemical vapor deposition of benzene with simultaneous pyrolysis at 800 °C, these membranes were appropriate for N_2/O_2 separation based on capacity and selectivity. It is anticipated that a careful control of the pore mouth treatment might result in membranes suitable for the separation of hydrogen purification.

5.7. Carbon Nanotubes

The discovery[355,356] of carbon nanotubes (CNTs) in 1991 stimulated a great deal of interest due to their unusual mechanic and electronic properties. With a hundred times the strength of steel and their high gas uptake capacity, applications ranging from lightweight fuel tanks to cables for elevators into space were envisioned.[357]

CNTs can be thought of as graphite sheets that have been wrapped into a tube and capped at each end with half a fullerene (C_{60}) sphere.[340] Their electronic properties depend on tube diameter and helicity.[358,359] Depending on the degree of twist along their length, nanotubes encompass many structural types ranging from the chiral "armchair" (metallic) over other chiral types to the achiral "zigzag" (semiconducting) tubes. Oxidation procedures allow the selective removal of end caps, yielding open-ended CNTs. Tube diameters lie typically in the range of several angstroms to a few nanometers. Besides the single-walled variety (SWNTs), multiwalled CNTs (MWNTs) exist which are composed of concentric layers of single-walled tubes separated roughly by the same distance as the planar sheets in graphite (ca. 3.4 Å). Here, each individual layer can have a different helicity.

Carbon nanotubes are typically synthesized by one of three major production methods: laser ablation, chemical vapor deposition, and electric arc discharge. Metal catalysts such as Fe, Co, Mo, and Ni and combinations thereof are necessary to grow SWNTs and are generally also used for making MWNTs. These metallic particles remain as impurities in the final product. In addition, other forms of carbon such as amorphous carbonaceous materials, graphitic particles, graphitic carbon fibers, nano-onions, and the like are formed.

In order to remove these impurities, the CNTs are subjected to post-treatment. Most purification techniques exploit the fact that the nanotube carbon network is extremely stable and usually not affected by oxidation, while other forms of carbon are readily oxidized to CO_2. Simultaneously, metal particles are converted into their oxides, which can then be dissolved by acid. It should be noted that, in this process, tubes may be cut into shorter pieces, possibly leaving tube ends opened and tube walls damaged or exfoliated.

Due to van der Waals forces between the tubes, SWNTs typically aggregate in the form of bundles with 50 or more tubes. O'Connell et al.[360] introduced a method to create a stable suspension of individual SWNTs using ultrasound. Most methods for separation of metallic and semiconducting SWNTs require initial debundling or solubilization of the nanotubes, which is generally achieved through surfactant aided dispersion by ultrasonication or chemical functionalization.[361]

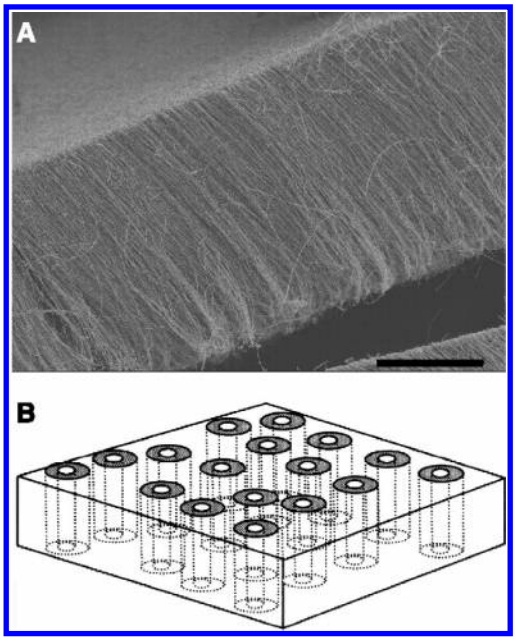

Figure 8. (A) An as-grown, dense, multiwalled CNT array. Scale bar, 50 μm. (B) Schematic of the target membrane structure. With a polymer embedded between the CNTs, a viable membrane structure can be readily produced, with the pore being the rigid inner-tube diameter of the CNT.[370] (From ref 370 (http://www.sciencemag.org). Reprinted with permission from AAAS.)

SWNTs possess several possible adsorption sites. While the binding energy is highest for interstitial channel sites, the surface area of pore sites is largest. These sites, however, are only accessible when the tube walls or caps are broken, as typically happens under harsh oxidation conditions.[362] Since multiwalled tubes rarely bundle, groove and interstitial channel sites do not exist. The interlayer spaces may be possible adsorption sites for small molecules.[363] The pores of MWNTs may be occupied, but the volume fraction of these sites is very small compared with SWNTs, considering their thick walls.

Recent breakthroughs in molecular dynamics (MD) simulations[364−368] and membrane fabrications[369,370] have put carbon nanotubes at the forefront of carbon-based membranes. Because the walls of the nanotubes are considered very smooth as compared to the other materials (i.e., zeolite membranes), they have been predicted by Sholl and Johnson to contain rapid transport rates for gases.[364,365] Holt et al.[369] and Hinds et al.[370] fabricated single- and double-walled nanotube membranes (1.3−2 nm diameter), and multiwalled nanotube (6−10 nm diameter) membranes, respectively (Figure 8).

Diffusion of single gas molecules (both light gases and hydrocarbons) was studied by both groups. Rapid transport of gases was recorded. Transport rates by Holt et al.[369] were 1−2 orders of magnitude larger than Knudsen diffusion predictions (Figure 9).

Multiple gas diffusion experiments have still not been reported. However, MD calculations have been reported for CH_4/H_2 mixtures.[367] They predict a preferential adsorption

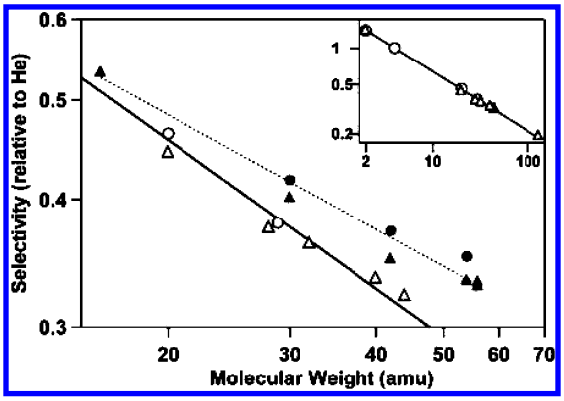

Figure 9. Pure gas selectivity (defined as permeability relative to He) data for sub-2-nm DWNT (double-walled nanotube; triangles) and MWNT (circles) membranes. Open symbols denote nonhydrocarbon gases (H_2, He, Ne, N_2, O_2, Ar, CO_2, Xe); solid symbols denote hydrocarbon gases (CH_4, C_2H_6, C_3H_6, C_4H_6, C_4H_8). The solid line is a power-law fit of the nonhydrocarbon gas selectivity data, showing a scaling predicted by the Knudsen diffusion model (exponent of -0.49 ± 0.01). The dashed line is a power-law fit of the hydrocarbon gas data, showing a deviation from the Knudsen model (exponent of -0.37 ± 0.02). The inset shows the full mass range of the nonhydrocarbon gas data, illustrating agreement with the Knudsen model scaling.[369] (From ref 369 (http://www.sciencemag.org). Reprinted with permission from AAAS.)

of CH_4 over H_2, with selectivities greater than 10, which is much higher than Knudsen diffusion predictions (<3).[368]

6. Polymer Membranes for H_2 Separations

Organic polymers have a long rich history which can be traced back to the 1840s with the discovery of nitrocellulose and the vulcanization of polyisoprene (natural rubber). Since then, the amazing variety and ubiquitous presence of polymeric materials in modern society has had an enormous impact on virtually all facets of large-scale industry and the global economy. It follows then that these materials be considered and exploited as a potential cornerstone of the proposed hydrogen economy. Membrane separations have been considered for a variety of gas separations since at least the 1950s;[371] however, it was not until the mid-1970s that DuPont pioneered the use of small-diameter hollow fibers as a viable gas separation membrane.[372,373] Among the numerous industrial targets, H_2 recovery, separation, and purification remains one of the most highly prized yet most elusive applications of polymer separation membranes.[373] Typical strategies for these separations include variation of the H_2/CO ratio in synthesis gas (commonly referred to as syn-gas), removal of H_2 from hydrocarbon streams, and, finally, removal from purge gases in ammonia production and other large-scale/commercial petrochemical processes.[372−376] This particular section of the review examines various polymeric membranes for H_2 separations, provides comparative data, and addresses active areas in need of expansion.

While DuPont's hollow fibers were groundbreaking, their low permeance was not efficient or productive enough to provide economically sustainable gas separations. Several years later, this performance shortfall was addressed by Monsanto when they developed asymmetric polysulfone hollow fiber membranes for H_2 recovery from ammonia purge gases.[375] The next advance was introduced by Separex in the form of spiral wound cellulose acetate membranes (Separex) for H_2 and natural gas separations.[376] As the transport properties of polymeric H_2 separation membranes evolved (Table 10), they became more commonly utilized on commercial scales for various recovery processes that eventually included H_2 reclamation from recycled refinery gas.[377,378]

Table 10. Hydrogen Separation Ability of First-Generation, Commercial Membranes for Gas Separations

membrane material(s)	developer	H_2/N_2	H_2/CO	H_2/CH_4	ref
polysulfone silicone rubber	Monsanto	39	23	24	375
polyimide	Ube	35.4	30		484
cellulose acetate	Separex	33	21	26	372, 376

Table 11. Hydrogen Purity Required in Industry[380]

purposes	hydrogen purity (%)
rocket engine fuel semiconductor manufacture	99.999999
polymer electrolyte fuel cell on-site hydrogen generating equipment	99.99
hydrodesulfurization	90
adjustment of molecular weight distribution	70−80
fuel gas	54−60

One of the primary polymer-based technologies for energy production is proton exchange membrane (PEM)-based fuel cells, which convert the chemical energy of H_2 directly and efficiently to electrical energy with dramatically reduced emissions of greenhouse gases (hydrocarbons, CO, CO_2, NO_x, and SO_x).[379] However, for these fuel cells to become widely applicable, a well distributed supply of hydrogen is required.

While polymer-based H_2 separation membranes are capable of H_2 production at very high purities, palladium composites, inorganic membranes, or more advanced separation processes are required to produce the highest of purities for many applications (Table 11).[380] However, it is quite clear that further scientific developments are needed to fully realize the hydrogen economy, since the current technologies do not yet meet the performance criteria set forth by the U.S. Department of Energy. Gas separation membranes have significant potential for application in this growing process.

6.1. Dense Polymeric Membranes

Dense type polymer membranes can be divided into glassy and rubbery polymeric membranes. The former have higher selectivity and lower flux, whereas the latter have higher flux but lower selectivity.[19] According to Kluiters,[19] operating temperatures for polymer membranes are ~100 °C. Several key advantages are that they possess the ability to cope with high-pressure drops and low cost. However, limited mechanical strength, relatively high sensitivity to swelling and compaction, and susceptibility to certain chemicals such as hydrochloric acid (HCl), sulfur oxides (SO_x), and CO_2 make polymeric membranes less attractive. Polymer membranes used for separation processes operate according to the solution diffusion mechanism. An in depth study on polymer membranes can be found elsewhere.[19] Table 14 gives hydrogen permeabilities (at 27 °C temperature and 206.8 kPa feed gas pressure) for the selected polymer membranes and the selectivities for nitrogen (N_2), methane (CH_4), and CO_2. The polystyrene shows the best combination of hydrogen permeability and selectivities for N_2, CH_4, and CO_2.[6,19,372]

Polymeric membranes are separated into porous and nonporous, and the hydrogen transport mechanisms of these

Table 12. Common Hydrogen Sources and Their Impurities[380]

hydrogen source	impurities
electrolysis of water	CH_4, O_2, N_2, CO_2, and CO
steam reforming gas	CO, CO_2, and CH_4
petroleum refining	C_1-C_6, and BTX[a]
ammonia purge gas	NH_3, N_2, and CH_4
coke oven gas	CH_4, N_2, BTX,[a] CO, CO_2, and O_2

[a] BTX = benzene, toluene, and xylene.

membranes may occur through five different diffusion processes (see Figure 1). If the polymeric membrane is porous, then diffusion occurs through mechanisms which depend largely on pore size and the size(s) of the diffusing gas molecule(s): (i) Knudsen diffusion, (ii) surface diffusion, (iii) capillary condensation, and (iv) molecular sieving. In Knudsen diffusion (i), the diffusing gaseous molecules collide more frequently with the pore walls than with other diffusing molecules, thus facilitating differential retention times.[381] With surface diffusion (ii), gaseous molecules adsorb onto the pore surfaces (walls) and then move from along a specific decreasing concentration gradient from one site to the next.[382,383] Capillary condensation (iii) occurs under very specific circumstances when diffusing gas molecules condense within a given pore to generate capillary forces which inhibit diffusion rates.[384] Finally, the molecular sieving (iv) mechanism is again a specific case where the diffusing gas molecules and the pore size are sufficiently close in size to require an energy of activation (directly related to molecule size).[385]

In nonporous, or dense, polymeric membranes, transport is controlled by the (v) solution diffusion.[18,386-388] In the solution diffusion mechanism, the gaseous molecules absorb to the surface, dissolve into the bulk of the polymer membrane, and are finally transported across the membrane by a gradient of chemical potential from the feed stream to the product stream. The equations which govern this particular diffusion mechanism are discussed at length in the introduction of this review and in refs 388-390.

6.2. Hydrogen Selective Polymeric Membranes

Polymeric membranes which are selective for hydrogen are designed such that the concentration of hydrogen is increased in the product stream (*permeate*) and the remaining components of the gas mixture remain in the feed stream or a secondary waste stream (*retentate*).

The variety of H_2 sources (feed stock streams) provides a modest number of impurities (Table 12) which could potentially interfere with the separation membrane. But as Table 13 shows, H_2 has the lowest critical temperature (T_c) compared to those of most of the other gases, and it has one of the smallest kinetic diameters of any gas molecule. This low T_c indicates lower potential hydrogen solubility while the small kinetic diameter suggests substantially higher diffusivities.[382,391,392] Thus, current research on selective polymeric H_2 membranes is aimed at the exploitation of high diffusivities while minimizing the consequential effects of the lower solubilities. Since dense membranes of this type operate entirely on the solution diffusion mechanism, polymeric membranes are engineered in an attempt to use these two major components to their advantage. Improving the performance of polymeric H_2 selective membranes is largely based on targeted separation, which rejects more condensable compounds (impurities) and allows the less condensable H_2 to permeate.

Table 13. Properties of Several Common Gas Molecules

compound	molecule	k[a] ($\times 10^{10}$ m)	σ[b] ($\times 10^{10}$ m)	T_C[c] (°C)
helium	He	2.6	2.551	−277.0
ammonia	NH_3	2.6	2.900	132.4
water	H_2O	2.65	2.641	374.2
hydrogen	H_2	2.89	2.827	−240.0
carbon dioxide	CO_2	3.3	3.941	31.0
carbon monoxide	CO	3.73	3.690	−140.3
oxygen	O_2	3.46	3.467	−118.6
nitrogen	N_2	3.64	3.798	−147.0
methane	CH_4	3.8	3.758	−82.8
propane	C_3H_8	4.3	5.118	96.7
BTX[d]	*d*	≥5.85	≥5.349	288-357

[a] Kinetic diameter calculated from the minimum equilibrium cross-sectional diameter.[485] [b] Lennard-Jones collision diameter.[382] [c] Critical temperature.[381] [d] BTX = benzene (C_6H_6), toluene (C_7H_8), and xylene (C_8H_{10}).

The idea of an "upper bound", originally introduced by Robeson in 1991,[393] is the carefully modulated balance between permeability and selectivity. This proposed upper bound provides insight into the maximum selectivity that is attainable for a given membrane permeability while using polymeric membranes for a given composition of gases in the H_2 feed stream. For example, at the low end of H_2 permeability, the separation of H_2 from a mixture of H_2/N_2 has been established by various poly(methyl methacrylate)s (PMMs), and at the high end of H_2 permeability, poly(1-trimethylsilyl-1-propyne) (PTMSP) has been used. Figure 10 illustrates the substantial amount of research directed toward more effective gas separation membranes, but Robeson's upper bound hypothesis, which was established over a decade ago, still remains.[394-414] This has been further explained by Benny Freeman, who presents[415] a clear and physically meaningful rationale behind the existence of this upper bound. Thus, membranes are now being designed from polymers along this upper bound. However, if separations exceeding this upper bound are required, then alternative membranes (zeolitic, metallic, etc.) and technologies must be employed.

The use of cross-linkable polymers is another more recent methodology which has been used to improve the performance of polymeric membranes.[237,416-418] These cross-linking moieties have been shown to provide a selectivity improvement for H_2 at least ten times the magnitude of their non-cross-linked counterparts. However, the complexity of implementing this approach on large industrial scale membranes has yet to be overcome and must be addressed before they find widespread commercial use. Although polymeric membrane research in the open literature appears to be shifting toward membrane processing[419,420] membrane systems and new supports,[421-428] the patent literature still reveals substantial efforts toward the development of new membrane materials.[401,429-433]

A specific application for polymer membranes is as hydrogen rejective membranes (as mentioned above). Rejective membranes use the significantly higher sorption of other gases to overcome the potential selective preference of the small size of the hydrogen molecule.[434] Rubbery polymers such as polydimethylsiloxane (PDMS) have been shown to reduce the diffusion selectivity.[435,436] The higher mobility of the chain structures in these rubbery polymers increases the diffusivity of all gaseous species. Since smaller molecules are already highly mobile, larger molecules benefit most from this chain mobility, which ultimately causes reductions in

Table 14. Permselective Properties of CO_2-selective Polymeric Facilitated Transport Membranes

membrane	other gas	CO_2 (kPa)	CO_2 permeance[a]	CO_2 selectivity	ref
sulfonated polystryene−EDAH	N_2	0.29	4.13×10^{-6}	600	449, 450
Nafion−EDAH	CH_4	0.16	7.99×10^{-7}	550	378, 452
Nafion−EDAH	H_2	101	3.63×10^{-7}	6.8	453, 486
Nafion−EDAH	H_2		1.88×10^{-6}	55	379, 454
sulfonated polystryene−divinyl benzene−EDAH	N_2	0.407	4.97×10^{-8}	524	456, 487
EDAH−alginate	N_2	1	1.05×10^{-8} [b]	50	457, 488
EDAH−polyacrylate	N_2	4.76	7.50×10^{-6}	4700	458, 459, 489, 490
poly(acrylate−EDAH)/poly(vinyl alcohol)	N_2	6.18	5.25×10^{-6}	1900	380, 460
poly(vinyl alcohol)−amino acid salts	H_2	76.0	6.38×10^{-7}	30	381, 461
poly(ethylenimine)−lithium glycinate	H_2	76.0	2.80×10^{-6}	75	382, 462
polyvinylalcohol−tetramethylammonium fluoride	H_2	76.0	5.33×10^{-7}	19	383, 463
polyvinylalcohol−cesium fluoride	H_2	4.4	5.96×10^{-7}	60	384, 464
cesium polyacrylate−cesium fluoride	H_2	4.4	6.09×10^{-7}	61	384, 464
poly(diallydimethylammonium fluoride)	H_2	40.0	1.35×10^{-7}	81	385, 465
poly(vinylbenzyltrimethylammonium fluoride)	H_2	4.21	4.52×10^{-7}	87	386, 466
poly(vinylbenzyltrimethylammonium fluoride)	H_2	113.9	2.22×10^{-7}	207	18, 467
poly(vinylbenzyltrimethylammonium fluoride)−cesium fluoride	H_2	4.08	1.93×10^{-6}	127	387, 468
poly-2-(*N*,*N*-dimethyl)aminoethyl methacrylate	N_2	4.76	3.75×10^{-7}	130	18, 388
poly-(2-(*N*,*N*-dimethyl)aminoethyl acrylate-*co*-acrylonitrile)	N_2	0.48	1.53×10^{-9}	90	389, 491
hydrolyzed polyvinylpyrrolidone	N_2	1.62	1.27×10^{-5}	48.1	390,492
poly(ethylenimine)/poly(vinyl alcohol)-	N_2	6.59	2.93×10^{-7}	230	392,493
poly(vinylamine)-ammonium fluoride	CH_4	200.0	2.33×10^{-8}	1143	393,494
poly(vinylamine)-cesium fluoride	H_2	4.29	5.03×10^{-7}	120	384,464
Biomimetic carbonic anhydrase	N_2	0.10	1.28×10^{-5}	>1000	398,495

[a] Permeance in units of $m^3/(m^2\ s\ kPa)$; literature P_0 values converted to permeance using reported membrane thicknesses. [b] Membrane thickness not reported, assumed a value of 50 μm.

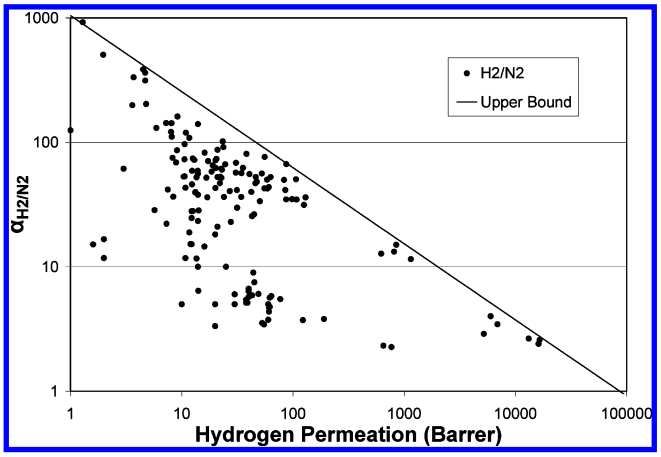

Figure 10. Permeability and selectivity data for hydrogen/nitrogen separation.[394−414] The upper bound was developed by Robeson[393] [1 Barrer = 7.50062×10^{-18} m^3(STP) m/(m^2 s Pa)]. (Reprinted from ref 393, copyright 1991, with permission from Elsevier.)

the diffusion selectivity. Unfortunately, this is not the case in glassy polymers because the low mobility of the polymer chains prevents any significant reduction in diffusion selectivities.

As alluded to above, increasing the solubility selectivity is another technique to improve the properties of H_2 rejective polymeric membranes. There have been several methods reported to increase the solubility selectivities. These include the incorporation of polar groups such as poly(propylene oxide),[321,435,437] poly(ether oxide),[438−440] poly(ester-ether),[432] or poly(urethane-ether).[433] These polymers provide an improved environment to solubilize polarizable feed-stream molecules such as CO, CO_2, and NO_x while the nonpolarizable feed-stream components such as H_2 do not experience this improved solubility. A very significant development in these types of polymeric membranes was reported by the Research Institute of Innovative Technology for the Earth (RITE).[441] RITE developed a novel gating membrane based on poly(amido-amine) dendrimers. This membrane has a unique CO_2 gating property and is predicted to provide unmatched CO_2/H_2 selectivity in polymeric materials. The rejective properties of polymeric membranes have also been achieved through careful production and processing control of the fractional free volumes.[442,443] For example, the fractional free volumes of H_2 *selective* PTMSP membranes can be modified to produce reverse selective membranes that favor hydrocarbons over hydrogen.[444−448]

Because the distinct properties of each gas (size, shape, chemistry, etc.) play a major role in the sorption selectivity and solubilities of a polymer, it is often not possible to generate a membrane which performs uniformly for all gas compositions. Therefore, it is often necessary to design these types of membranes for specific pairs of target gases.

The separation and purification of H_2 in SMR (steam-methane reforming) plants is presently accomplished through PSA (pressure swing adsorption) and/or amine-based acid gas scrubbers.[9] As implied above, polymeric membranes are well suited to remove bulk CO_2 and to retain H_2, and they offer a particularly attractive economic alternative to these well-established technologies. While there are various classes of membranes whose function may be considered for H_2 purification at SMR plants, the temperature of the product gas stream (450−650 °C) prevents conventional polymeric membranes from being used. However, they can be used if the temperature of the gas stream is sufficiently cooled. If product gas stream cooling is not a viable option, then microporous inorganic or palladium (Pd)-based proton conducting or carbon molecular sieving membranes are used.[6] The H_2 is removed from the minor component (CO_2), and the product is recovered. However, since these types of membranes usually permeate both H_2 and CO_2, the recovered H_2 will also contain CO_2, since it also permeates to some extent.

6.3. H_2 versus CO_2 Selective Polymeric Membranes

A CO_2-selective polymeric membrane permeates CO_2 by means of a reversible reaction, where an amine-based carrier gas species reacts with CO_2 on the high-pressure feed side of the membrane to form an adduct, R_2N-CO_2. The R_2N-CO_2 adduct diffuses through the membrane to the low-pressure product stream side, where it reforms free carrier species and CO_2 is liberated. Both CO_2 and H_2 permeate by Fickian diffusion, in which gas molecules dissolve at the high-pressure feed side, diffuse across the membrane, and desorb into the gas phase on the lower pressure permeate side (see eq 1 and Figure 1).[9]

The ideal polymeric H_2 separation membrane is one that maximizes both CO_2 permeability and CO_2/H_2 selectivity without reducing the relative H_2 fluxes. The increase in CO_2 permeability translates to low membrane area and, hence, lower costs. High permeability, however, cannot be achieved at the expense of selectivity, since H_2 losses are commercially and economically unacceptable. While H_2 permeates only by a solution diffusion mechanism (v), the key to resolving this issue is to avoid a membrane that has very low H_2 solubility because it functions as a barrier to H_2 permeation. A wide range of polymeric materials have been investigated as candidates, including ion exchange resins, hydrophilic polymers, blended polymers with CO_2-reactive salts, polyelectrolytic membranes, and polyanilines. Membranes consisting of ion exchange resins, polyelectrolytes, and polymer/salt blends contain mobile carrier species which preferentially react with CO_2 and diffuse across the membranes. The following sections are brief summaries of these classes of membranes that have been reported for CO_2/H_2 separations.

6.4. Ionic and Ion Exchange Polymer Membranes

Pioneering work in this area was carried out in the early 1980s using ion exchange membranes.[449,450] Membranes consisting of polyvinylpyridines and simple anions (carbonate (CO_3^-) or glycinate ($NH_2CH_2CO_2^-$)) resulted in high CO_2 permeabilities relative to standard chloride containing polyvinylpyridine membranes. Polystryenesulfonic acid (PSSA) membranes neutralized with ethylenediamine (EDA) improved the permselective properties. However, the resulting monoprotonated ethylenediamine, $NH_2CH_2CH_2NH_3^+$ ($EDAH^+$), can form carbamates ($R_2NCO_2^-$) based on the reversible reaction of R_2NH with CO_2, which provides a robust pathway for reversible carbon dioxide sequestration.

Following diffusion to the low-pressure side of the membrane, the carbamate decomposes, or rather dissociates, to form the original components, $EDAH^+$ and CO_2 in the gas phase. However, the CO_2 permeabilities were not constant because of carrier saturation (carbamate formation) at higher CO_2 pressures.[451] The ionic nature of this membrane provides a substantial barrier to permeation of nonpolarizable gases and, by extension, H_2. Ion exchange membranes, containing $EDAH^+$, have fueled intense research on these membrane technologies. One particular group of membranes, Nafion, consists of poly(perfluorosulfonic acid), which contains $EDAH^+$, and was reported to mediate the transport of CO_2,[452] with only a modest CO_2/H_2 selectivity.[453] Since Nafion has a relatively low ion exchange capacity, it provides only a moderate H_2 permeation barrier. However, highly hydrated Nafion−EDAH membranes exhibited increased CO_2/H_2 selectivities.[454] A sulfonated polybenzimidazole−EDAH (PBI−EDAH) membrane with a higher ionic site density than that of Nafion was shown to permeate CO_2 through a facilitated transport mechanism.[455] A water-swollen sulfonated styrene-divinylbenzene (2.2 mequiv/g) containing $EDAH^+$ exhibited a high CO_2 permeance of 5.0×10^{-8} $m^3/(m^2\ s\ kPa)$ at 0.41 kPa CO_2 feed pressure. Although H_2 data were not reported, the CO_2/N_2 selectivity was still quite promising.[456] A novel ion exchange membrane was obtained by cross-linking a polysaccharide, sodium alginate, followed by exchange to form the $EDAH^+$ containing membrane.[457] Exponential increases in both CO_2 permeance and selectivity resulted from increasing the $EDAH^+$ concentration in the membrane, but a modest CO_2/N_2 selectivity of about 50 strongly suggests that this membrane may not be suitable for CO_2/H_2 separations.

Ion exchange membranes prepared by polymerizing of acid containing monomers onto microporous or highly permeable surfaces have shown great promise.[458,459] Plasma graft polymerization of acrylic acid gave membranes with higher exchange capacities than those of typical ion exchange membranes. The result is a higher CO_2-carrier density and a more highly ionic barrier to H_2 permeation. Following neutralization with EDA to form $EDAH^+$, facilitated transport of CO_2 with very high selectivity was observed: CO_2 permeance, 7.5×10^{-6} $m^3/(m^2\ s\ kPa)$; CO_2/N_2 selectivity, 4700 at 4.8 kPa CO_2 feed pressure.[458,459] With such a high selectivity, these membranes are expected to be effective for removal of CO_2 from H_2.

Another novel class of polymeric membranes consists of polyvinyl alcohol/poly(acrylic acid) block copolymer blends neutralized with EDA.[460] Depending on the nature and ratio of polymers, ion exchange capacities ranged from 1.3 to 4.5 mequiv/g. A maximum CO_2/N_2 selectivity of 1500 at 6.2 kPa CO_2 feed pressure was obtained for the highest exchange capacity membrane. Such a high CO_2/N_2 selectivity would suggest utility for CO_2/H_2 separations.

Hydrophilic polymers blended with basic or CO_2-reactive salts have also proved effective for CO_2/H_2 separations. These membranes contain mobile carrier species that react to form bicarbonate or carbamates. Membranes consisting of polyvinylalcohol blended with various amino acid salts exhibited CO_2 permeabilities ranging from 0.72×10^{-11} to 1.6×10^{-11} $m^3/(m^2\ s\ kPa)$ with CO_2/H_2 selectivities of 13−30 at a CO_2 feed pressure of 76 kPa.[461] Membranes consisting of polyethylenimine alone, or blended with polyvinylalcohol, have been utilized. When blended with 50 wt % lithium glycinate, the resulting CO_2 permeabilities range from 1.4 to 1.6×10^{-11} $m^3/(m^2\ s\ kPa)$ and CO_2/H_2 selectivities range from 28 to 37 at ambient temperature and 1230 Barrers [1 Barrer = 7.50062×10^{-18} $m^3(STP)\ m/(m^2\ s\ Pa)$] and a selectivity of 75 is obtained at 80 °C.[462] Polyvinylalcohol membranes containing 50 wt % tetramethylammonium fluoride tetrahydrate had a reported CO_2/H_2 selectivity of 19 at 76 kPa CO_2 feed pressure.[463] Membranes consisting of blends of cesium fluoride with polyvinylalcohol or cesium polyacrylate exhibited CO_2/H_2 selectivities of about 60 at a CO_2 feed pressure of about 4.4 kPa.[464]

Polyelectrolytes are polymers that have high ionic content—up to one ionic unit per polymer repeat unit. Unlike ion exchange polymers, polyelectrolytes are water soluble. The high ionic site density of polyelectrolytes provides a high concentration of CO_2-reactive sites and an ionic medium with a low H_2 solubility. Polyelectrolytes that have utility for H_2 purification have cationic groups on the polymer backbone coupled with anions, particularly fluoride (F^-) and acetate ($CH_3CO_2^-$). One common example is poly(vinylbenzyltri-

methylammonium fluoride) (PVBTAF).[465,466] PVBTAF has quaternary nitrogen groups on the polymer backbone. These functional groups cannot interact with CO_2; rather, CO_2 reactivity arises from the counteranion. As described in reaction 4, such anions act as bases to promote formation of HCO_3^-.

$$2F^- \cdot nH_2O + CO_2 \rightarrow HCO_3^- + HF_2^- \cdot (2n-1)H_2O \quad (4)$$

PVBTAF and related membranes exhibited facilitated transport[451−455] of CO_2 and CO_2/H_2 selectivities greater than 80.[465,466] Permselective properties were, not surprisingly, strongly dependent on the feed and sweep gas relative humidities. Membranes consisting of two polyelectrolyte layers exhibited an unexpected improvement in selectivity to 207 without sacrificing CO_2 permeance.[467] Much like the hydrophilic polymers discussed above, incorporation of various fluoride and acetate containing salts into polyelectrolyte membranes yielded improved permselective properties.[464,468] Incorporating 4 mol of cesium fluoride/mole of repeat unit gave membranes with a 4- to 6-fold higher CO_2 permeance and a CO_2/H_2 selectivity of 127 at a CO_2 pressure of 4.1 kPa.

7. Conclusion

We have outlined some of the basic requirements and concepts central to the application of metallic membranes for H_2 separation into a clean, useable energy source, for the Hydrogen economy. Metallic membranes containing group IV (Ti, Zr, Hf) and group V (V, Nb, Ta) metals are of great focus in the research community for H_2 separations. As shown in Table 5, amorphous alloys offer greater mechanical durability and resistance to H_2 embrittlement, although it is not yet known whether they can produce higher H_2 fluxes or display higher thermal stability than their crystalline counterparts. The modeling of H_2 permeation through a metal membrane and complications associated with thin membranes, amorphous metals, and membranes with complex microstructures have been discussed, and a brief summary of the key chemical and physical properties of non-Pd-based metals and alloys is highlighted. Despite this, the preparation of amorphous and nanocrystalline alloys through melt techniques provides a readily accessible avenue for novel membrane design. In addition, it should be noted that the processing and production techniques must also be sufficiently able to manipulate the defect structure if amorphous metals are to be useful for H_2 separations. Undoubtedly, the advances in the fundamental science and understanding will continue to play a significant role in improving the performance characteristics of metallic H_2 separation membranes.

Inorganic silica and zeolite membranes hold the potential for full and near-term industrial implementation due to their tunable nature and high-temperature and high-pressure stability. Silica membranes are one of the candidates for hydrogen separation due to their ease of fabrication, low cost of production, and scalability. Because of their porosity and composition, silica membranes are also less expensive than metals (due to the lack of precious elements) and not susceptible to H_2 embrittlement. Similarly, zeolite membranes have inherent chemical, mechanical, and thermal stability. The trends in zeolite membrane research show clearly the improvements in selectivity, fabrication methodology, and energy-production applications. In the near future, the ability to inexpensively fabricate these membranes for tuned selectivity will put them at the forefront of separations technology. Currently, they are interesting candidates for streamlined hydrogen production via natural gas reformation because of their stability at high temperatures and their ability to be regenerated without loss to performance. Concerns associated with inorganic membranes center on their fabrication reproducibility. Compared with organic membranes, inorganic membranes are currently expensive to manufacture. However, introduction into large-scale production facilities should result in more competitive production costs.

Carbon-based membranes have the potential for a wide variety of applications associated with the separation and purification of hydrogen gas. A recent review[33] summarizes the literature for performances of carbon membranes for the separation of mixtures of permanent gases. However, to become economically viable as commercial products, these membranes will have to have better selectivity, thermal stability, and chemical stability. Today, the production of carbon membranes involves a very high cost; it is on the order of 1−3 orders of magnitude greater than that of the typical polymeric membranes. Therefore, it must achieve a superior performance in order to compensate for the higher cost. Areas of fundamental research aimed at achieving that superior performance include[8] (1) optimization of fabrication parameters during the pyrolysis process, (2) development of effective yet inexpensive carbon membrane precursors, and (3) enhancing the stability of these membranes when exposed to water vapor (as found in reforming processes).

Over the past 25 years, substantial progress had been achieved in developing polymeric membranes for hydrogen purification. However, much remains to be done before such membranes become a commercial reality. While polymeric membranes are successfully employed for large-scale commercial H_2 recovery programs, there is still plenty of room for further improvement. Advanced polymeric membranes with improved selectivity, diffusivity, H_2 fluxes, and permeabilities are being developed. A wider range of operating conditions, specifically temperature and pressure, in addition to higher chemical resistance to hydrocarbons and other aggressive feed streams are all important properties where research efforts are being conducted by the global research community. Cross-linkable polymers show promise in addressing some of these concerns; however, there is still a lot of research needed with those materials. Further development in the area of membrane processing and applications should improve the effectiveness of polymeric membranes in some cases, and focusing this research on very specific applications should allow membranes to play an increasing role in the growing hydrogen separation market.

While many of the challenges are associated with polymeric H_2 separations, it may eventually prove necessary to blend multiple membrane technologies together into mixed-matrix systems such as hybrid membranes (metal−polymer, ceramic−polymer, metal−ceramic), which attempt to incorporate the benefits of each component to improve the overall membrane performance. While there are still some major technical barriers that must be overcome, the future of polymeric membranes for hydrogen separations is very promising and has excellent potential for growth, especially in the area of functionalization and chemical resistivity.

Polymeric membranes are a dense type of membrane, transporting species through the bulk of the material. Depending on their state, polymeric membranes can be subdivided into glassy (prepared at temperatures below the glass transition temperature) and rubbery (prepared at temperatures above the glass transition temperature) polymeric

Table 15. Comparison of Membrane Classes

	metallic: Pd, Ta, V, Nb, and alloys		ceramic: silica, alumina, zirconia, titania, and zeolites		carbon: porous carbons," single-wall carbon nanotubes	polymer: polyesters, ethers, imides, urethanes, etc.	
	dense	porous	dense	porous	porous	dense	porous
T range (°C)	300−600		600−900	200−600	500−900	<100	
selectivity	>1000		>1000	5−139	4−20	low	
flux	60−300		6−80	60−300	10−200	low	
mechanical issues	phase transitions		brittle		very brittle	swelling and compaction	
chemical stability	poisoned by H_2S, HCl, CO_2, SO_x		potential degradation with H_2O, H_2S or CO_2		oxidizing and susceptible to organic vapors	degraded H_2S, HCl, CO_2, SO_x	
transport mechanism[a]	SolD	SolD/MS	SolD	MS	SolD/MS	SolD	MS

[a] KD, Knudson diffusion; SurD, surface diffusion; CC, capillary condensation; MS, molecular sieving; SolD, solution diffusion.

membranes. Glassy membranes have relatively high selectivity and low flux, whereas rubbery membranes have increased flux but lower selectivity. In absolute terms, both types have moderate fluxes and selectivity. They are usually produced using the phase inversion method. Operating temperatures are limited to 90−100 °C. Advantages in most applications are a good ability to cope with large pressure drops, low cost, and good scalability. Possible problems are limited chemical resistance to certain chemicals, such as HCl, SO_x, but also CO_2, limited mechanical strength, and relatively high sensitivity to swelling and compaction. Polymeric membranes are in an advanced stage of development and are being considered for industrial commercialization by gas producing companies such as Air Products, Linde, BOC, and Air Liquide.[19]

8. Comparisons and Perspectives

Given the tremendous body of literature and the ever growing global research efforts on H_2 separation membranes, it is not surprising to find such diverse materials and engineering approaches. This review is intended to provide a distinct cross section of these major efforts and current state-of-the art materials. Beyond this, there is a comparatively small but growing body of literature on composite or hybrid materials which attempt to integrate the ideal performance of several classes of H_2 membrane materials. We suspect that research on these types of materials will become an increasingly important effort toward overcoming the many scientific and technological hurdles that exist between the present state of hydrogen production, utilization, and storage capabilities and those required for a competitive sustainable hydrogen economy. Table 15 provides a comparison of the classes of the H_2 separation membrane materials presented throughout this review. When this information is compared against the 2015 targets, we quickly see that each individual class has its own distinct advantages and disadvantages.

While polymer-based membranes are arguably the cheapest and easiest processed of the materials, they are less thermally robust and lack sufficient selectivity and flux capacities. Unlike other classes of materials, polymers possess the greatest flexibility in their synthetic compositions and the available organic chemistries for component pre- and postfabrication modification. This offers a distinctly unique opportunity over zeolite, metal, and carbon membranes in that precise synthetic control, which clearly has an impact on their performance, can be systematically tailored as the knowledge and performance base grows. Although closely related, carbon-based separation membranes do not suffer from the thermal limitations of the polymers. Generally, their flux capacities are on par with those of zeolite and silica membranes. However, the lack of robust mechanical properties makes processing and modular design very difficult and adversely effects the performance lifetime of the membrane.

Metal and zeolite separation membranes operating on the solution diffusion mechanism easily provide the highest selectivities and flux capacities of all the membrane classes. The typically higher operating temperature ranges are additional parasitic energy costs which must be considered over the lifetime of the membrane. In addition, the potential phase transitions and hydride embrittlement experienced by many pure metals and alloys offer a substantial obstacle for a permanent membrane solution.

Perhaps the biggest hurdle which is faced by all classes of H_2 separation membranes is the lack of chemical stability. Water, sulfur containing species, acidic vapors, and CO_2 are the most commonly encountered problematic contaminants which must be dealt with. The combined result of these chemical and thermal performance issues ultimately determines the cost and viability of a given material for application in commercial H_2 separation technologies and how it addresses the five performance targets for H_2 separation set forth by the U.S. Department of Energy listed in Table 1.[14] With the predicted doubling of global energy consumption by 2050, our research efforts must unambiguously overcome the many scientific and technological hurdles that exist in H_2 separation membranes.[1] Regardless of which method is used, separation and purification of the nearly 6 Exajoules ($1\ EJ = 10^{18}$ joules) of H_2 which is produced industrially per year is a paramount task which the membrane research community must endeavor to address before the "hydrogen economy" can become a reality.

9. Acknowledgments

Sandia is a multiprogram laboratory operated by Sandia Corporation, a Lockheed Martin Company, for the U.S. Department of Energy's National Nuclear Security Administration, under Contract DE-AC04-94AL85000. T.M.N. thanks the U.S. DOE Hydrogen, Fuel Cells, & Infrastructure Technologies Program for continued support.

10. References

(1) Report from the Basic Energy Sciences Advisory Committee (Feb 2003); available electronically at http://www.sc.doe.gov/bes/besac/Basic_Research_Needs_To_Assure_A_Secure_Energy_Future_FEB2003.pdf.
(2) Report from the Basic Energy Sciences Workshop on Hydrogen Production, Storage, and Use (Feb 2004); available electronically at http://www.sc.doe.gov/bes/hydrogen.pdf.
(3) Ogden, J. Lecture (Oct 2004); available electronically at http://www.its.ucdavis.edu/education/classes/pathwaysclass/7-StationaryH2-(Ogden).pdf.

(4) Sircar, S.; Golden, T. C. *Sep. Sci. Technol.* **2000**, *35*, 667.
(5) Stocker, J.; Whysall, M.; Miller, G. Q. *30 years of PSA technology for hydrogen purification 2005*; UOP LLC: Des Plaines, IL, 1998.
(6) Bredesen, R.; Jordal, K.; Bollard, O. *Chem. Eng Process.* **2004**, *43*, 1129.
(7) Adhikari, S.; Fernando, S. *Ind. Eng. Chem. Res.* **2006**, *45*, 875.
(8) Spillman, R. W.; Grace, W. R. *Chem. Eng. Prog.* **1989**, *85*, 41.
(9) Gunardson, H. *Industrial Gases in Petrochemical Processing*; Marcel Dekker, Inc.: 1998.
(10) Molburg, J. C.; Doctor, R. D. 20th Annual International Pittsburg Coal Conference (2003).
(11) Lin, Y. S. *Sep. Purif. Technol.* **2001**, *25*, 39.
(12) Norby, T. *Solid State Ionics* **1999**, *125*, 1.
(13) Guan, J.; Dorris, S. E.; Balachandran, U.; Liu, M. *Solid State Ionics* **1997**, *100*, 45.
(14) U.S. Department of Energy, Small Business Innovation Research Program and Small Business Technology Transfer Program FY 2005 Solicitations, Technical Topic Descriptions, 15. Materials Research, Office of Fossil Energy, 2005.www.science.doe.gov/sbir/solicitations/fy%202005/15_FE3.htm.
(15) The President Hydrogen Fuel Initiative: A Clean and Secure Energy Future; available electronically at http://www.hydrogen.energy.gov/presidents_initiative.html.
(16) Broehl, J. *Energy Bulletin* 2004, http://www.energybulletin.net/3342.html.
(17) Rosen, M. A.; Scott, D. S. *Int. J. Hydrogen Energy* **1998**, *23*, 631.
(18) Koros, W. J.; Fleming, G. K. *J. Membr. Sci.* **1993**, *83*, 1.
(19) Kluiters, S. C. A. *Status review on membrane systems for hydrogen separation*; Energy Center of Netherlands: Petten, The Netherlands, 2004.
(20) Malek, K.; Coppens, M. O. *J. Chem. Phys.* **2003**, *119*, 2801.
(21) Jaguste, D. N.; Bhatia, S. K. *Chem. Eng. Sci.* **1995**, *50*, 167.
(22) Noble, R. D.; Stern, S. A. *Membrane Separations Techology—Principles and Applications*; Elsevier: Amsterdam, 1995.
(23) Mulder, M.; Mulder, J. *Basic principles of membrane technology*; Kluwer Academic Publishers: Dordretch, The Netherlands, 1996.
(24) Fick, A. *Ann. Phys., Leipzig* **1855**, *170*, 59.
(25) Buxbaum, R. E.; Kinney, A. B. *Ind. Eng. Chem. Res.* **1996**, *35*, 530.
(26) Wipf, H. *Phys. Scr.* **2001**, *T94*, 43.
(27) Lewis, F. A. *Pure Appl. Chem.* **1990**, *62*, 2091 and references therein.
(28) Gao, H. Y.; Lin, Y. S.; Li, Y. D.; Zhang, B. Q. *Ind. Eng. Chem. Res.* **2004**, *43*, 6920.
(29) Uemiya, S. *Sep. Purif. Method* **1999**, *28*, 51.
(30) Paglieri, S. N.; Way, J. D. *Sep. Purif. Method* **2002**, *31*, 1.
(31) Ma, Y. H.; Mardilovich, I. P.; Engwall, E. E. *Ann. N. Y. Acad. Sci.* **2003**, *984*, 346 and references therein.
(32) Sholl, D. S. *MRS Bull.* **2006**, *31*, 770 and references therein.
(33) Ma, Y. H.; Mardilovich, P. P.; She, Y. U.S. Patent 6,152,987.
(34) Ma, Y. H.; Mardilovich, I. P.; Engwall, E. E. U.S. Patent Applications 0,244,590; 0,244,583; and 0,237,779.
(35) Criscuoli, A.; Basile, A.; Drioli, E.; Loiacono, O. *J. Membr. Sci.* **2001**, *181*, 21.
(36) Middelton, P.; Solgaard-Anderson, H.; Rostrup-Nielson, H. T. *Proceedings of the 14th World Energy Conference*, Montreal, Canada, June 9−13, 2000.
(37) Bryden, K. J.; Ying, J. Y. *J. Membr. Sci.* **2002**, *203*, 29.
(38) Castro, F. J.; Meyer, G.; Zampieri, G. *J. Alloys Compd.* **2002**, *330*, 612.
(39) Hoyos, L. J.; Primet, P.; Praliaud, H. *J. Chem. Soc., Faraday Trans.* **1992**, *22*, 3367.
(40) Rutlowski, W.; Wetzig, D.; Zacharias, H. *Phys. Rev. Lett.* **2001**, *87*, 246101.
(41) Roa, F.; Block, M. J.; Way, J. D. *Desalination* **2002**, *147*, 411.
(42) Frieske, H.; Wicke, E. *Ber. Bunsen-Ges. Phys. Chem.* **1973**, *77*, 48.
(43) Wicke, E.; Nernst, G. H. *Ber. Bunsen-Ges. Phys. Chem.* **1964**, *68*, 224.
(44) Ma, Y. H.; Akis, B. C.; Ayturk, M. E.; Guazzone, F.; Engwall, E. E.; Mardilovich, I. P. *Ind. Eng. Chem. Res.* **2004**, *43*, 2936.
(45) Sholl, D. S.; Ma, Y. H. *MRS Bull.* **2006**, *31*, 770.
(46) Phair, J. W.; Donelson, R. *Ind. Eng. Chem. Res.* **2006**, *45*, 5657.
(47) Hara, S.; Sakaki, K.; Itoh, N.; Kimura, H. M.; Asami, K.; Inoue, A. *J. Membr. Sci.* **2000**, *164*, 289.
(48) Hara, S.; Sakaki, K.; Itoh, N. Amorphous Ni alloy membrane for separation/dissociation of hydrogen. U.S. Patent 6,478,853.
(49) Yamaura, S.-I.; Shimpo, Y.; Okouchi, H.; Nishida, M.; Kajita, O.; Kimura, H.; Inoue, A. *Mater. Trans., JIM* **2003**, *44*, 1885.
(50) Newsome, D. S. *Catal. Rev.* **1980**, *21*, 275.
(51) Pasel, J.; Samsun, R. C.; Schmitt, D.; Peters, R.; Stolten, D. *J. Power Sources* **2005**, *152*, 189.
(52) Rostrup-Nielsen, J. R.; Rostrup-Nielsen, T. *Caltech* **2002**, *6*, 150.
(53) Ruth, L. A. *Mater. High Temp.* **2003**, *20*, 7.
(54) Amadeo, N. E.; Laborde, M. A. *Int. J. Hydrogen Energy* **1995**, *20*, 949.
(55) Andreeva, D.; Idakiev, V.; Tabakova, T.; Andreev, A.; Giovanoli, R. *Appl. Catal., A* **1996**, *134*, 275.
(56) Morreale, B. D.; Ciocco, M. V.; Enick, R. M.; Morsi, B. I.; Howard, B. H.; Cugini, A. V.; Rothenberger, K. S. *J. Membr. Sci.* **2003**, *212*, 87.
(57) Kajiwara, M.; Uemiya, S.; Kojima, T. *Int. J. Hydrogen Energy* **1999**, *24*, 839.
(58) Buxbaum, R. E.; Marker, T. L. *J. Membr. Sci.* **1993**, *85*, 29.
(59) Castello, G.; Biagini, E.; Munari, S. *J. Chromatogr., A* **1965**, *20*, 447.
(60) Rothenberger, K. S.; Howard, B. H.; Killmeyer, R. P.; Cugini, A. V.; Enick, R. M.; Bustamante, F.; Ciocco, M. V.; Morreale, B. D.; Buxbaum, R. M. *J. Membr. Sci.* **2003**, *218*, 19.
(61) Makrides, A. C.; Wright, M. A.; Jewett, D. A. U.S. Patent 3,350,-846.
(62) Moss, T. S.; Peachey, N. M.; Snow, R. C.; Dye, R. C. *Int. J. Hydrogen Energy* **1998**, *23*, 99.
(63) Uemiya, S.; Kato, W.; Uyama, A.; Kajiwara, M.; Kojima, T.; Kikuchi, E. *Sep. Purif. Technol.* **2001**, *22−3*, 309.
(64) Ward, T. L.; Dao, T. *J. Membr. Sci.* **1999**, *153*, 211.
(65) Shu, J.; Grandjean, B. P. A.; Vanneste, A.; Kaliaguine, S. *Can. J. Chem. Eng.* **1991**, *69*, 1036.
(66) Hara, S.; Hatakeyama, N.; Itoh, N.; Kimura, H. M.; Inoue, A. *J. Membr. Sci.* **2003**, *211*, 149.
(67) Kajiwara, M.; Uemiya, S.; Kojima, T.; Kikuchi, E. *Catal. Today* **2000**, *56*, 65.
(68) Hara, S.; Hatakeyama, N.; Itoh, N.; Kimura, H. M.; Inoue, A. *Desalination* **2002**, *144*, 115.
(69) Heinze, S.; Vuillemin, B.; Colson, J. C.; Giroux, P.; Leterq, D. *Solid State Ionics* **1999**, *122*, 51.
(70) Pick, M. A. *J. Nucl. Mater.* **1987**, *147*, 297.
(71) Makhlouf, M. M.; Sisson, R. D. *Metall. Mater. Trans. A* **1991**, *22*, 1001.
(72) Fukada, S.; Nakahara, T.; Mitsuishi, N. *J. Nucl. Mater.* **1990**, *171*, 399.
(73) Zhang, Y.; Ozaki, T.; Komaki, A.; Nishimura, C. *J. Membr. Sci.* **2003**, *224*, 81.
(74) Liu, B. S.; Li, H. X.; Cao, Y.; Deng, J. F.; Sheng, C.; Zhou, S. Y. *J. Membr. Sci.* **1997**, *135*, 33.
(75) Liu, B. S.; Zhang, W. D.; Dai, W. L.; Deng, J. F. *J. Membr. Sci.* **2004**, *244*, 243.
(76) Peachey, N. M.; Snow, R. C.; Dye, R. C. *J. Membr. Sci.* **1996**, *111*, 123.
(77) Lu, K.; Wang, J. T.; Wei, W. D. *J. Phys. D: Appl. Phys.* **1992**, *25*, 808.
(78) Siriwardane, R. V.; Poston, J. A.; Fisher, E. P.; Lee, T. H.; Dorris, S. E.; Balachandran, U. *Appl. Surf. Sci.* **2000**, *167*, 34.
(79) Birnbaum, H. K. *J. Less-Common. Met.* **1984**, *104*, 31.
(80) Mundschau, M. V. Hydrogen transport membranes. U.S. Patent 6,-899,744.
(81) Roark, S. E.; Mackay, R.; Mundschau, M. V. Dense, layered membranes for hydrogen separation. U.S. Patent 7,001,446.
(82) Paglieri, S. N.; Birdsell, S. A.; Barbero, R. S.; Snow, R. C.; Smith, F. M. Tubular hydrogen permeable metal foil membrane and method of fabrication. U.S. Patent 0,045,034 A1.
(83) Villars, P.; Prince, A.; Okamoto, H. *Handbook of Ternary Alloy Phase Diagrams*; ASM International: Materials Park, OH, 1995.
(84) Massalski, T. B.; Okamoto, H.; Subramanian, P. R.; Kacprzak, L. *Binary Alloy Phase Diagrams*; ASM International: Materials Park, OH, 1990.
(85) Dos Santos, D. S.; De Miranda, P. E. V. *J. Non-Cryst. Solids* **1998**, *234*, 133.
(86) Yukawa, H.; Yamashita, D.; Ito, S.; Morinaga, M.; Yamaguchi, S. *Mater. Trans., JIM* **2002**, *43*, 2757.
(87) Yukawa, H.; Teshima, A.; Yamashita, D.; Ito, S.; Yamaguchi, S.; Morinaga, M. *J. Alloys Compd.* **2002**, *337*, 264.
(88) Yukawa, H.; Yamashita, D.; Ito, S.; Morinaga, M.; Yamaguchi, S. *J. Alloys Compd.* **2003**, *356*, 45.
(89) Komiya, K.; Ito, S.; Yukawa, H.; Morinaga, M.; Nagata, K.; Nambu, T.; Ezaki, H. *Mater. Trans., JIM* **2003**, *44*, 1686.
(90) Dorris, S. E.; Lee, T. H.; Balachandran, U. Metal/ceramic composites with high hydrogen permeability. U.S. Patent 6,569,226.
(91) Edlund, D. J.; Newbold, D. D.; Frost, B. Composite hydrogen separation element and module. U.S. Patent 5,645,626.
(92) Gleiter, H. *Phys. Status Solidi B* **1992**, *172*, 41.
(93) Kirchheim, R. *Phys. Scr.* **2001**, *T94*, 58.
(94) Gleiter, H. *Prog. Mater. Sci.* **1989**, *33*, 223.
(95) Gleiter, H. *Nanostruct. Acta Mater.* **2000**, *48*, 1.
(96) Bryden, K. J.; Ying, J. Y. *Mater. Sci. Eng., A* **1995**, *204*, 140.
(97) Bryden, K. J.; Ying, J. Y. *Nanostruct. Mater.* **1997**, *9*, 485.
(98) Papaefthymiou, G. C.; Bryden, K. J.; Ying, J. Y. *Physica B* **2002**, *311*, 279.
(99) McCool, B. A.; Lin, Y. S. *J. Mater. Sci.* **2001**, *36*, 3221.

(100) Xomeritakis, G.; Lin, Y. S. *AIChE J.* **1998**, *44*, 174.
(101) Yang, K.; Cao, M. Z. *Scr. Metall. Mater.* **1991**, *25*, 2139.
(102) Galano, M.; Audebert, F.; Cantor, B.; Stone, I. *Mater. Sci. Eng., A* **2004**, *375*, 1206.
(103) Eliaz, N.; Eliezer, D.; Abramov, E.; Zander, D.; Koster, U. *J. Alloys Compd.* **2000**, *305*, 272.
(104) Luck, R. *Quasicrystals. An Introduction to Structure, Physical Properties, and Applications*; Springer: Berlin, 2002.
(105) Senechal, M. *Notes AMS* **2006**, *53*, 886.
(106) Gapontsev, A. V.; Kondrat'ev, V. V. *Phys.-Usp.* **2003**, *46*, 1077.
(107) Steward, S. A. *Review of Hydrogen Isotope Permeabilities Through Materials*; Lawrence Livermore National Laboratory: Livermore, CA, 1983.
(108) Liu, L.; Zhang, J. *MRS Bull.* **2001**, *36*, 2073.
(109) Shimpo, Y.; Yamaura, S.; Okouchi, H.; Nishida, M.; Kajita, O.; Kimura, H.; Inoue, A. *J. Alloys Compd.* **2004**, *372*, 197.
(110) Yamaura, S.-I.; Shimpo, Y.; Okouchi, H.; Nishida, M.; Kajita, O.; Inoue, A. *Mater. Trans., JIM* **2004**, *45*, 330.
(111) Evard, E. A.; Kurdumov, A. A.; Berseneva, F. N.; Gabis, I. E. *Int. J. Hydrogen Energy* **2001**, *26*, 457.
(112) Evard, E. A.; Sidorov, N. I.; Gabis, I. E. *Tech. Phys.* **2000**, *45*, 377.
(113) Nishimura, C.; Komaki, M.; Hwang, S.; Amano, M. *J. Alloys Compd.* **2002**, *330-332*, 902.
(114) Ozaki, T.; Zhang, Y.; Komaki, M.; Nishimura, C. *Int. J. Hydrogen Energy* **2003**, *28*, 1229.
(115) Nishimura, C.; Ozaki, T.; Komaki, M.; Zhang, Y. *J. Alloys Compd.* **2003**, *356-357*, 295.
(116) Zhang, Y.; Ozaki, T.; Komaki, M.; Nishimura, C. *Scr. Metall. Mater.* **2002**, *47*, 601.
(117) Amano, M.; Komaki, M.; Nishimura, C. *J. Less-Common. Met.* **1991**, *172*, 727.
(118) Eliaz, N.; Eliezer, D. *Adv. Perform. Mater.* **1999**, *6*, 5.
(119) Kirchheim, R.; Mutschele, T.; Kieninger, W.; Gleiter, H.; Birringer, R.; Koble, T. D. *Mater. Sci. Eng. A* **1988**, *99*, 457.
(120) Rush, J. J.; Rowe, J. M.; Maeland, A. J. *J. Phys. F: Met. Phys.* **1980**, *10*, L283.
(121) Bankmann, J.; Pundt, A.; Kirchheim, R. *J. Alloys Compd.* **2003**, *356−357*, 566.
(122) Dos Santos, D. S.; De Miranda, P. E. V. *J. Mater. Sci.* **1997**, *32*, 6311.
(123) Wu, Q. Y.; Xu, J.; Sun, X. K.; Hu, Z. Q. *J. Mater. Sci. Technol.* **1997**, *13*, 443.
(124) Maeland, A. J.; Tanner, L. E.; Libowitz, G. G. *J. Less-Common. Met.* **1980**, *74*, 279.
(125) Suzuki, K. *J. Less-Common. Met.* **1983**, *89*, 183.
(126) Dos Santos, D. S.; De Miranda, P. E. V. *Int. J. Hydrogen Energy* **1998**, *23*, 1011.
(127) Shimizu, E.; Aoki, K.; Masumoto, T. *J. Alloys Compd.* **1999**, *295*, 526.
(128) Kim, J. J.; Stevenson, D. A. *J. Non-Cryst. Solids* **1988**, *101*, 187.
(129) Eliaz, N.; Fuks, D.; Eliezer, D. *Mater. Lett.* **1999**, *39*, 255.
(130) Kirchheim, R.; Stolz, U. *Acta Metall. Mater.* **1987**, *35*, 281.
(131) Zander, D.; Leptien, H.; Koster, U.; Eliaz, N.; Eliezer, D. *J. Non-Cryst. Solids* **1999**, *252*, 893.
(132) Aoki, K.; Kamachi, M.; Masumoto, T. *J. Non-Cryst. Solids* **1984**, *61−62*, 679.
(133) Eliaz, N.; Moshe, E.; Eliezer, S.; Eliezer, D. *Metall. Mater. Trans. A* **2000**, *31*, 1085.
(134) Ishida, M.; Takeda, H.; Watanabe, D.; Amiya, K.; Nishiyama, N.; Kita, K.; Saotome, Y.; Inoue, A. *Mater. Trans., JIM* **2004**, *45*, 1239.
(135) Kim, W. B.; Ye, B. J.; Yi, S. *Met. Mater. Int.* **2004**, *10*, 1.
(136) Park, E. S.; Kim, D. H. *Met. Mater. Int.* **2005**, *11*, 19.
(137) Inoue, A.; Nishiyama, N.; Amiya, K.; Zhang, T.; Masumoto, T. *Mater. Lett.* **1994**, *19*, 131.
(138) Peker, A.; Johnson, W. L. *Appl. Phys. Lett.* **1993**, *63*, 2342.
(139) Wesseling, P.; Nieh, T. G.; Wang, W. H.; Lewandowski, J. J. *Scr. Metall. Mater.* **2004**, *51*, 151.
(140) Zhang, Q. S.; Zhang, H. F.; Deng, Y. F.; Ding, B. Z.; Hu, Z. Q. *Scr. Metall. Mater.* **2003**, *49*, 273.
(141) Bakonyi, I.; Cziraki, A. *Nanostruct. Mater.* **1999**, *11*, 9.
(142) Fan, C.; Takeuchi, A.; Inoue, A. *Mater. Trans., JIM* **1999**, *40*, 42.
(143) Li, J. M.; Du, Y. W.; Feng, D.; Quan, M. X.; Hu, Z. Q. *Adv. Eng. Mater.* **1999**, *1*, 137.
(144) Inoue, A. *Mater. Sci. Eng., A* **2001**, *304*, 1.
(145) Fan, C.; Li, C. F.; Inoue, A. *J. Non-Cryst. Solids* **2000**, *270*, 28.
(146) Murty, B. S.; Hono, K. *Appl. Phys. Lett.* **2004**, *84*, 1674.
(147) Kamakoti, P.; Morreale, B. D.; Ciocco, M. V.; Howard, B. H.; Killmeyer, R. P.; Cugini, A. V.; Sholl, D. S. *Science* **2005**, *307*, 569.
(148) Kamakoti, P.; Sholl, D. S. *J. Membr. Sci.* **2006**, *279*, 94.
(149) Kamakoti, P.; Sholl, D. S. *Phys. Rev. B* **2005**, *71*, 14301.
(150) Sonwane, C. G.; Wilcox, J.; Ma, Y. H. *J. Chem. Phys.* **2006**, *125*, 184714.
(151) Brouwer, R. C.; Griessen, R. *Phys. Rev. B* **1989**, *40*, 1481.
(152) Cockayne, D. J. H.; McKenzie, D. R.; McBride, W.; Goringe, C.; McCulloch, D. *Microsc. Microanal.* **2000**, *6*, 329.
(153) Miracle, D. B. *Nat. Mater.* **2004**, *3*, 697.
(154) Treacy, M. M. J.; Gibson, J. M. *Acta Crystallogr., A* **1996**, *52*, 212.
(155) Hufnagel, T. C. Finding order in disorder. *Nat. Mater.* **2004**, *3*, 666.
(156) Warde, J.; Knowles, D. M. *ISIJ Int.* **1999**, *39*, 1006.
(157) Warde, J.; Knowles, D. M. *ISIJ Int.* **1999**, *39*, 1015.
(158) Amis, E. J. *Nat. Mater.* **2004**, *3*, 83.
(159) Amis, E. J.; Xiang, X. D.; Zhao, J. C. *MRS Bull.* **2002**, *27*, 295.
(160) Xiang, X. D.; Sun, X. D.; Briceno, G.; Lou, Y. L.; Wang, K. A.; Chang, H. Y.; WallaceFreedman, W. G.; Chen, S. W.; Schultz, P. G. *Science* **1995**, *268*, 1738.
(161) Koinuma, H.; Takeuchi, I. *Nat. Mater.* **2004**, *3*, 429.
(162) Yoo, Y. K.; Xiang, X. D. *J. Phys.: Condens. Matter* **2002**, *14*, R49.
(163) Yoo, Y. K.; Ohnishi, T.; Wang, G.; Duewer, F.; Xiang, X. D.; Chu, Y. S.; Mancini, D. C.; Li, Y. Q.; O'Handley, R. C. *Intermetallics* **2001**, *9*, 541.
(164) Xiang, X. D. *Appl. Surf. Sci.* **2004**, *223*, 54.
(165) Zhao, J. C. *Annu. Rev. Mater. Res.* **2005**, *35*, 51.
(166) Xiang, X. D.; Schultz, P. G. *Physica C* **1997**, *282*, 428.
(167) Wei, T.; Xiang, X. D.; WallaceFreedman, W. G.; Schultz, P. G. *Appl. Phys. Lett.* **1996**, *68*, 3506.
(168) Zhao, J. C. *J. Mater. Res.* **2001**, *16*, 1565.
(169) Rao, X.; Xia, Q. F.; Li, X. J.; Si, P. C. *Intermetallics* **2000**, *8*, 499.
(170) Takeuchi, A.; Inoue, A. *J. Optoelectron. Adv. M* **2004**, *6*, 533.
(171) Miracle, D. B.; Senkov, O. N.; Sanders, W. S.; Kendig, K. L. *Mater. Sci. Eng., A* **2004**, *375−377*, 150.
(172) Yeung, K. L.; Varma, A. *AIChE J.* **1995**, *41*, 2131.
(173) Jayaraman, N.; Lin, Y. S.; Pakala, M.; Lin, R. Y. *J. Membr. Sci.* **1995**, *99*, 89.
(174) Saracco, G.; Specchia, V. *Catal. Rev.* **1994**, *36*, 305.
(175) Xue, D.; Chen, H.; Wu, G. H.; Deng, J. F. *Appl. Catal., A* **2001**, *214*, 87.
(176) Burchardt, T. *Int. J. Hydrogen Energy* **2000**, *25*, 627.
(177) Burchardt, T.; Hansen, V.; Valand, T. *Electrochim. Acta* **2001**, *46*, 2761.
(178) Deng, J. F.; Li, H.; Wang, W. *Catal. Today* **1999**, *51*, 113.
(179) Bozzolo, G.; Ferrante, J.; Noebe, R. D.; Good, B.; Honecy, F. S.; Abel, P. *Comput. Mater. Sci.* **1999**, *15*, 169.
(180) Good, B.; Bozzolo, G. *Surf. Sci.* **2002**, *507-510*, 730.
(181) Besenbacher, F.; Chorkendorff, I.; Clausen, B. S.; Hammer, B.; Molenbroek, A. M.; Nørskov, J. K.; Stensgaard, I. *Science* **1998**, *279*, 1913.
(182) Greeley, J.; Mavrikakis, M. *Nat. Mater.* **2004**, *3*, 810.
(183) Symons, D. M.; Young, G. A.; Scully, J. R. *Metall. Mater. Trans. A* **2001**, *32*, 369.
(184) Song, Z.; Tan, D.; He, F.; Bao, X. *Appl. Surf. Sci.* **1999**, *137*, 142.
(185) Dong, J.; Liu, W.; Lin, Y. S. *AIChE J.* **2000**, *46*, 1957.
(186) Prabhu, A. K.; Radhakrishnan, R.; Oyama, S. T. *Appl. Catal., A* **1999**, *183*, 241.
(187) Prabhu, A. K.; Oyama, S. T. *Chem. Lett.* **1999**, 213.
(188) Morooka, S.; Kusakabe, K. *MRS Bull.* **1999**, *24*, 25.
(189) Tsapatis, M.; Gavalas, G. R. *MRS Bull.* **1999**, *24*, 30.
(190) Prabhu, A. K.; Oyama, S. T. *J. Membr. Sci.* **2000**, *176*, 233.
(191) Verweij, H. *J. Mater. Sci.* **2003**, *38*, 4677.
(192) Tsuru, T.; Tsuge, T.; Kubota, S.; Yoshida, K.; Yoshioka, T.; Asaeda, M. *Sep. Sci. Technol.* **2001**, *38*, 3721.
(193) Kurungot, S.; Yamaguchi, T.; Nakao, S.-I. *Catal. Lett.* **2003**, *86*, 273.
(194) Kurungot, S.; Yamaguchi, T. *Catal. Lett.* **2004**, *92*, 181.
(195) Nair, B. N.; Okubo, T.; Nakao, S.-I. *Membranes* **2000**, *25*, 73.
(196) Kitao, S.; Kameda, H.; Asaeda, M. *Membranes* **1990**, *15*, 222.
(197) de Lange, R. S. A.; Keizer, K.; Burggraaf, A. J. *J. Membr. Sci.* **1995**, *104*, 81.
(198) Asaeda M.; Kashimoto, M. Proceedings of the Fifth International Conference Inorganic Membranes, Nagoya, Japan, 1998; p A-405.
(199) Nomura, M.; Ono, K.; Gopalakrishnan, S.; Sugawara, T.; Nakao, S.-I. *J. Membr. Sci.* **2005**, *251*, 151.
(200) Nomura, M.; Yamaguchi, T.; Kumakiri, I.; Nakao, S.-I. *Membranes* **2001**, *23*, 124.
(201) Okubo, T.; Inoue, H. *J. Membr. Sci.* **1989**, *42*, 109.
(202) Gavalas, G. R.; Megiris, C. E.; Nam, S.-W. *Chem. Eng. Sci.* **1989**, *44*, 1829.
(203) Megiris, C. E.; Glezer, J. H. E. *Ind. Eng. Chem. Res.* **1992**, *31*, 1293.
(204) Tsapatsis, M.; Gavalas, G. R. *AIChE J.* **1992**, *38*, 847.
(205) Ha, H.-Y.; Nam, S.-W.; Hong, S.-A.; Lee, W.-K. *J. Membr. Sci.* **1993**, *85*, 279.
(206) Xomeritakis, G.; Lin, Y.-S. *Ind. Eng. Chem. Res.* **1994**, *33*, 2607.
(207) Morooka, S.; Yan, S.-C.; Kusakabe, K.; Akiyama, Y. *J. Membr. Sci.* **1995**, *101*, 89.
(208) Nakao, S.-I.; Suzuki, T.; Sugawara, T.; Tsuru, T.; Kimura, S. *Microporous Mesoporous Mater.* **2000**, *37*, 145.
(209) Yamaguchi, T.; Ying, X.; Tokimasa, Y.; Nair, B. N.; Sugawara, T.; Nakao, S.-I. *Phys. Chem. Chem. Phys.* **2000**, *2*, 4465.

(210) Nenoff, T. M.; Spontak, R. J.; Aberg, C. M. *MRS Bull.* **2006**, *31*, 735.
(211) Fotou, G. P.; Lin, Y. S.; Pratsinis, S. E. *J. Membr. Sci.* **1995**, *30*, 2803.
(212) Nair, B. N.; Elferink, J. W.; Keizer, K.; Verweij, H. *J. Colloid Interface Sci.* **1996**, *178*, 565.
(213) Nair, B. N.; Keizer, K.; Maene, N.; Okubo, T.; Nakao, S.-I. In *Surface Chemistry and Electrochemistry of Membranes*; Sorenson, T. S., Ed.; Marcel Dekker: New York, 1999; p 125.
(214) Maier, W. F.; Schramm, H. O. *Mater. Res. Soc. Symp. Proc.* **1992**, *271*, 493.
(215) Asaeda, M.; Yamamichi, A.; Satoh, M.; Kamakura, M. In *Proceedings of ICIM3*; Ma, Y. H., Ed.; 1994; p 315.
(216) Asaeda, M. Proceedings of 1999 International Conference on Membranes, Toronto, 1999.
(217) Asaeda, M.; Yamasaki, S. *Sep. Purif. Technol.* **2001**, *25*, 151−159.
(218) Julbe, A.; Balzer, C.; Guizard, C.; Cot, L. *J. Sol-Gel Sci. Technol.* **1995**, *4*, 89.
(219) Cao, G. Z.; Lu, Y.; Delattre, L.; Brinker, C. J.; Lopez, G. P. *Adv. Mater.* **1996**, *8*, 588.
(220) Raman, N. K.; Anderson, M. T.; Brinker, C. J. *Chem. Mater.* **1996**, *8*, 1682.
(221) de Vos, R. M.; Maier, W. F.; Verweij, H. *J. Membr. Sci.* **1999**, *158*, 277.
(222) Brinker, C. J.; Ward, T. L.; Sehgal, R.; Raman, N. K.; Hietala, S. L.; Smith, D. M.; Hua, D.-W.; Headley, T. J. *J. Membr. Sci.* **1993**, *77*, 165.
(223) Koros, W. J.; Ma, Y. H.; Shimidzu, T. *Pure Appl. Chem.* **1996**, *68*, 1479.
(224) Lin, Y. S.; Baxbaum, R. E. In *Encyclopedia of Separation Science*; Wilson, I. D., Adlard, T. R., Poole, C. F., Cooke, M., Eds.; Academic Press: San Diego, CA, 2000; p 3365.
(225) Lai, Z. P.; Bonilla, G.; Diaz, I.; Nery, J. G.; Sujaoti, K.; Amat, A. M.; Kokkoli, E.; Terasaki, O.; Thompson, R. W.; Tsapatsis, M.; Vlachos, D. G. *Science* **2003**, *300*, 456.
(226) Tsai, C. Y.; Tam, S. Y.; Lu, Y. F.; Brinker, C. J. *J. Membr. Sci.* **2000**, *169*, 255.
(227) Hoenicke D.; Dietzsch, E. In *Handbook of Porous Solids*; Schueth, F., Sing, K. S. W., Weitkamp, J., Eds.; Wiley: Weinheim, 2002; p 1395.
(228) van Rijn, C. J. M.; Nijdam, W.; Kuiper, S.; Veldhuis, G. J.; van Wolferen, H. A. G. M.; Elwenspoek, M. C. *J. Micromech. Microeng.* **1999**, *9*, 170.
(229) Richardson, J. T.; Paripatyadar, S. A. *Appl. Catal.* **1990**, *61*, 293.
(230) Kusakabe, K.; Shibao, F.; Zhao, G.; Sotowa, K.-I.; Watanabe, K.; Saito, T. *J. Membr. Sci.* **2003**, *215*, 321.
(231) Nomura, M.; Yamaguchi, T.; Nakao, S. *Ind. Eng. Chem. Res.* **1997**, *36*, 4217.
(232) Mottern, M. L.; Quickel, G. T.; Shi, J. Y.; Yu, D.; Verweij, H. In *Proceedings of the 8th International Conference on Inorganic Membranes*, Cincinnati, OH, July 18−22, 2004; Lin, Y. S., Ed.; p 26.
(233) Liang, J.; Jiang, X.; Liu, G.; Deng, Z.; Zhuang, J.; Li, F.; Li, Y. *Mater. Res. Bull.* **2003**, *38*, 161.
(234) Shi, J. Y.; Verweij, H. *Langmuir* **2005**, *21*, 5570.
(235) Lee, D.; Zhang, L.; Oyama, S. T.; Niu, S.; Saraf, R. F. *J. Membr. Sci.* **2004**, *231*, 117.
(236) Nijmeijer, A.; Huiskes, C.; Sibelt, N. G. M.; Kruidhof, H.; Verweij, H. *Am. Ceram. Soc. Bull.* **1998**, *77*, 95.
(237) Yoshino, Y.; Suzuki, T.; Nair, B. N.; Taguchi, H.; Itoh, N. *J. Membr. Sci.* **2005**, *267*, 8.
(238) Brinkman, H. W.; van Eijk, J. P. G. M.; Meinema, H. A.; Terpstra, R. A. *Am. Ceram. Soc. Bull.* **1999**, *78*, 51.
(239) Millan, A. J.; Nieto, M. I.; Moreno, R.; Baudin, C. *J. Eur. Ceram. Soc.* **2002**, *22*, 2223.
(240) Toy, C.; Whittemore, O. J. *Ceram. Int.* **1989**, *15*, 167.
(241) Giessler, S.; Jordan, L.; da Costa, J. C. D.; Lu, G. Q. *Sep. Purif. Technol.* **2003**, *32*, 255.
(242) Yoshida, K.; Hirano, Y.; Fujii, H.; Tsuru, T.; Asaeda, M. *J. Chem. Eng. Jpn.* **2001**, *34*, 523.
(243) Iler, R. K. *The Chemistry of Silicas*; Wiley: New York, 1979.
(244) (a) Kanezashi, M.; Fujita, T.; Asaeda, M. *Sep. Sci. Technol.* **2005**, *40*, 225. (b) Kanezashi, M.; Asaeda, M. *J. Membr. Sci.* **2006**, *271*, 86.
(245) Hasegawa, Y.; Kusakabe, K.; Morooka, S. *J. Membr. Sci.* **2001**, *190*, 1.
(246) Lin, Y. S.; Kumakiri, I.; Nair, B. N.; Alsyouri, H. *Sep. Purif. Methods* **2002**, *31*, 229.
(247) Benes, N. E.; Biesheuvel, P. M.; Verweij, H. *AIChE J.* **1999**, *45*, 1322.
(248) Verweij, H.; Lin, Y. S.; Dong, J. H. *MRS Bull.* **2006**, *31*, 756.
(249) Duke, M. C.; Diniz da Costa, J. C.; Lua, G. Q.; Petch, M.; Gray, P. *J. Membr. Sci.* **2004**, *241*, 325.
(250) den Exter, M. J.; Jansen, J. C.; van de Graaf, J. M.; Kapteijn, F.; Moulijn, J. A.; van Bekkum, H. *Recent Adv. New Horizons Zeolite Sci. Technol.* **1996**, *102*, 413.
(251) Suzuki, H. Composite membrane having a surface layer of an ultrathin film of cage-shaped zeolite and processes for production thereof. U.S. Patent 4,699,892.
(252) Bakker, W. J. W.; van den Broeke, L. J. P.; Kapteijn, F.; Moulijn, J. A. *AIChE J.* **1997**, *43*, 2203.
(253) Hedlund, J.; Sterte, J.; Anthonis, M.; Bons, A.-J.; Carstensen, B.; Corcoran, N.; Cox, D.; Deckman, H.; Gijnst, W. D.; de Moor, P.-P.; Lai, F.; McHenry, J.; Mortier, W.; Reinoso, J.; Peeters, J. *Micropororous Mesoporous Mater.* **2002**, *52*, 179.
(254) Bowen, T. C.; Kalipcilar, H.; Falconer, J. L.; Noble, R. D. *J. Membr. Sci.* **2003**, *215*, 235.
(255) Sano, T.; Yanagishita, H.; Kiyozumi, Y.; Mizukami, F.; Haraya, K. *J. Membr. Sci.* **1994**, *95*, 221.
(256) Lovallo, M. C.; Gouzinis, A.; Tsapatsis, M. *AIChE J.* **1998**, *44*, 1903.
(257) Burggraaf, A. J.; Vroon, Z. A. E. P.; Keizer, K.; Verweij, H. *J. Membr. Sci.* **1998**, *44*, 77.
(258) Noack, M.; Kolsch, P.; Caro, J.; Schneider, M.; Toussaint, P.; Sieber, I. *Microporous Mesoporous Mater.* **2000**, *35*, 253.
(259) Wegner, K.; Dong, J. H.; Lin, Y. S. *J. Membr. Sci.* **1999**, *158*, 17.
(260) Lin, X.; Kita, H.; Okamoto, K. *Chem. Commun.* **2000**, *19*, 1889.
(261) Gardner, T. Q.; Flores, A. I.; Noble, R. D.; Falconer, J. L. *AIChE J.* **2002**, *48*, 1155.
(262) Aoki, K.; Kusakabe, K.; Morooka, S. *J. Membr. Sci.* **1998**, *141*, 197.
(263) Kita, H.; Horii, K.; Ohtoshi, Y.; Tanaka, K.; Okamoto, K. I. *J. Mater. Sci. Lett.* **1995**, *14*, 206.
(264) Hedlund, J.; Schoeman, B.; Sterte, J. *Chem. Commun.* **1997**, *13*, 1193.
(265) Navajas, A.; Mallada, R.; Téllez, C.; Coronas, J.; Menéndez, M.; Santamaría, J. *Desalination* **2002**, *148*, 25.
(266) Nishiyama, N.; Korekazu, U.; Masahiko, M. *Chem. Commun.* **1995**, *19*, 1967.
(267) Yamazaki, S.; Tsutsumi, K. *Adsorption* **1997**, *3*, 165.
(268) Kita, H.; Asamura, H.; Tanaka, K.; Okamoto, K.-I.; Kondo, M. *Abstr. Papers Am. Chem. Soc.* **1997**, *214*, 269.
(269) Kusakabe, K.; Kuroda, T.; Uchino, K.; Hasegawa, Y.; Morooka, S. *AIChE J.* **1999**, *45*, 1220.
(270) Li, S.; Tuan, V. A.; Falconer, J. L.; Noble, R. D. *Microporous Mesoporous Mater.* **2002**, *53*, 59.
(271) Geus, E. R.; Den Exter, M. J.; Van Bekkum, H. *J. Chem. Soc., Faraday Trans.* **1992**, *88*, 3101.
(272) van Bekkum, H.; Geus, E. R.; Kouwenhoven, H. W. *Stud. Surf. Sci. Catal.* **1994**, *85*, 509.
(273) Coronas, J.; Santamaria, J. *Sep. Purif. Methods* **1999**, *28*, 127.
(274) Bein, T. *Chem. Mater.* **1996**, *8*, 1636.
(275) Caro, J.; Noack, M.; Kolsch, P.; Schafer, R. *Microporous Mesoporous Mater.* **2000**, *38*, 3.
(276) Chiang, A. S. T.; Chao, K.-J. *J. Phys. Chem. Solids* **2001**, *62*, 1899.
(277) Matsukata, M.; Kikuchi, E. *Bull. Chem. Soc. Jpn.* **1997**, *70*, 2341.
(278) Mizukami, F. *Stud. Surf. Sci. Catal.* **1999**, *125*, 1.
(279) Tavolaro, A.; Drioli, E. *Adv. Mater.* **1999**, *11*, 975.
(280) Davis, M. E. *Nature* **2002**, *417*, 813.
(281) Nair, S.; Tsapatsis, M. In *Handbook of Zeolite Science and Technology*; Auerbach, S. M., Carrado, K. A., Dutta, P. K., Eds.; Marcel Dekker: New York, 2003.
(282) Bowen, T. C.; Noble, R. D.; Falconer, J. L. *J. Membr. Sci.* **2004**, *245*, 1 and references therein.
(283) Cui, Y.; Kita, H.; Okamoto, K. *J. Mater. Chem.* **2004**, *14*, 924.
(284) Husain, S.; Koros, W. J. *J. Membr. Sci.* **2007**, *288*, 195.
(285) Pechar, T. W.; Kim, S.; Vaughan, B.; Marand, E.; Tsapatsis, M.; Jeong, H. K.; Cornelius, C. J. *J. Membr. Sci.* **2006**, *277*, 195.
(286) Choi, J.; Ghosh, S.; Lai, Z.; Tsapatsis, M. *Angew. Chem., Int. Ed.* **2006**, *45*, 1154.
(287) Lai, Z.; Tsapatsis, M.; Nicolich, J. P. *Adv. Funct. Mater.* **2004**, *14*, 716.
(288) Barrer, R. M. *J. Chem. Soc., Faraday Trans.* **1990**, *86*, 1123.
(289) Bakker, W. J. W.; Kapteijn, F.; Poppe, J.; Moulijn, J. A. *J. Membr. Sci.* **1996**, *117*, 57.
(290) Jost, S.; Bar, N.-K.; Fritzsche, S.; Haberlandt, R.; Karger, J. *J. Phys. Chem.* **1992**, *B102*, 6375.
(291) Krishna, R.; Paschek, D. *Phys. Chem. Chem. Phys.* **2002**, *4*, 1891.
(292) Sanborn, M. J.; Snurr, R. Q. *Sep. Purif. Technol.* **2000**, *20*, 1.
(293) Sanborn, M. J.; Snurr, R. Q. *AIChE J.* **2001**, *47*, 2032.
(294) Skoulidas, A. I.; Sholl, D. S.; Krishna, R. *Langmuir* **2003**, *19*, 7977.
(295) Skoulidas, A. I.; et al. *J. Membr. Sci.* **2003**, *227*, 123.
(296) Skoulidas, A. I.; Sholl, D. S. *AIChE J.* **2005**, *51*, 876.
(297) Sholl, D. S. *Acc. Chem. Res.* **2006**, *39*, 403.
(298) Cussler, E. L. *Diffusion Mass Transfer in Fluid Systems*, 2nd ed.; Cambridge University Press: Cambridge, U.K., 1997.
(299) Burggraaf, A. J. *Transport and separation properties of membranes with gases and vapors*; Elsevier: Amsterdam, 1996.

(300) Masuda, T.; Fukumoto, N.; Kitamura, M.; Mukai, S. R.; Hahimoto, K.; Tanaka, T.; Funabiki, T. *Microporous Mesoporous Mater.* **2001**, *48*, 239.
(301) Park, D. H.; Nishiyama, N.; Egashira, Y.; Ueyama, K. *Ind. Eng. Chem. Res.* **2001**, *40*, 6105.
(302) Sano, T.; Hasegawa, M.; Ejiri, S.; Kawakami, Y.; Yanagishita, H. *Microporous Microporous Mater.* **1995**, *5*, 179.
(303) Falconer, J. L.; George, S. M.; Ott, A. W.; Klaus, J. W.; Noble, R. D.; Funke, H. H. Modification of zeolite or molecular sieve membranes using atomic layer controlled chemical vapor deposition. U.S. Patent 6,043,177.
(304) Yan, Y. S.; Davis, M. E.; Gavalas, G. R. *J. Membr. Sci.* **1997**, *123*, 95.
(305) Nenoff, T. M.; Kartin, M.; Thoma, S. G. Enhanced Selectivity of Zeolites by Controlled Carbon Deposition. U.S. Patent 7,041,616.
(306) Gu, X.; Dong, J. H.; Nenoff, T. M.; Ozokwelu, D. E. *J. Membr. Sci.* **2006**, *280*, 624.
(307) Hong, M.; Falconer, J. L.; Noble, R. D. *Ind. Eng. Chem. Res.* **2005**, *44*, 4035.
(308) Guan, G.; Kusakabe, K.; Morooka, S. *Sep. Sci. Technol.* **2001**, *36*, 2233.
(309) Guan, G. Q.; Tanaka, T.; Kusakabe, K.; Sotowa, K. I.; Morooka, S. *J. Membr. Sci.* **2003**, *214*, 191.
(310) Mitchell, M. C.; Autry, J. D.; Nenoff, T. M. *Mol. Phys.* **2001**, *99*, 1831.
(311) Mitchell, M.; Gallo, M.; Nenoff, T. M. *J. Chem. Phys.* **2004**, *121*, 1910.
(312) Gallo, M.; Nenoff, T. M.; Mitchell, M. C. *Fluid Phase Equilib.* **2006**, *247*, 135.
(313) Adams, K. L.; Li, L.; Gu, X.; Dong, J. H.; Mitchell, M. C.; Nenoff, T. M. *J. Membr. Sci.*, in preparation.
(314) Seike, T.; Matsuda, M.; Miyake, M. *J. Mater. Chem.* **2002**, *12*, 366.
(315) Bernal, M. P.; Coronas, J.; Menéndez, M.; Santamaría, J. *AIChE J.* **2004**, *50*, 127.
(316) Gu, X.; Dong, J. H.; Nenoff, T. M. *Ind. Eng. Chem. Res.* **2005**, *44*, 937.
(317) Li, S.; Martinek, J. G.; Falconer, J. L.; Noble, R. D.; Gardner, T. Q. *Ind. Eng. Chem. Res.* **2005**, *44*, 3220.
(318) DOE/H2 Multi-Year Research, Development and Demonstration Plan, available electronically at http://www.1.eere.energy.gov/hydrogenandfuelcells/.
(319) FutureGen coalition formed. *Power Eng.* **2005**, *109*, 16.
(320) Peltier, R. *Power* **2003**, *147*, 52.
(321) Williams, M. C.; Strakey, J. P.; Surdoval, W. A. *J. Power Sources* **2005**, *143*, 191.
(322) Saufi, S. M.; Ismail, A. F. *Carbon* **2004**, *42*, 241.
(323) Fuertes, A. B.; Centeno, T. A. *J. Membr. Sci.* **1998**, *144*, 105.
(324) Ismail, A. F.; David, L. I. B. *J. Membr. Sci.* **2001**, *193*, 1.
(325) Shiflett, M. B.; Foley, H. C. *J. Membr. Sci.* **2000**, *179*, 275.
(326) Shiflett, M. B.; Foley, H. C. *Science* **1999**, *285*, 1902.
(327) Hayashi, J.; Mizuta, H.; Yamamoto, M.; Kusakabe, K.; Morooka, S. *J. Membr. Sci.* **1997**, *124*, 243.
(328) Wang, H.; Zhang, L.; Gavalas, G. R. *J. Membr. Sci.* **2000**, *177*, 25.
(329) Fuertes, A. B.; Centeno, T. A. *Microporous Mesoporous Mater.* **1998**, *26*, 23.
(330) Acharya, M.; Foley, H. C. *J. Membr. Sci.* **1999**, *161*, 1.
(331) Liang, C.; Sha, G.; Guo, S. *Carbon* **1999**, *37*, 1391.
(332) Morthon-Jones, D. H. *Polymer processing*; Chapman and Hall: London, 1984; Chapter 2.
(333) Soffer, A.; Rosen, D.; Saguee, S.; Koresh, J. Carbon membranes. GB patent 2207666.
(334) Schindler, E.; Maier, F. Manufacture of porous carbon membranes. U.S. patent 4919860.
(335) Suda, H.; Haraya, K. *J. Phys. Chem. B* **1997**, *101*, 3988.
(336) Geiszler, V. C.; Koros, W. J. *Ind. Eng. Chem. Res.* **1996**, *35*, 2999.
(337) Strathmann, H. *Membr. Technol.* **1999**, *113*, 9.
(338) Yoneyama, H.; Nishihara, Y. Carbon based porous hollow fiber membrane and method for producing same. U.S. patent 5089135.
(339) Petersen, J.; Matsuda, M.; Haraya, K. *J. Membr. Sci.* **1997**, *131*, 85.
(340) Pietrass, T. *MRS Bull.* **2006**, *31*, 765.
(341) Rao, A. M.; Sircar, S. *Gas Sep. Purif.* **1993**, *7*, 279.
(342) Rao, A. M.; Sircar, S. *J. Membr. Sci.* **1993**, *85*, 253.
(343) Viera-Linhares, A. M.; Seaton, N. A. *Chem. Eng. Sci.* **2003**, *58*, 4129.
(344) Sircar, S.; Waldron, W. E.; Rao, M. B.; Anand, M. *Sep. Purif. Technol.* **1999**, *17*, 11.
(345) Viera-Linhares, A. M.; Seaton, N. A. *Chem. Eng. Sci.* **2003**, *58*, 5251.
(346) Koresh, J. E.; Soffer, A. *Sep. Sci. Technol.* **1987**, *22*, 973.
(347) Villar-Rodil, S.; Denoyel, R.; Rouquerol, J.; Martínez-Alonso, A.; Tascón, J. M. D. *Chem. Mater.* **2002**, *14*, 4328.
(348) Koresh, J. E.; Soffer, A. *J. Chem. Soc., Faraday Trans. 1* **1980**, *76*, 2457.
(349) Koresh, J. E.; Soffer, A. *J. Chem. Soc., Faraday Trans. 1* **1980**, *76*, 2472.
(350) Koresh, J. E.; Soffer, A. *J. Chem. Soc., Faraday Trans. 1* **1980**, *76*, 2507.
(351) Koresh, J. E.; Soffer, A. *J. Chem. Soc., Faraday Trans. 1* **1981**, *77*, 3005.
(352) Koresh, J. E.; Soffer, A. *Sep. Sci. Technol.* **1983**, *18*, 723.
(353) Koresh, J. E.; Soffer, A. *J. Chem. Soc., Faraday Trans. 1* **1986**, *82*, 2057.
(354) Hatori, H.; Takagi, H.; Yamada, Y. *Carbon* **2004**, *42*, 1169.
(355) Choudhary, T. V.; Sivadinarayana, C.; Goodman, D. W. *Chem. Eng. J.* **2003**, *93*, 69.
(356) Iijima, S. *Nature* **1991**, *354*, 56.
(357) Service, R. F. *Science* **2000**, *290*, 246.
(358) Odom, T. W.; Huang, J.-L.; Kim, P.; Lieber, C. M. *Nature* **1998**, *391*, 62.
(359) Wildöer, J. W. G.; Venema, L. C.; Rinzler, A. C.; Smalley, R. E.; Dekker, C. *Nature* **1998**, *391*, 59.
(360) O'Connell, M. J.; Bachilo, S. M.; Huffman, C. B.; Moore, V. C.; Strano, M. S.; Haroz, E. H.; Rialon, K. L.; Boul, P. J.; Noon, W. H.; Kittrell, C.; Ma, J.; Hauge, R. H.; Weisman, R. B.; Smalley, R. E. *Science* **2002**, *391*, 593.
(361) Dyke, C. A.; Tour, J. M. *Chem.—Eur. J.* **2004**, *10*, 812.
(362) Williams, K. A.; Eklund, P. C. *Chem. Phys. Lett.* **2000**, *320*, 352.
(363) Dresselhaus, M. S.; Williams, K. A.; Eklund, P. C. *Mat. Res. Bull.* **1999**, *24*, 45.
(364) Skoulidas, A. I.; Ackerman, D. M.; Johnson, J. K.; Sholl, D. S. *Phys. Rev. Lett.* **2002**, *89*, 185901.
(365) Sokhan, V. P.; Nicholson, D.; Quirke, N. *J. Chem. Phys.* **2002**, *117*, 8531.
(366) Skoulidas, A. I.; Johnson, J. K.; Sholl, D. S. *J. Chem. Phys.* **2006**, *124*, 154708.
(367) Chen, H.; Sholl, D. S. *J. Membr. Sci.* **2006**, *269*, 152.
(368) Sholl, D. S.; Johnson, K. J. *Science* **2006**, *312*, 1003.
(369) Holt, J. K.; Park, H. G.; Wang, Y.; Stadermann, M.; Artyukhin, A. B.; Grigoropoulos, C. P.; Noy, A.; Bakajin, O. *Science* **2006**, *312*, 1034.
(370) Hinds, B. J.; Chopra, N.; Rantell, T.; Andrews, R.; Gavalas, V.; Bachas, L. G. *Science* **2004**, *303*, 62.
(371) Weller, S.; Steiner, W. A. *Chem. Eng. Prog.* **1950**, *46*, 585.
(372) Zolandz, R. R.; Fleming, G. K. Gas Permeation Applications. In *Membrane Handbook*; Ho, W. S. W., Sirkar, K. K., Eds.; Chapman and Hall: New York, 1992; p 78.
(373) Gardner, R. J.; Crane, R. A.; Hannan, J. F. *Chem. Eng. Prog.* **1977**, *73*, 76.
(374) Koros, W. J.; Mahajan, R. *J. Membr. Sci.* **2000**, *175*, 181.
(375) Henis, J. M. S.; Tripodi, M. K. Multicomponent Membranes for Gas Separations. United States Patent 4,230,463, 1980.
(376) Schell, W. J.; Houston, C. D. *Chem. Eng. Prog.* **1982**, *78*, 33.
(377) Bollinger, W. A.; Long, S. P.; Metzger, T. R. *Chem. Eng. Prog.* **1984**, *80*, 51.
(378) Bollinger, W. A.; Maclean, D. L.; Narayan, R. S. *Chem. Eng. Prog.* **1982**, *78*, 27.
(379) Farrauto, R.; et al. *Annu. Rev. Mater. Res.* **2003**, *33*, 1.
(380) Sato, S.; Nagai, K. *Membranes* **2005**, *30*, 20.
(381) Knudsen, M. *The Kinetic Theory of Gases; Some Modern Aspects*; Methuen's Monographs on Physical Subjects; Methuen: London, 1952.
(382) Hines, A. L.; Maddox, R. N. *Mass Transfer*; Prentice Hall PTR: Upper Saddle River, NJ, 1985; p 553.
(383) Hwang, S. T.; Kammerme, K. *Can. J. Chem. Eng.* **1966**, *44*, 82.
(384) Lee, K. H.; Hwang, S. T. *J. Colloid Interface Sci.* **1986**, *110*, 544.
(385) Masaryk, J. S.; Fulrath, R. M. *J. Chem. Phys.* **1973**, *59*, 1198.
(386) Baker, R. W. *Membrane Technology and Applications*; McGraw-Hill: New York, 2000.
(387) Rautenbach, R.; Albrecht, R. *Membrane Processes*; John Wiley & Sons: Chichester, 1989.
(388) Stern, S. A. *J. Membr. Sci.* **1994**, *94*, 1.
(389) Vu, D. Q.; Koros, W. J.; Miller, S. J. *J. Membr. Sci.* **2003**, *211*, 311.
(390) Singh, A.; Koros, W. J. *Ind. Eng. Chem. Res.* **1996**, *35*, 1231.
(391) Lin, H.; Freeman, B. D. *J. Membr. Sci.* **2004**, *239*, 105.
(392) Reid, R. C.; Prausnitz, J. M.; Poling, B. E. *The Properties of Gases and Liquids*, 4th ed.; McGraw Hill: Boston, MA, 1987; p 752.
(393) Robeson, L. M. *J. Membr. Sci.* **1991**, *62*, 165.
(394) Aitken, C. L.; Koros, W. J.; Paul, D. R. *Macromolecules* **1992**, *25*, 3651.
(395) Aitken, C. L.; Koros, W. J.; Paul, D. R. *Macromolecules* **1992**, *25*, 3424.
(396) Aitken, C. L.; Paul, D. R.; Mohanty, D. K. *J. Polym. Sci., Part B: Polym. Phys.* **1993**, *31*, 983.
(397) Aitkin, C. L.; Paul, D. R. *J. Polym. Sci., Part B: Polym. Phys.* **1993**, *31*, 1061.
(398) Bixler, H. J.; Sweeting, O. J. Barrier Properties of Polymer Films. In *The Science and Technology of Polymer Films*; Sweeting, O. J., Ed.; Wiley-Interscience: New York, 1971; pp 1−130.

(399) Fritsch, D.; Peinemann, K. V. *J. Membr. Sci.* **1995**, *99*, 29.
(400) Hofman, D.; et al. *Polymer* **1996**, *37*, 4773.
(401) Kita, H.; Tabuchi, M.; Sakai, T. Polymer Separation Membrane. U.S. Patent 6,656,252 B2.
(402) McHattie, J. S.; Koros, W. J.; Paul, D. R. *Polymer* **1991**, *32*, 2618.
(403) McHattie, J. S.; Koros, W. J.; Paul, D. R. *J. Polym. Sci., Part B: Polym. Phys.* **1991**, *29*, 731.
(404) McHattie, J. S.; Koros, W. J.; Paul, D. R. *Polymer* **1991**, *32*, 840.
(405) McHattie, J. S.; Koros, W. J.; Paul, D. R. *Polymer* **1992**, *33*, 1701.
(406) Min, K. E.; Paul, D. R. *J. Polym. Sci., Part B: Polym. Phys.* **1988**, *26*, 1021.
(407) Mohr, J. M.; et al. *J. Membr. Sci.* **1991**, *56*, 77.
(408) Mohr, J. M.; et al. *Polymer* **1991**, *32*, 2387.
(409) Nagasaki, Y.; et al. *Makromol. Chem., Rapid Commun.* **1989**, *10*, 255.
(410) Srinivasan, R.; Auvil, S. R.; Burban, P. M. *J. Membr. Sci.* **1994**, *86*, 67.
(411) Stern, S. A.; et al. *J. Polym. Sci., Part B: Polym. Phys.* **1989**, *27*, 1887.
(412) Takada, K.; et al. *J. Appl. Polym. Sci.* **1985**, *30*, 1605.
(413) Tanaka, K.; et al. *Polymer* **1992**, *33*, 585.
(414) Yamamoto, H.; et al. *J. Polym. Sci., Part B: Polym. Phys.* **1990**, *28*, 2291.
(415) Freeman, B. D. *Macromolecules* **1999**, *32*, 375.
(416) Kita, H.; et al. *J. Membr. Sci.* **1994**, *87*, 139.
(417) Liu, Y.; Ding, M. X.; Xu, J. P. *J. Appl. Polym. Sci.* **1995**, *58*, 485.
(418) Wright, C. T.; Paul, D. R. *J. Membr. Sci.* **199**7, *129*, 47.
(419) Ding, Y.; Bikson, B.; Nelson, J. K. Polymide Gas Separation Membranes. U.S. Patent 6,790,263.
(420) Kawakami, H.; et al. Gas Separation Membrane and Method of Producing the Same. U.S. Patent 6,709,491 B2.
(421) Baker, R. W.; et al. Gas Separation using Organic-Vapor-Resistant Membranes in Conjunction with Organic-Vapor-Selective Membranes. U.S. Patent 6,572,697 B2.
(422) Bikson, B.; et al. Hollow Fiber Membrane Gas Separation Cartridge and Gas Purification Assembly. U.S. Patent 6,814,780 B2.
(423) Engler, Y.; Fuentes, F. Plant for the Production of Hydrogen and of Energy. U.S. Patent 5,989,501.
(424) Fuentes, F. Installation for the Production of Pure Hydrogen from a Gas Containing Helium. U.S. Patent 6,669,922 B1.
(425) Lokhandwala, K. A.; Baker, R. W. Hydrogen/Hydrocarbon Separation Process, Including PSA and Membranes. U.S. Patent 6,592,749.
(426) Siadous, N.; Engler, Y.; Monereau, C. Method for Separating a Gas Mixture with a Permeation Membrane Unit. U.S. Patent 6,977,007 B2.
(427) Wallace, P. S.; Kasbaum, J. L.; Johnson, K. A. Hydrogen Recycle and Acid Gas Removal Using a Membrane. U.S. Patent 6,416,568 B1.
(428) Yamashita, N.; Yamamoto, T. Method and Apparatus for Recovering a gas from a gas mixture. U.S. Patent 6,197,090 B1.
(429) Ekiner, O. M. Gas Separation Membranes of Blends of Polyethersulfones with Aromatic Polyimides. U.S. Patent 5,917,137.
(430) MacKinnon, S. M., Process for Preparing Graft Copolymers and Membranes Formed Therefrom. U.S. Patent 6,828,386 B2.
(431) Nakanishi, S.; et al. Gas Separation Membrane and Method for its Use. U.S. Patent 6,464,755.
(432) Simmons, J. W. Block Polyurethane-ether and Polyurea-ether Gas Separation Membranes. U.S. Patent 6,843,829.
(433) Simmons, J. W. Block Polyester-ether Gas Separation Membranes. U.S. Patent 6,860,920 B2.
(434) Perry, J. D.; Nagai, K.; Koros, W. J. *MRS Bull.* **2006**, *31*, 745.
(435) Merkel, T. C.; et al. *J. Membr. Sci.* **2001**, *191*, 85.
(436) Pinnau, I.; He, Z. J. *J. Membr. Sci.* **2004**, *244*, 227.
(437) Hirayama, Y.; et al. *J. Membr. Sci.* **1999**, *160*, 87.
(438) Nagai, K.; et al. *J. Membr. Sci.* **2000**, *172*, 167.
(439) Nagai, K.; Nakagawa, T. Adv. Materials for Membrane Separations; *ACS Symposium Series*; American Chemical Society: Washington, DC, 2004.
(440) Suzuki, H.; et al. *J. Membr. Sci.* **1998**, *146*, 31.
(441) Kazama, S.; et al. 7th International Conference on Greenhouse Gas Control Technologies, Vancouver, Canada, 2004.
(442) Nagai, K. *KOUBUSHIRONBUNSHU* **2004**, *61*, 420.
(443) Nagai, K. *Membrane* **2004**, *29*, 42.
(444) Anand, M.; et al. *J. Membr. Sci.* **1997**, *123*, 17.
(445) Bondar, V. I.; Freeman, B. D.; Pinnau, I. *J. Polym. Sci., Part B: Polym. Phys.* **2000**, *38*, 2051.
(446) Pinnau, I.; et al. *J. Polym. Sci., Part B: Polym. Phys.* **1996**, *34*, 2613.
(447) Raharjo, R. D.; et al. *Polymer* **2005**, *46*, 6316.
(448) Robeson, L. M.; et al. *Polymer* **1994**, *35*, 4970.
(449) LeBlanc, O. H.; Ward, W. J.; Matson, S. L.; Kimura, S. G. *J. Membr. Sci.* **1980**, *6*, 339.
(450) Kimura, S. G.; Ward, W. J.; Matson, S. L. U.S. Patent No. 4,318,-714.
(451) Way, J. D.; Noble, R. D. In *Membrane Handbook*; Ho, W. S. W., Sirkar, K. K., Eds.; Van Nostrand Reinhold: New York, 1992; p 833.
(452) Way, J. D.; Noble, R. D.; Reed, D. L.; Ginley, G. M.; Jarr, L. A. *AIChE J.* **1987**, *33*, 480.
(453) Way, J. D.; Hapke, R. L. *Prepr. Pap.—Am. Chem. Soc., Div. Fuel Chem.* **1988**, *33*, 283.
(454) Pelligrino, J. J.; Nassimbene, R.; Ko, M.; Noble, R. D. *Proc. Ninth Annu. Gasification Gas Stream Cleanup Syst. Contractors Rev. Meeting* **1989**, 211.
(455) Noble, R. D.; Pellegrino, J. J.; Grosgogeat, E.; Sperry, D.; Way, J. D. *Sep. Sci. Techmol.* **1988**, *23*, 1595.
(456) Langevin, D.; Pinoche, M.; Selegny, E.; Metayer, M.; Roux, R. *J. Membr. Sci.* **1993**, *82*, 51.
(457) Kim, M.; Park, Y.; Youm, K.; Lee, K. *J. Membr. Sci.* **2004**, *245*, 79.
(458) Matsuyama, H.; Teramoto, M.; Iwai, K. *J. Membr. Sci.* **1994**, *93*, 237.
(459) Matsuyama, H.; Teramoto, M.; Sakakura, H.; Iwai, K. *J. Membr. Sci.* **1996**, *117*, 251.
(460) Matsuyama, H.; Teramoto, M.; Matsui, K.; Kitaura, Y. *J. Appl. Polym. Sci.* **2001**, *81*, 936.
(461) Ho, W. S. W. U.S. Patent No. 5,611,843.
(462) Ho, W. S. W. U.S. Patent No. 6,099,621.
(463) Ho, W. S. W. U.S. Patent No. 6,579,331.
(464) Quinn, R.; Laciak, D. V. U.S. Patent 6,315,968.
(465) Quinn, R.; Laciak, D. V.; Appleby, J. B.; Pez, G. P. U.S. Patent 5,336,298.
(466) Quinn, R.; Laciak, D. V. *J. Membr. Sci.* **1997**, *131*, 49.
(467) Quinn, R. *J. Membr. Sci.* **1998**, *139*, 97.
(468) Quinn, R.; Laciak, D. V.; Pez, G. P. *J. Membr. Sci.* **1997**, *131*, 61.
(469) Namboodhiri, T. K. G. *Trans. Indian Inst. Met.* **1984**, *37*, 764.
(470) Birnbaum, H. K. In Environmental Sensitive Fracture of Engineering Materials; *Proceedings of Symposium on Environmental Effects on Fracture*, Chicago, Illinois, 1977; Foroulis, Z. A., Ed.; Metallurgical Society of AIME: Warendale, PA, pp 326−360.
(471) Buschow, K. H. J.; Bouten, P. C. P.; Miedema, A. R. *Rep. Prog. Phys.* **1982**, *9*, 937.
(472) Shkolnik, I. V.; Kulsartov, T. V.; Tazhibaeva, I. L.; Shestakov, V. P. *Fusion Technol.* **1998**, *34*, 868.
(473) Cermák, J.; Rothová, V. *Intermetallics* **2001**, *9*, 403.
(474) Takano, T.; Ishikawa, K.; Matsuda, T.; Aoki, K. *Mater. Trans., JIM* **2004**, *45*, 3360.
(475) Komiya, K.; Shinzato, Y.; Yukawa, H.; Morinaga, M.; Yasuda, I. *Fifth Pacific Rim Int. Conf. Adv. Mater. Process., Pts 1−5* **2005**, *475−479*, 2497.
(476) Cheng, X. Y.; Wu, Q. Y.; Sun, Y. K. *J. Alloys Compd.* **2005**, *389*, 198.
(477) Hashi, K.; Ishikawa, K.; Matsuda, T.; Aoki, K. *Mater. Trans., JIM* **2005**, *46*, 1026.
(478) Aoki, K.; Matsuda, T.; Ishikawa, K. U.S. Patent 0,217,480 A1.
(479) Jang, T. H.; Lee, J. Y. *J. Non-Cryst. Solids* **1990**, *116*, 73.
(480) Yan, S.; Maeda, H.; Kusakabe, K.; Morooka, S.; Akiyama, Y. *Ind. Eng. Chem. Res.* **1994**, *33*, 2696.
(481) Hwang, G. J.; Onuki, K.; Shimizu, S.; Ohya, H. *J. Membr. Sci.* **1999**, *162*, 83.
(482) Koukou, M. K.; Papayannakos, N.; Markatos, N. C.; Bracht, M.; Van Veen, H. M.; Roskam, A. *J. Membr. Sci.* **1999**, *155*, 241−259.
(483) Schafer, R.; Noack, M.; Kolsch, P.; Thomas, S.; Seidel-Morgenstern, A.; Caro, J. *Sep. Purif. Technol.* **2001**, *25*, 3.
(484) Tsuru, T.; Yamaguchi, K.; Yoshioka, T.; Asaeda, M. *AIChE J.* **2004**, *50*, 2794.
(485) Makino, H.; et al. Process for Preparing Aromatic Polyimide Semipermeable Membranes. U.S. Patent 4,378,324.
(486) Breck, D. W. *Zeolite Molecular Sieves*; John Wiley & Sons: New York, 1974; p 783.
(487) Agrawal, R.; Offutt, M.; Ramage, M. P. *AIChE J.***2005**, *51*, 1582.
(488) Ramage, M. P. *The Hydrogen Economy: Opportunities, Costs, Barriers, and R&D Needs*; National Research Council of the National Academies: 2004; pp ES-1 to ES-14.
(489) Simbeck, D. R. *Energy* **2004**, *29*, 1633.
(490) Summers, W. A.; Gorensek, M. B. *Chem. Eng. Prog.* **2005**, *101*, 4.
(491) Winter, C. J. *Int. J. Hydrogen Energy* **2005**, *30*, 681.
(492) Orme, C. J.; Stone, M. L.; Benson, M. T.; Peterson, E. S. *Sep. Sci. Technol.* **1995**, *38*, 3225−3283.
(493) Zhang, Y.; Wang, Z.; Wang, S. *J. Appl. Polym. Sci.* **2002**, *86*, 2222.
(494) Matsuyama, H.; Terada, A.; Nakagawara, T.; Kitamura, Y.; Teramoto, M. *J. Membr. Sci.* **1999**, *163*, 221.
(495) Kim, T. J.; Li, B.; Hägg, M. B. *J. Polym. Sci. B* **2004**, *42*, 4326.
(496) Trachtenberg, M. C. *Proceedings of EFC-conference on Advanced Membrane Technology*, Barga, Italy, 2001.

CR0501792